

**CONTROLLED RELEASE FROM A BIODEGRADABLE ELASTOMER FOR
APPLICATIONS IN CARDIOVASCULAR REGENERATIVE MEDICINE**

by

Priya Ramaswami

BSE, Duke University, 2001

Submitted to the Graduate Faculty of the
Swanson School of Engineering in partial fulfillment
of the requirements for the degree of
Doctor of Philosophy

University of Pittsburgh

2008

UNIVERSITY OF PITTSBURGH
SWANSON SCHOOL OF ENGINEERING

This dissertation was presented

by

Priya Ramaswami

It was defended on

April 28, 2008

and approved by

Eric J. Beckman, PhD, Professor, Chemical & Petroleum Engineering

Toby Chapman, PhD, Associate Professor, Chemistry

Johnny Huard, PhD, Professor, Orthopaedic Surgery and Bioengineering

Bruno Péault, PhD, Professor, Pediatrics and Cell Biology & Physiology

Dissertation Director:

William R. Wagner, PhD, Professor, Bioengineering & Chemical & Petroleum Engineering

CONTROLLED RELEASE FROM A BIODEGRADABLE ELASTOMER FOR APPLICATIONS IN CARDIOVASCULAR REGENERATIVE MEDICINE

Priya Ramaswami, PhD

University of Pittsburgh, 2008

Insulin-like growth factor-1 (IGF-1) and hepatocyte growth factor (HGF) have been implicated in the intrinsic response of the heart to myocardial infarction (MI), and it has been postulated that exogenous administration of one or both of these growth factors may enhance myocardial repair and regeneration. We hypothesized that a biodegradable, elastomeric poly(ester urethane)urea (PEUU) capable of sustained, local delivery of IGF-1 or HGF to ischemic myocardium would improve left ventricular (LV) dimension and function. PEUU scaffolds without growth factor or scaffolds containing either IGF-1 or HGF were applied onto the hearts of rats injured by MI. Improvement in LV function and restoration of LV wall thickness, muscle mass, and angiogenesis were assessed 8 weeks post-patch implantation. Improvement in LV dimension and function due to IGF-1-loaded patches was not significant compared to control patches, while HGF-loaded patches significantly worsened LV dimension compared to IGF-loaded and control patches. No significant differences in muscle or capillary formation or LV function were noted between groups. Although no significant improvements were noted with growth factor-loaded patches, trends towards improved LV dimension with IGF-1-loaded patches and trends towards worsened LV dimension and function with HGF-loaded patches may warrant additional investigation.

Furthermore, we evaluated the ability of PEUU to deliver molecules designed to induce cellular gene expression in a spatially-controlled manner *in vitro*. PEUU films and scaffolds with spatially-defined regions containing or omitting inducer molecules were fabricated, and cells transduced to express green fluorescent protein (GFP) were cultured on films and within scaffolds to evaluate spatial control of gene expression. PEUU demonstrated an extended period of controlled release of the inducer molecule as well as providing spatial control over GFP expression in both PEUU films and three-dimensional scaffolds. Hence, these scaffolds may provide a means to control progenitor cell commitment in a spatially-defined manner *in vivo* for tissue repair and regeneration. With an elastic scaffold delivery system, such a technique might ultimately find application in cardiovascular tissue engineering.

TABLE OF CONTENTS

PREFACE.....	xvi
1.0 INTRODUCTION.....	1
1.1 SIGNIFICANCE.....	1
1.2 CELL THERAPY FOR CARDIAC REPAIR AND REGENERATION.....	4
1.2.1 Cellular cardiomyoplasty.....	4
1.2.2 Cardiomyocytes	4
1.2.3 Skeletal muscle precursor cells.....	5
1.2.3.1 Skeletal myoblasts.....	5
1.2.3.2 Muscle-derived stem cells.....	6
1.2.4 Stem and progenitor cells.....	7
1.2.4.1 Cardiac stem cells.....	7
1.2.4.2 Embryonic stem cells	8
1.2.4.3 Bone marrow-derived mesenchymal stem cells.....	9
1.2.4.4 Bone marrow-derived hematopoietic stem cells.....	10
1.2.4.5 Endothelial progenitor cells	10
1.2.4.6 Umbilical cord blood cells	11
1.2.5 Gene therapy and cell transplantation	11
1.3 BIOMATERIALS FOR CARDIAC REPAIR AND REGENERATION.....	13

1.3.1	Natural biomaterials.....	14
1.3.2	Synthetic biomaterials.....	16
1.3.3	Biomaterials for growth factor delivery	18
1.3.4	Biomaterials for gene therapy	22
1.4	OBJECTIVES	26
1.4.1	Objective #1: Biodegradable PEUU as a controlled release system	27
1.4.2	Objective #2: A cardiac patch for post-MI myocardial repair	28
1.4.3	Objective #3: Spatial control of gene expression via a polymer scaffold .	29
2.0	CONTROLLED RELEASE POLYURETHANE SCAFFOLDS FOR SOFT TISSUE ENGINEERING	30
2.1	INTRODUCTION	30
2.2	METHODS.....	33
2.2.1	Biodegradable poly(ester urethane)urea synthesis.....	33
2.2.2	Fabrication of ligand-loaded PEUU films	34
2.2.3	Quantification of ligand release from PEUU films.....	35
2.2.4	Verification of bioactivity of released ligand	35
2.2.5	Fabrication of factor-loaded PEUU scaffolds	36
2.2.5.1	Fabrication of ligand-loaded scaffolds	37
2.2.5.2	Fabrication of growth factor-loaded scaffolds	37
2.2.6	Mechanical testing of PEUU scaffolds	38
2.2.7	Quantification of growth factor release from PEUU scaffolds.....	38
2.2.8	Verification of bioactivity of released growth factor.....	39
2.2.9	Statistical methods.....	40
2.3	RESULTS	41

2.3.1	RSL1 release from PEUU films.....	41
2.3.2	Bioactivity of released RSL1.....	42
2.3.3	Mechanical properties of PEUU scaffolds.....	44
2.3.4	Growth Factor Release from PEUU scaffolds	45
2.3.5	Bioactivity of released IGF-1	46
2.3.6	Bioactivity of released HGF	48
2.4	DISCUSSION.....	50
3.0	IGF-1- AND HGF-LOADED CARDIAC PATCHES FOR MYOCARDIAL REPAIR AND REGENERATION.....	56
3.1	INTRODUCTION	56
3.2	METHODS.....	58
3.2.1	Preparation of cardiac patches from biodegradable, elastomeric PEUU	58
3.2.2	Animal model of subacute myocardial infarction	58
3.2.3	PEUU patch implantation.....	59
3.2.4	Echocardiography analysis.....	60
3.2.5	Histological assessment	60
3.2.6	Statistical methods.....	62
3.3	RESULTS	62
3.3.1	Gross morphology	62
3.3.2	LV wall thickness, formation of muscle bundles, and capillary density ..	63
3.3.3	LV cavity size and contractile function	66
3.4	DISCUSSION.....	68
4.0	SPATIAL CONTROL OF GENE EXPRESSION VIA A BIODEGRADABLE POLYURETHANE.....	75
4.1	INTRODUCTION	75

4.2	METHODS	77
4.2.1	Cells.....	77
4.2.2	Polyurethane synthesis.....	78
4.2.3	Preparation of RSL1-loaded PEUU films.....	79
4.2.4	Gene expression via PEUU films.....	79
4.2.5	Preparation of RSL1 loaded PEUU scaffolds.....	80
4.2.6	Seeding PEUU scaffolds with B16 cells.....	80
4.2.7	Spatial control of gene expression on PEUU films.....	81
4.2.8	Spatial control of gene expression in PEUU scaffolds.....	82
4.3	RESULTS	82
4.3.1	Gene expression via media manipulation.....	82
4.3.2	Gene expression via PEUU films.....	83
4.3.3	Gene expression in TIPS scaffolds.....	86
4.3.4	Spatial Control of gene expression on PEUU films.....	86
4.3.5	Spatial control of gene expression in TIPS scaffolds.....	88
4.4	DISCUSSION	89
5.0	CONCLUSIONS	94
5.1	FUTURE DIRECTIONS	96
5.1.1	Quantification of the <i>in vitro</i> release kinetics of IGF-1 and HGF.....	96
5.1.2	Development of IGF-1- and HGF-loaded PEUU patches for myocardial repair.....	97
5.1.3	Development of angiogenic and myogenic growth factor-loaded PEUU patches for myocardial repair.....	99
5.1.4	<i>In vivo</i> evaluation of PEUU scaffolds for spatial control of gene expression.....	100

APPENDIX A	102
APPENDIX B	103
APPENDIX C	104
APPENDIX D	105
APPENDIX E	106
APPENDIX F	107
APPENDIX G	108
APPENDIX H	109
BIBLIOGRAPHY	110

LIST OF FIGURES

Figure 1.1: MI results when one or more of the coronary arteries supplying blood to the heart are blocked leading to ischemic injury and death of muscle cells in the infarct zone. (Image modified from www.medicinenet.com/peripheral_vascular_disease/article.htm)	2
Figure 1.2: Skeletal muscle cells can be isolated from patients, expanded and/or modified <i>ex vivo</i> , and transplanted into infarcted myocardium for repair. (Image from www.med.umich.edu/opm/newspage/2002/musclecell.htm)	5
Figure 1.3: A biomaterial can be placed over infarcted myocardium in order to repair it by providing mechanical support or by delivering cells and/or biomolecules (Image modified from www.mirm.pitt.edu/news/article.asp?qEmpID=46)	13
Figure 1.4: The building blocks of tissue-engineered constructs [81]	19
Figure 1.5: “Tet-off”-regulated gene expression system.	24
Figure 1.6: RheoSwitch Ligand 1 (RSL1)	25
Figure 1.7: Transcriptional control using the RheoSwitch system. (Image from www.neb.com/nebecomm/products/productE3000.asp)	26
Figure 2.1: Poly(ester urethane)urea synthesis [169].	34
Figure 2.2: Ligand release curves for 2-5 μ M loading concentration of RSL1. An initial release of 49%-63% of RSL1 occurred over the first 7 days. This was followed by a slower release of RSL1 over the next two weeks, resulting in 73%-95% of ligand being released over a three week period <i>in vitro</i>	41
Figure 2.3: Ligand release curves for 50-150 μ M loading concentration of RSL1. An initial release of 6%-18% occurred over the first 7 days. A total of 20%-60% of ligand was released over a four week period <i>in vitro</i>	42

Figure 2.4: Gene expression in cells treated with release medium from PEUU films containing (a) 0 μ M, (b) 1 μ M, (c) 2 μ M, (d) 3 μ M, (e) 4 μ M, and (f) 5 μ M RSL1. Scale bar = 500 μ m for all images.....	43
Figure 2.5: Dose-dependent GFP expression in cells in degradation solutions from polymer containing 1-5 μ M RSL1. % GFP positive cells quantified as % of cells visibly positive for green fluorescence.....	44
Figure 2.6: IGF-1 ELISA standard curves in distilled water and in degradation solution from scaffolds without growth factor.....	45
Figure 2.7: HGF ELISA standard curves in distilled water and in degradation solution from polymer without growth factor.....	46
Figure 2.8: MG-63 cell growth in degradation solutions relative to growth medium (* p <0.05).	47
Figure 2.9: Balb/3T3 cell growth in degradation solutions relative to growth medium (* p <0.05).	48
Figure 2.10: HUVEC average cell velocity.....	49
Figure 2.11 Wound infiltration by HUVECs with time (* p <0.05 compared to cells in growth medium and cells in degradation solutions from polymer without growth factor)..	49
Figure 3.1: Representative image of a patched heart (albumin control) 8 weeks after implantation. Arrows point to the patched region. P = patch.....	62
Figure 3.2: LV wall thickness.....	63
Figure 3.3: Representative histological sections of H&E staining of hearts receiving (a) high IGF-1, (b) control, and (c) HGF patches 8 weeks after implantation. Black arrows indicate patch. Scale bars are 500 μ m in all images.....	64
Figure 3.4: Smooth muscle bundles and capillaries in (a) patch control, (b) high IGF-1, (c) low IGF-1, and (d) HGF patched hearts. Red: α -SMA, Green: vWF, Blue: Hoechst dye (nuclear stain). Scale bars are 200 μ m in all images.....	65
Figure 3.5: LV end-diastolic area (EDA) for infarction control, patch control, IGF-1, and HGF groups. EDA for the infarction control and HGF groups significantly increased at 8 weeks compared to 0 weeks (* p <0.05). No significant difference in EDA was seen between experimental groups.....	66
Figure 3.6: Fractional Area Change (%FAC) for infarction control, patch control, IGF-1, and HGF groups. %FAC for the infarction control significantly decreased at 8 weeks compared to 0 weeks (* p <0.05). No significant difference in %FAC was seen between experimental groups.....	67
Figure 4.1. Vector map for pRG-1012b-hrGFP.....	78

Figure 4.2: Typical slide layout for 2-dimensional spatial control experiments.	81
Figure 4.3: Gene expression via media manipulation. 48 hours post-RSL1 administration, cells in growth medium without ligand did not express GFP (left), while cells in growth medium containing 1-5 μM ligand expressed GFP (5 μM concentration shown on right). Scale bars = 500 μm	83
Figure 4.4: Gene expression on PEUU films containing (a) 0 μM , (b) 1 μM , (c) 2 μM , (d) 3 μM , (e) 4 μM , and (f) 5 μM RSL1. Blue: nuclear stain, Green: GFP. Scale bar = 500 μm for all images.	83
Figure 4.5: Gene expression on PEUU films containing (a) 0 μM , (b) 1 μM , (c) 3 μM , (d) 5 μM , (e) 7 μM , and (f) 10 μM RSL1. Blue: nuclear stain, Red: phalloidin, Green: GFP. Scale bar = 250 μm for all images.	84
Figure 4.6: Dose-dependent GFP expression in cells on PEUU films containing 0-10 μM RSL1.	85
Figure 4.7: Dose-dependent GFP expression in cells on PEUU films containing 1-5 μM RSL1. 85	
Figure 4.8: Cells within TIPS scaffolds without RSL1 did not express GFP (left), while cells within scaffolds containing RSL1 expressed GFP. Scale bars = 500 μm	86
Figure 4.9: Cells on sections of slides containing PEUU without ligand did not express GFP (left), whereas cells on sections of slides containing PEUU loaded with RSL1 clearly expressed GFP (right), thereby demonstrating spatial control of gene expression via 2-dimensional PEUU films. Scale bar = 500 μm for all images.	87
Figure 4.10: Spatial control of gene expression within 3D PEUU scaffolds. Cells in the outer ring of the scaffold, where ligand was omitted, did not express GFP (left), whereas cells in the center of the scaffold, which contained RSL1, clearly expressed GFP (right), thereby demonstrating spatial control of gene expression within a 3-dimensional PEUU scaffold. Scale bar = 500 μm for all images.	88

NOMENCLATURE

α -SMA - alpha-smooth muscle actin

ACE - angiotensin-converting enzyme

ANOVA - analysis of variance

BDI - butane diisocyanate

bFGF, FGF2 - basic fibroblast growth factor

BSA - bovine serum albumin

CCM - cellular cardiomyoplasty

CHF - congestive heart failure

DMEM - Dulbecco's modified Eagle medium

DMSO - dimethyl sulfoxide

ECM - extracellular matrix

EcR - ecdysone receptor

EDA - end-diastolic area

ELISA - enzyme-linked immunosorbant assay

EPC - endothelial progenitor cell

ePTFE – expanded poly(tetrafluoroethylene)

ESA - end-systolic area

ESC - embryonic stem cell

FAC - fractional area change

GFP - green fluorescent protein

HDI - 1,6-diisocyanatohexane

H&E - hematoxylin and eosin

HSC - hematopoietic stem cell

HGF- hepatocyte growth factor

HUVEC - human umbilical vein endothelial cell

IGF-1- insulin-like growth factor-1

LDI - lysine methyl ester diisocyanate

LV - left ventricle

LVAD - left ventricular assist device

MDSC - muscle-derived stem cell

MDI - 4,4'-diphenylmethane diisocyanate

MI - myocardial infarction

MSC - mesenchymal stem cell

MW - molecular weight

MyoD - myogenic determination gene

PBS - phosphate buffered saline

PCL - polycaprolactone diol

PDGF - platelet derived growth factor

PEG - poly(ethylene glycol)

PEI - poly(ethylene imine)

PEO - poly(ethylene oxide)

PET - polyethylene terephthalate

PEUU - poly(ester urethane)urea

PGA - poly(glycolic acid)

PLA - poly(lactic acid)

PU - polyurethane

RSL1 - RheoSwitch ligand 1

RXR - retinoid X receptor

skMBs - skeletal myoblasts

SMC - smooth muscle cell

SPU - segmented polyurethane

TCPS - tissue culture polystyrene

TDI - 2,4-toluene diisocyanate

tetO - tetracycline operator

tetR - tetracycline-dependent repressor

TGF - transforming growth factor

TIPS - thermally induced phase separation

tTA - tetracycline-controlled transcriptional regulator

UCB - umbilical cord blood cell

VEGF - vascular endothelial growth factor

vWF - von Willebrand factor

PREFACE

It is with much gratitude to a great many people that this work was completed.

First and foremost, I convey my most genuine thankfulness to my thesis advisor, Dr. William R. Wagner, for his infinite patience and encouragement, and for allowing me to work on projects that were of interest to me. I have learned much from him in terms of being a disciplined scientist, and one of uncompromising integrity.

Tremendous thanks to my esteemed committee members, Dr. Eric Beckman, Dr. Toby Chapman, Dr. Johnny Huard, and Dr. Bruno Péault. Your expertise, encouragement, and guidance helped make my dream a reality.

I am very grateful to Dr. Kimimasa Tobita and Dr. Kazuro Fujimoto for their guidance and expertise with all animal experiments. Without them, those experiments would not have been possible.

To all those who were always ready and willing to share their knowledge with me, thank you – Dr. Ann Stewart-Akers, Doug Chew, Dr. Bridget Deasy, Dr. Burhan Gharaibeh, and Dr. Rick Koepsel – your guidance will always be much appreciated. Thank you also to the wonderful staff at the Center for Biologic Imaging for all their help with microscopy.

To all members of the Wagner Lab past and present, thank you for your support, friendship, and guidance. In particular, special thanks to Nick Amoroso, Dr. Yi Hong, Carl

Johnson, Dr. Zuwei Ma, Dr. Tim Maul, Devin Nelson, Dr. Trevor Snyder, Erin Wacker, and Dr. Sang-ho Ye. To Josh Woolley, a very heartfelt thank you for being a phenomenal friend and for always making lab an entertaining and fun place regardless of experimental strife! I will miss all the laughs.

Many thanks to Carole Stewart, Vera Pawlowski, Gilliane McShane, and Kelly Andres for all you have done for me in my time at Pitt. Thanks also to Marla Harris and Lynette Spataro for all their help and friendship through the years. Very special thanks also go to LaShon Jackson and Joan Schanck for giving me wonderful opportunities to be a part of the Pittsburgh community and to give back in so many ways. It has been an honor and a pleasure.

To the wonderful girlfriends (many also colleagues) who laughed and cried with me, for your love and friendship, I am eternally grateful. Charu Agarwal, Lynn Bonacci, Beth Boswell, Jenn Debarr, Lynn Ekis, Paola Florez de Sessions, Diana Gaitan, Amy Lazarus, Jess LoSurdo, Christy Milburn, Aarthi Sowrirajan, Sumathi Subbiah, and Indu Subbiah...thank you.

Last, and of course, not least, I owe everything to my wonderful family. One can only dream of having such an encouraging and supportive clan to always turn to. My brother was my anchor since I first started graduate school, and my parents have always been pillars of strength and incredible role models. And when I couldn't ask for more, I find myself blessed with absolutely loving in-laws-to-be. Words cannot express my gratitude to my fiancé, Andy for his support, his belief that I can do anything, his willingness to be there for me even when I'm a monster, and his ability to always make me laugh. None of this would have been possible had it not been for the unconditional love and support of my family, and to them goes the greatest thank you of all. Words cannot adequately express my love and respect for all of you.

1.0 INTRODUCTION

1.1 SIGNIFICANCE

Cardiovascular disease has been the leading cause of death in the United States since 1900, accounting for more American deaths each year than the next four leading causes of death combined [1]. It is estimated that over 850,000 people in the United States suffer from a myocardial infarction (MI, or heart attack) every year [1]. When one or more of the coronary arteries supplying blood to the heart are blocked, resulting in MI, oxygen and nutrient deprivation leads to ischemic injury and death of muscle cells in the infarct zone. **(Figure 1.1)** Since the mammalian heart cannot adequately regenerate after injury, progressive muscle atrophy (due to injury or death of cardiomyocytes) and the formation of noncontractile scar tissue result in cardiac cachexia [2]. Furthermore, intrinsic remodeling of the left ventricle (LV) following MI results in LV dilation, wall thinning, and sphericity. While allowing the heart to maintain cardiac output by increasing stroke volume, in the long-term, this remodeling leads to maladaptive changes in myocardial structure and function resulting in congestive heart failure (CHF) [3]. MI is a principle cause of CHF, with approximately 22% of men and 46% of women being disabled with CHF within six years of their first MI [1]. CHF affects 5 million Americans and 22 million people worldwide and is a leading cause of adult hospitalizations, resulting in an

estimated healthcare cost of \$29.6 billion in the United States in 2006 alone [1]. As such, medical interventions for MI and CHF are in dire need.

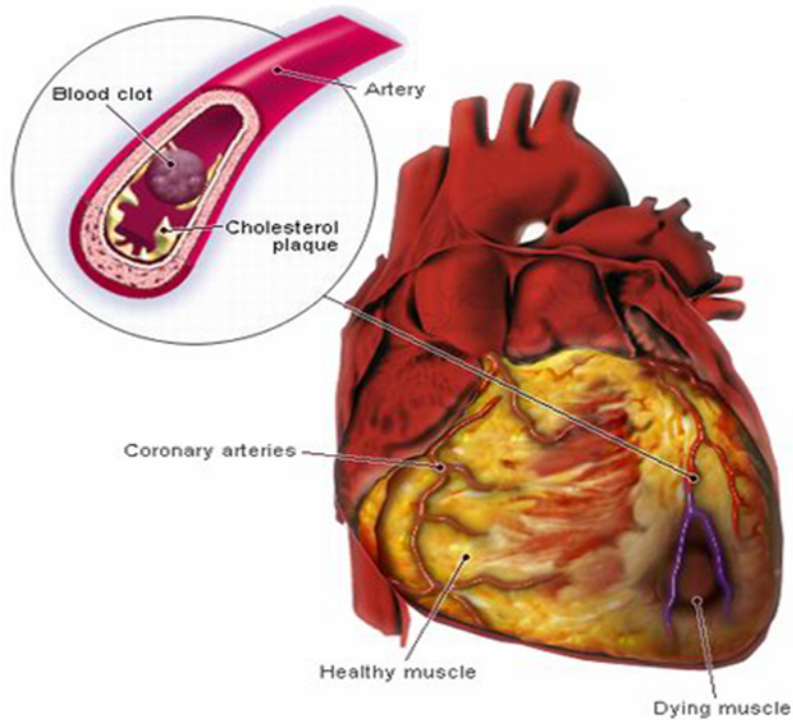


Figure 1.1: MI results when one or more of the coronary arteries supplying blood to the heart are blocked leading to ischemic injury and death of muscle cells in the infarct zone. (Image modified from www.medicinenet.com/peripheral_vascular_disease/article.htm)

The most effective treatment for CHF, to date, is heart transplantation; however, in the last 13 years, while the number of organ donors has tripled, the overall number of transplants has stayed constant and is limited to less than 3000 patients worldwide each year due to severe organ shortage. Furthermore, organ transplantation requires long-term immunosuppression in patients, resulting in substantial postoperative risk [4]. Thus, alternatives to heart transplantation are needed. Mechanical circulatory assist devices (i.e. left ventricular assist devices (LVADs)) provide a ‘bridge to transplant’ for many patients awaiting organ donation, but a substantial number of patients still die on the waiting list, while others are subject to the same immunosuppression regimens and subsequent perioperative risks as transplant patients [5].

Pharmaceutical strategies to antagonize LV remodeling (such as treatment with beta-blockers and angiotensin-converting enzyme (ACE) inhibitors) have proven limited in their ability to stem the progression from MI to CHF, and surgical interventions for advanced CHF have been limited to patients with severe dilation and dysfunction (as with the Dor and Batista procedures) or have resulted in complications arising from the intervention (e.g. foreign body encapsulation of the epicardium following epicardial restraint therapy) [3].

In light of these limitations, in recent years, tissue engineering approaches including cell transplantation and the use of bioactive biomaterials for myocardial repair and regeneration have come to be seen as promising alternatives to heart transplantation. The challenge for engineering myocardial tissue is multifaceted and complex. Cardiac muscle is compact and highly vascularized, containing a high density of metabolically active, well-differentiated cells in a complex 3-dimensional assembly of myocardial cells and collagen fibers in parallel. The metabolic demands require a high degree of vascularity. Cardiomyocytes contract synchronously with electrical stimulation, and myocardial fibers are therefore both electrically and mechanically anisotropic. For this reason, cells implanted into infarcted myocardium (through cell injection or the introduction of a cell-seeded scaffold) must not only survive and proliferate, but also become electrically coupled with the surrounding native myocardium and be able to withstand the mechanical loads imposed by contractile myocardium. To date, a number of cell sources and biomaterials have been investigated for this purpose with much debate as to the ideal combination.

1.2 CELL THERAPY FOR CARDIAC REPAIR AND REGENERATION

1.2.1 Cellular cardiomyoplasty

Cellular cardiomyoplasty (CCM), also known as cellular cardiomyogenesis, is the transplantation of cells into injured myocardium to restore blood flow and contractility to infarcted, scarred, or dysfunctional heart tissue, thereby reversing heart failure [6]. To this end, a number of cell types have been tested in the laboratory using experimental models of heart failure, and have led to multiple human clinical trials [7-13]. The choice of optimal cell type for CCM may depend on the type of injury and the clinical objective for the patient in question. However, at a fundamental level, any cell type used to repair and regenerate the myocardium must engraft and survive in the heart, differentiate into cardiomyocytes and vasculature, and integrate both mechanically and electrically with native cardiomyocytes.

1.2.2 Cardiomyocytes

While cardiomyocytes may seem the ideal and obvious cell type for CCM, there are a number of major limitations to their use. Any clinically-feasible cell type for CCM must be readily available. Since mammalian cardiomyocytes lose their proliferative abilities soon after birth, it is highly unlikely that these cells will be a viable off-the-shelf option. Furthermore, cardiomyocytes demand a high vascular supply for *in vivo* survival [6]. Such a blood supply is unlikely to be found or obtained in infarcted myocardium, thereby bringing the engraftment and survival of these cells into question.

1.2.3 Skeletal muscle precursor cells

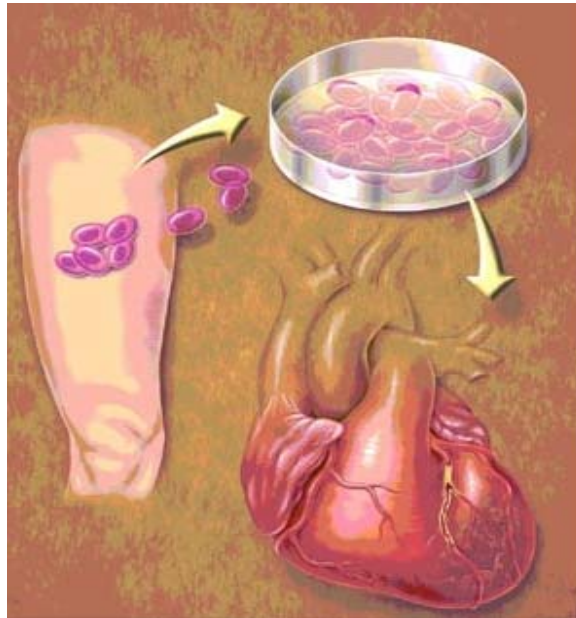


Figure 1.2: Skeletal muscle cells can be isolated from patients, expanded and/or modified *ex vivo*, and transplanted into infarcted myocardium for repair. (Image from www.med.umich.edu/opm/newspage/2002/musclecell.htm)

1.2.3.1 Skeletal myoblasts

Since heart muscle is a mesodermally-derived tissue, it follows that a mesodermal progenitor cell should possess the capability to differentiate to the cardiac lineage. To this end, researchers have investigated the use of skeletal myoblasts (skMBs), skeletal muscle precursor cells with the ability to expand and form new fibers following muscle injury, to repair infarcted myocardium.

(Figure 1.2) Successful engraftment of skMBs into infarcted myocardium resulting in improved LV function and attenuation of LV remodeling was first demonstrated in 1998 [14]. Since then, several clinical trials have demonstrated improved LV functional outcomes in patients treated with skMBs [15-17]. However, these cells have not, as yet, demonstrated definitive differentiation into cardiomyocytes, and the mechanism by which they improve LV function is

unknown [18]. While some research has suggested that transplanted skMBs undergo electrophysiological changes and down-regulate voltage-gated ion channels to integrate with surrounding myocardium, these cells remain electrically-isolated from host cells [19, 20]. Furthermore, the effective clinical use of skMBs is questioned by research pointing to poor survival rates and engraftment of cells in native tissue [21]. It has been demonstrated that only a small subpopulation of transplanted skMBs actually plays a role in muscle regeneration [22, 23], and research has led to the discovery of a stem cell population within skeletal muscle that has been shown to participate in this process [24-28].

1.2.3.2 Muscle-derived stem cells

In the last decade, researchers have identified a population of muscle-derived stem cells (MDSCs) within the skeletal muscle cell population [24-28]. These cells appear to be less committed to the myogenic lineage than myoblasts and possess the ability to differentiate towards multiple lineages *in vitro*, including the muscle, endothelial, and hematopoietic lineages [24, 28, 29]. When transplanted into muscle of dystrophic mice, MDSCs generated large grafts of muscle [28]. Additionally, when these cells were transplanted into ischemic myocardium in a mouse infarct model, they resulted in greater cell engraftment and increased neoangiogenesis compared to skMBs, prevented cardiac remodeling, and led to significant improvement in cardiac function [30, 31]. Further evaluation of these cells demonstrated their ability to secrete vascular endothelial growth factor (VEGF) in response to cyclic stretch and hypoxia *in vivo*. Furthermore, the ability to genetically engineer these cells to overexpress VEGF for *in vivo* myocardial repair, specifically for increased neoangiogenesis has been demonstrated [32, 33].

While skeletal muscle provides a promising autologous source of precursor cells for myocardial repair, numerous other populations of stem and progenitor cells for myocardial repair and regeneration have also been studied.

1.2.4 Stem and progenitor cells

1.2.4.1 Cardiac stem cells

For years, scientific convention dictated that the heart was incapable of self-renewal. In the past several years, however, a growing body of data have emerged supporting the notion that the heart is capable of regeneration and is not arrested in a post-mitotic state [34]. Several groups have identified multipotent, undifferentiated cells in postnatal myocardium and have shown that these cell populations express a number of stem cell markers [35-37], side population cell markers [38], and cardiac transcription factors [39, 40]. While these cells are present in adult myocardium, they obviously lack the ability to prevent scar formation and remodeling following MI. However, when isolated, expanded in culture, and injected into infarcted myocardium, it has been demonstrated that these cells can differentiate into cardiomyocytes, endothelial cells, and smooth muscle cells and facilitate functional repair [37, 40] while avoiding some of the safety concerns related to the clinical use of other stem cell populations [40].

1.2.4.2 Embryonic stem cells

The early years of the 21st Century have seen a flurry of activity with reports on the ability of rodent, murine, and human embryonic stem cells (ESCs) to differentiate to the cardiac phenotype. While ESCs have been known to form spontaneously beating patches in culture, the conditions for this differentiation are poorly defined. Furthermore, differentiation is inefficient (i.e. limited to a small percentage of cells in a given culture) and is relatively nonselective [41]. Methods resulting in more directed and efficient differentiation of these cells would clearly benefit cardiac repair efforts. It has been demonstrated that cardiogenols A-D induce cardiomyogenesis in murine ESC cultures, with cardiogenol C being the most potent in a recent report. ESCs treated with cardiogenols formed beating patches and expressed cardiac specific markers, genes, and transcription factors [41]. The downregulation of protein kinase- β (PKC- β) and PKC- ζ as well as the upregulation of PKC- ϵ (a major set of signal transduction components implicated in certain heart diseases in humans and mice) have also been implicated in the *in vitro* differentiation of ESCs to cardiomyocytes [42]. Furthermore, ESCs maintained in serum free medium have been shown to effectively differentiate to cardiomyocytes with the addition of insulin, transferrin, and platelet derived growth factor-BB (PDGF-BB) to the culture medium [43]. However, despite their ability to differentiate into cardiomyocytes, the clinical use of ESCs is currently limited by the ethical debate surrounding them and their potential for *in vivo* tumor formation.

1.2.4.3 Bone marrow-derived mesenchymal stem cells

The bone marrow contains a population of multipotent CD34⁺ CD45⁻ stem cells known as mesenchymal stem cells (MSCs) or stromal cells. These cells have the ability to differentiate to a number of mesenchymal lineages *in vitro* and *in vivo*, including bone, fat, cartilage, and skeletal muscle [44], and in some instances cardiomyocytes [45]. Murine and rodent MSCs, when treated with 5-azacytidine, developed spontaneously beating patches and stained positively for markers of cardiac differentiation [46-48]. Human MSCs have been shown to differentiate to cardiac-like cells, expressing contractile and myofibrillar proteins, when cultured in defined medium containing dexamethasone, insulin, and ascorbic acid [49]. Human MSCs cultured in cardiomyocyte-conditioned media or co-cultured with human cardiomyocytes also differentiated to a cardiac phenotype and expressed cardiac markers [50]. It should be noted that the aforementioned results are still a topic of debate, with some investigators claiming that differentiation with 5-azacytidine treatment is not reproducible [51]. Additionally, 5-azacytidine and co-culture treatments are not currently perceived to be clinically applicable due to their overall inefficiency and possible harmful side effects [50]. However, *in vivo*, it has been demonstrated that MSCs can engraft in high numbers in infarcted heart and that they lend functional benefits including neovascularization [52] and improved regional contractility and global diastolic function [53]. Furthermore, research suggests that MSCs are immunoprivileged, [54] allowing for allogeneic, off-the-shelf delivery of these cells without *in vitro* manipulation prior to implantation.

1.2.4.4 Bone marrow-derived hematopoietic stem cells

Also found in the bone marrow is a population of CD34⁺, lineage negative (Lin⁻), AC133⁺, sca-1⁺ cells (human markers) known as hematopoietic stem cells (HSCs). These blood-forming cells differentiate into a number of cell types *in vitro* and *in vivo*, including all blood cell types and lymphoid lineages. These cells have also been shown to differentiate to smooth muscle cells, endothelial cells, and cardiomyocytes [55]. However, there is no conclusive evidence that, when injected into infarcted myocardium, HSCs differentiate into cardiomyocytes or restore function [56, 57].

1.2.4.5 Endothelial progenitor cells

Endothelial progenitor cells (EPCs) are also found in the bone marrow and home to the site of injury to repair damaged endothelium and promote neoangiogenesis. These cells can be separated from peripheral blood cells using vascular endothelial growth factor receptor-2 (VEGFR-2), CD34, and CD133 antigens for identification. Following myocardial infarction, EPCs have been shown to mobilize to the site of injury [58] and improve LV dimension and regional wall motion [59]. These cells have not, however, been shown to give rise to cardiomyocytes *in vivo* [60].

1.2.4.6 Umbilical cord blood cells

Obtained from human umbilical cord blood, this progenitor cell population is CD13⁺, CD34⁺, CD44⁺, and human leukocyte antigen-1⁺ (HLA-1⁺). Cord blood cells (UCBs), which contain mesenchymal and hematopoietic cell populations, have the potential to differentiate into a number of lineages *in vitro* and *in vivo*. These cells are highly attractive for cell therapy applications as they do not pose the ethical dilemma raised by the use of ESCs and are less immunogenic than MSCs, thereby providing an off-the-shelf option for cell therapy. Previous reports have reported that UCBs improve LV function, attenuate remodeling, and decrease infarct size when injected into infarcted myocardium [61]. UCBs have also been shown to induce neoangiogenesis *in vivo* [62]. However, no evidence exists demonstrating the ability of UCBs to differentiate into cardiomyocytes [62, 63]. Recently, reports have emerged that the injection of UCBs into a porcine myocardial infarct failed to improve LV function and that the treatment resulted in more extensive infarcts with greater inflammatory cell infiltration and calcifications [64]. These conflicting results suggest that more research is necessary before UCBs can be considered a viable option for cardiac cell therapy.

1.2.5 Gene therapy and cell transplantation

Irrespective of the ideal cell source for cardiac regeneration, ischemic myocardium is a difficult milieu for cell engraftment and survival due to lack of oxygen and nutrients, dysfunctional mechanical forces, and altered biochemical environments [65]. As such, research has emerged focusing on the use of cells as carriers for genes implicated in angiogenesis and myogenesis,

thereby increasing the efficiency of CCM with gene therapy. Genetically modified cells transplanted into ischemic myocardium provide for the localized and sustained delivery of therapeutic proteins at the site of cell administration. A variety of cell types including smooth muscle cells, skeletal muscle cells, cardiac cells, and mesenchymal stem cells have been investigated as carriers of exogenous genes [66]. Cells have thus far been modified to overexpress VEGF, VEGF165, hepatocyte growth factor (HGF), and myogenic determination gene MyoD for pre-clinical studies for myocardial repair following MI. Preliminary results from these studies show increased commitment of cells to the myogenic lineage, increased cell engraftment, and increased angiogenesis in the ischemic region [32, 67-75]. Studies evaluating numerous other angiogenic and myogenic genes including other VEGF isoforms, PDGF, and transforming growth factor- β 1 (TGF- β 1) have been suggested for increasing the efficiency of cell therapy but have yet to be thoroughly investigated [66].

1.3 BIOMATERIALS FOR CARDIAC REPAIR AND REGENERATION

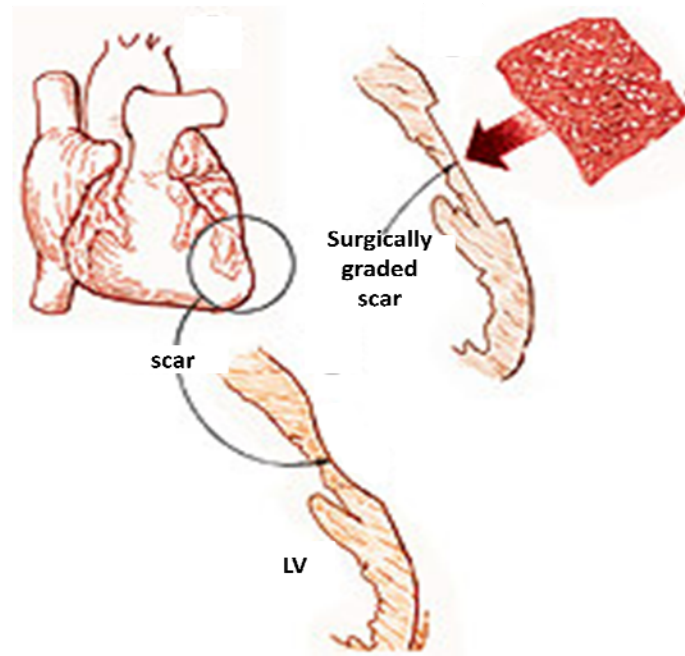


Figure 1.3: A biomaterial can be placed over infarcted myocardium in order to repair it by providing mechanical support or by delivering cells and/or biomolecules (Image modified from www.mirm.pitt.edu/news/article.asp?qEmpID=46)

While cell transplantation has shown promise in myocardial regeneration, the localized delivery of cells alone for regeneration and repair is limited by the ability of transplanted cells to remain in the area of injury at the proper concentrations and for the necessary time period [76, 77]. For this reason, researchers have focused on combining cells with a biomaterial scaffold for successful tissue repair and regeneration. **(Figure 1.3)** Upon implantation, biomaterials initially function as an artificial extracellular matrix (ECM) providing mechanical and biological support similar to that provided by native ECM [78]. Biomaterials provide cells with a surface for adhesion and with mechanical support against *in vivo* stresses at the site of repair until the cells can deposit new ECM and take over the process of regeneration. Furthermore, the biomaterial scaffold may act to retain the delivered cells in the defined 3-dimensional space to which they

were administered, thereby guiding new tissue growth at the site of injury [77, 79, 80]. Over the years, the field of tissue engineering has utilized a variety of biomaterials for tissue repair and regeneration. These polymers range from naturally derived materials and acellular tissue matrices to synthetic polymers. It should be noted that much of the following review of natural and synthetic biomaterials for myocardial regeneration was published in *An Introduction to Biomaterials* and is reproduced with permission from CRC Press [81]. (Copyright 2006 from *An Introduction to Biomaterials* by Priya Ramaswami and William R. Wagner. Reproduced by permission of Taylor and Francis Group, LLC, a division of Informa plc.)

1.3.1 Natural biomaterials

Several natural materials have been used as scaffolds for myocardial tissue repair. Commercially available collagen sponges composed of type I bovine collagen seeded with rat neonatal cardiomyocytes have been shown to support spontaneous contraction of cells as well as homogeneous cell distribution. Electrical stimulation, stretching, and stimulation with Ca^{2+} , epinephrine, or adrenaline of these constructs resulted in increased force development with physiological beating patterns [82-84]. Collagen sponges seeded with rat ventricular myocytes were also induced to contract via application of a pulsatile electric field, resulting in enhanced contractile and conductive properties of cells within the scaffold, increased expression of cardiac-specific proteins, and differentiation comparable to that of native myocardium [85].

Engineered Heart Tissue has also been formed from a liquid cell-matrix mixture composed of collagen type I, ECM proteins and rat heart cells. Spontaneously and synchronously beating Engineered Heart Tissue displayed morphological and functional

characteristics of differentiated heart muscle. These constructs could be made in a variety of shapes and sizes for potential *in vivo* use [86]. Furthermore, alginate scaffolds have been used to culture high-density cardiomyocyte populations with a uniform distribution. Contractile cell clusters were also found within these three-dimensional alginate constructs [87].

A novel approach to the formation of three-dimensional cardiac grafts has been developed in Japan without the use of a scaffold. The temperature-responsive polymer poly(N-isopropylacrylamide) was grafted onto tissue culture polystyrene. This slightly hydrophobic surface changed reversibly to become hydrophilic when temperature was reduced from 37°C to 32°C. Cultured cells detached spontaneously from the surface while maintaining cell-cell connections. Cardiomyocytes cultured on such a surface could detach as cell sheets with intact electrical connections. Layering of these cardiomyocyte cell sheets allowed for the formation of three-dimensional cardiac constructs for use in myocardial tissue regeneration. It has been demonstrated that layered sheets formed electrical connections between the sheets and beat synchronously in culture. The application of mechanical loads to strengthen tissue and inclusion of growth factors to stimulate vascularization allowed for the formation of three-dimensional, electrically coupled cardiac tissues without the need for a scaffold [88-90].

While naturally derived materials and acellular tissue matrices can be recognized by the body, variation can occur in these materials leading to poor reproducibility of results both *in vitro* and *in vivo*. Oftentimes, naturally derived scaffolds also exhibit poor mechanical properties [80, 91]. Furthermore, high purification of these substrates is necessary prior to clinical use in humans to avoid contamination with animal byproducts. As such, a number of synthetic polymers have emerged for use as a tissue engineered myocardial patch.

1.3.2 Synthetic biomaterials

Although synthetic biomaterials are not recognized by the body, they are reproducible and produce few batch-to-batch variations. These materials can also be modified to enhance specific biologic interactions [77, 79, 80]. In addition, synthetic biomaterials provide a number of parameters that can be adjusted for optimal mechanical, chemical, and biological properties for a given application. Design criteria for these materials include: adequate mechanical strength, controllable biodegradation rates, lack of toxic degradation products, integration into surrounding tissue without extensive inflammatory response or support of infection, adequate support of cell proliferation, differentiation, & maturation, and the potential to deliver biological molecules.

Patches used for ventricular or myocardial structural repair have consisted of synthetic materials such as Dacron (polyethylene terephthalate (PET)), expanded poly(tetrafluoroethylene) ePTFE, and polyglycolic acid (PGA). Dacron and ePTFE, however, are not biodegradable and lack the ability to grow with the patient. All three of the aforementioned materials can also be too stiff to comply with the contractions of the myocardial environment [92]. These materials have been used for the repair of cardiovascular defects including congenital heart disorders. However, patches for myocardial repair need not only be biocompatible and mechanically robust, but also resorbable at a rate similar to the intrinsic remodeling and repair process [92].

Consisting of a copolymer sponge of ϵ -caprolactone-co-L-lactide reinforced with poly-L-lactide fabric, PCLA patches exhibit a unique biodegradation; the spongy component is resorbed within two months, whereas the fibrous portion persists for one to two years [93]. Acellular PCLA patches, due to their spongy structure, have been shown to foster cell adhesion and infiltration into the matrix more so than PGA matrices when implanted into rat heart [92]. PCLA

patches seeded with vascular smooth muscle cells prior to implantation in rat hearts result in elastic tissue formation and reduced abnormal chamber distensibility when compared to unseeded grafts eight weeks post-implantation [94]. Furthermore, smooth muscle cell-seeded PCLA patches did not show evidence of dilation or produce a significant inflammatory response *in vivo* [93].

Electrospinning is a process that produces fibers with diameters in the submicron range that are in the form of a nonwoven mesh, resembling ECM topography. Neonatal rat cardiomyocytes have been successfully cultured on electrospun polycaprolactone (PCL) meshes extended over a wire ring acting as a passive load. Due to the high porosity of the scaffold, cells were able to be maintained throughout its thickness. Cells spontaneously contracted after three days in culture and expressed cardiac specific proteins on this synthetic scaffold [95]. Our group has successfully electrospun a biodegradable, elastomeric poly(ester urethane)urea (PEUU) with submicron morphology resembling that of native ECM. Furthermore, we have demonstrated successful microintegration of vascular smooth muscle cells (SMCs) into an electrospun PEUU mesh to fabricate an elastomeric tissue construct with high cell density that could be used in a number of cardiovascular tissue engineering applications [96, 97].

Amorphous, elastomeric biomaterials made of poly(trimethylene carbonate) and D,L-lactide (TMC-DLLA) have also been evaluated as three-dimensional scaffolds for myocardial tissue engineering, as have elastomeric, segmented polyurethanes (SPUs). Rat cardiomyocytes have been shown to attach and proliferate well on TMC-DLLA scaffolds *in vitro*, and these scaffolds exhibit high strength at physiological conditions and biodegradation rates of up to three years *in vitro* and *in vivo* [98]. Rat neonatal cardiomyocytes cultured on biodegradable, SPU elastomers patterned with lanes of laminin responded to these spatial constraints by forming

elongated, rod-shaped cells aligned parallel to the lanes. Patterned cardiomyocytes displayed a striking resemblance to intercalated disks. Furthermore, synchronously beating layers of patterned cardiomyocytes served as a suitable substrate for subsequent cardiomyocyte layers in order to build a 3-dimensional, organized sheet of cardiomyocytes [99]. Similar cell patterning was achieved on biodegradable PLGA [100]. This patterning provides an increased ability to govern the morphology and architecture of cultured cardiomyocytes. It is important to note, however, that while neonatal rat cardiomyocytes have a known capacity to spontaneously beat *in vitro*, this has not been successfully demonstrated for cardiomyocytes that might be harvested from an adult population.

Recently, our group has demonstrated the successful application of a biodegradable, elastomeric PEUU scaffold, fabricated by a thermally induced phase separation method, as a cardiac patch in a rat subacute infarct model. Eight weeks post-patch implantation, most of the material had been resorbed, and LV wall thickness was restored compared to the non-patched group. Smooth muscle bundles with contractile phenotype were seen under the PEUU patch. Such bundles were not apparent in infarcted myocardium that did not receive a patch. Furthermore, application of the cardiac patch stemmed LV dilation and improved contractile function compared to non-patched controls [3].

1.3.3 Biomaterials for growth factor delivery

Recent advances in biomaterials-related tissue engineering have included attempts to direct cell proliferation and differentiation and induce neoangiogenesis via the biomaterial itself. Bioactive, biodegradable scaffolds have been produced from a number of natural and synthetic materials

incorporating a variety of growth factors, cytokines, and proteins. The effects of these bioactive matrices on stem, progenitor, and terminally differentiated cells, both *in vitro* and *in vivo*, have been studied [76, 77, 101-113]. The combined use of an optimal cell source, scaffold for cell delivery and physical support, and biological signals may be a common pathway toward a viable tissue engineered construct for cardiovascular repair and regeneration (**Figure 1.4**).

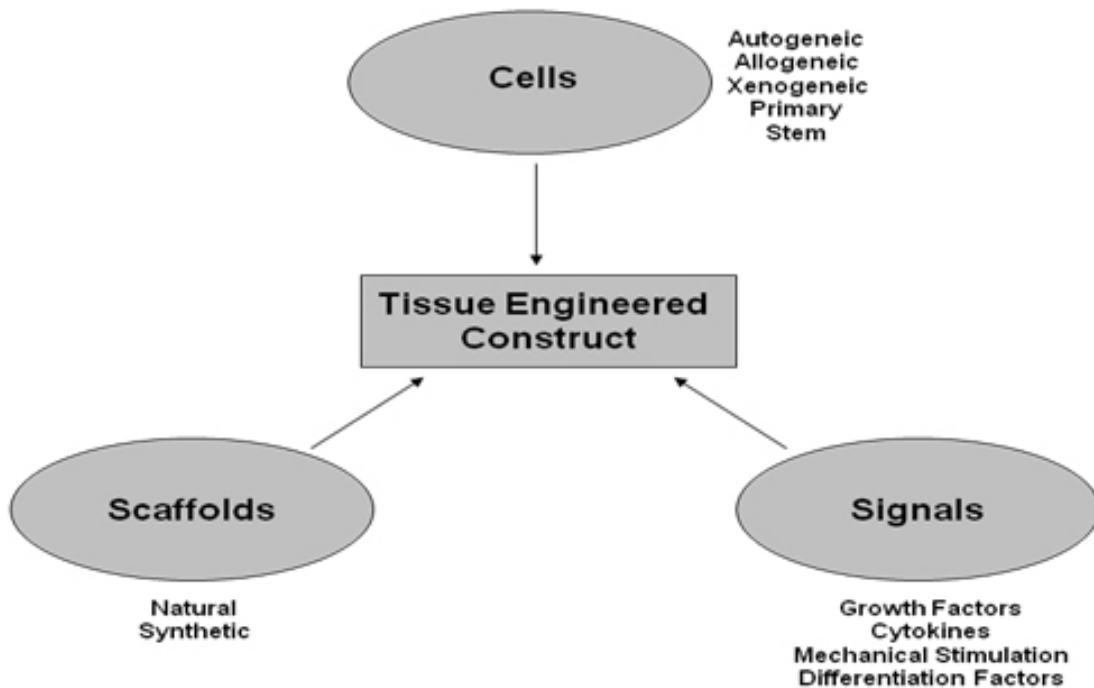


Figure 1.4: The building blocks of tissue-engineered constructs [81].

For myocardial regeneration, much research has focused on the sustained and controlled release of angiogenic factors within ischemic myocardium. When implanted into ischemic myocardium in patients undergoing coronary bypass surgery, alginate microspheres containing fibroblast growth factor-2 (FGF-2) resulted in increased perfusion and no adverse effects [114]. Gelatin microspheres loaded with basic fibroblast growth factor (bFGF) implanted into rat myocardium following MI induced therapeutic levels of angiogenesis [115]. Furthermore,

implantation of bFGF-loaded gelatin microspheres prior to cardiomyocyte cell transplantation resulted in prevascularization of the region, thereby improving the biological function of the transplanted cells and subsequent cardiac function in a rat MI model [116]. Hydrogels loaded with VEGF have also shown promise in promoting angiogenesis and improving cardiac function when implanted into ischemic myocardium [117].

Since successful angiogenesis requires cell recruitment and vessel maturation, researchers have used biomaterial scaffolds for multiple growth factor delivery to enhance blood vessel formation. While administration of FGF-2 or HGF alone did not yield increased blood flow in a murine model of hindlimb ischemia, the administration of collagen microspheres containing both growth factors resulted in increased blood flow, vessel formation, and vessel maturity [118]. Similarly, crosslinked hyaluronan hydrogels loaded with VEGF and keratinocyte growth factor or VEGF and angiopoietin-1 (Ang-1) led to increased vessel formation compared to either factor alone or the administration of soluble forms of both factors (i.e. via direct injection) in the ear pinnae of mice [119, 120]. While the aforementioned models of dual growth factor delivery for angiogenesis are not specific to an MI model, these studies prove promising for improved vascularization of ischemic myocardium.

HGF is not only known to be a potent angiogenic factor, but is also known for its anti-apoptotic and motogenic functions in cells [121-123]. HGF has been implicated in stem cell recruitment to ischemic myocardium and in the differentiation of stem cells to the cardiac lineage [124]. Local overexpression of adenovirus-encoded HGF in ischemic myocardium had anti-apoptotic effects on cardiomyocytes and induced angiogenesis [125], while implantation of MSCs overexpressing HGF into ischemic myocardium improved function, decreased scar size, and increased capillary number [68]. As such, research has emerged focusing on the sustained,

local delivery of HGF to ischemic myocardium. Following MI in a rat heart, the application of a gelatin sheet containing HGF over infarcts injected with skeletal muscle cells resulted in increased angiogenesis, decreased fibrotic area, and attenuation of LV dilation compared to controls [126]. Application of a polymer saturated with HGF to the infarcted anterior wall following MI in a rat model resulted in decreased scar size, decreased LV dimension, increased ejection fraction, and increased contractility [127]. These preliminary results suggest that a polymeric delivery system for HGF may prove successful in myocardial repair and regeneration.

Recently, insulin-like growth factor-1 (IGF-1) has been implicated in skeletal muscle regeneration as well as in cardiomyocyte survival post-MI [2, 128, 129]. IGF-1 has been shown to aid in muscle regeneration through the recruitment of MSCs to the site of injury [129]. Additionally, local overexpression of IGF-1 in ischemic myocardium protects against cardiomyocyte apoptosis and LV dilation and promotes engraftment, differentiation, and functional improvement when cells are transplanted into myocardium [130-134]. Subsequently, as with HGF, some research has emerged focusing on the sustained, local delivery of IGF-1 to ischemic myocardium via biomaterial scaffolds. To this end, biotinylated self-assembling peptide nanofibers have been used to deliver IGF-1 to ischemic myocardium, and in combination with cell therapy. Results suggest decreased apoptosis, increased cell growth, and improved systolic function [135]. IGF-1 has also been successfully incorporated into a number of biomaterials for enhanced bone regeneration [136-140]. These studies suggest that sustained, controlled delivery of IGF-1 may prove useful in a number of tissue engineering applications, including those in the cardiovascular arena.

1.3.4 Biomaterials for gene therapy

As discussed in section 1.2.5, gene therapy to augment cell transplantation is a viable option for tissue engineering. However, exogenous gene therapy approaches are limited by survival of transplanted cells as well as control over the amount of protein secreted by transfected cells [141]. Gene therapy approaches involving the injection of naked DNA into tissues have shown some promise, but are limited by toxicity concerns, degradation of DNA, low transfection efficiencies *in vivo*, and nonspecific targeting of cells [141-144]. Cardiomyocytes in particular have been shown to have very low transfection efficiencies [141]. Alternatively, viral delivery of genes has been investigated; however, their clinical application is limited due to concerns surrounding the use of viral vectors [141].

In lieu of growth factor presentation via a tissue-engineered construct, the use of polymers for non-viral gene delivery has been demonstrated. Biomaterials provide a means to quantitatively deliver DNA to target cell populations in a spatiotemporally-regulated manner. In addition to augmenting transfection efficiency, the use of biomaterial scaffolds may also enhance cell survival and prolong plasmid activity *in vivo* by protecting against DNA degradation [143]. Naturally-derived polymers such as collagen, and its derivatives, and fibrin have been used for this purpose [143]. Synthetic polymers such as poly(ethylene imine) (PEI) [143, 145] and copolymers of PEI with poly(ethylene glycol) (PEG) and poly(N-isopropylacrylamide) (PNIPAm) [146, 147] have also been used as delivery vehicles for plasmid DNA.

Cationized gelatin microspheres containing plasmid DNA enhanced the level as well as the time period of expression *in vivo* when compared to plasmid DNA administration in solution [148]. Furthermore, gelatin microspheres containing plasmid DNA for FGF-4 enhanced angiogenesis in ischemic rabbit hindlimb at concentrations significantly lower than free plasmid

delivery alone, thereby demonstrating increased transfection efficacy. Additionally, plasmid degradation was slower when plasmid was incorporated into the polymer, suggesting a protective effect of the material on plasmid DNA [149]. While plasmid delivery to myocardium has not been extensively studied to date, fibrin glue containing plasmid DNA for pleiotropin (an angiogenic gene) induced enhanced angiogenesis when injected into ischemic rat myocardium compared to fibrin glue or DNA injection alone [150].

Finally, “on-demand” systems to regulate activity of a selected gene have proven effective in the control of gene expression in cells. These systems rely on the use of a small molecule capable of modulating binding of transcriptional factors to specific promoters, thereby driving gene expression [151]. The tetracycline-controlled gene expression system was first introduced in 1992 [152], and the use of these molecular switches to regulate transcription has become popular in controlling mammalian gene expression [153, 154]. The two basic variants of this system are the rtTA “tet-on”- [154] and the more popularly used tTA “tet-off” systems [151]. The “tet-off” system uses control elements of the tetracycline-resistance operon from the Tn10 strain of *E. coli*, a tetracycline-resistant strain. Transcription of tetracycline-mediated genes is negatively regulated by the tetracycline-dependent repressor, tetR. Tetracycline-controlled transcriptional regulator (tTA) is generated by fusing the DNA-binding domain of tetR with the transcription activation domain of virion protein 16 (VP16) of herpes simplex virus. Minimal promoters fused to the tetracycline operator (tetO) are stimulated by tTA, and tTA must be constitutively expressed in target cells for this system to work. In the absence of tetracycline, tTA binds to tetO, activates the promoter, and initiates transcription and target gene expression. When tetracycline is present, tTA changes conformation and dissociates from tetO, resulting in termination of transcription and expression of the target gene [151]. **(Figure 1.5)**

While tetracycline-controlled systems are widely used, these switches can be leaky, resulting in undesirable background expression of the target gene [151, 154].

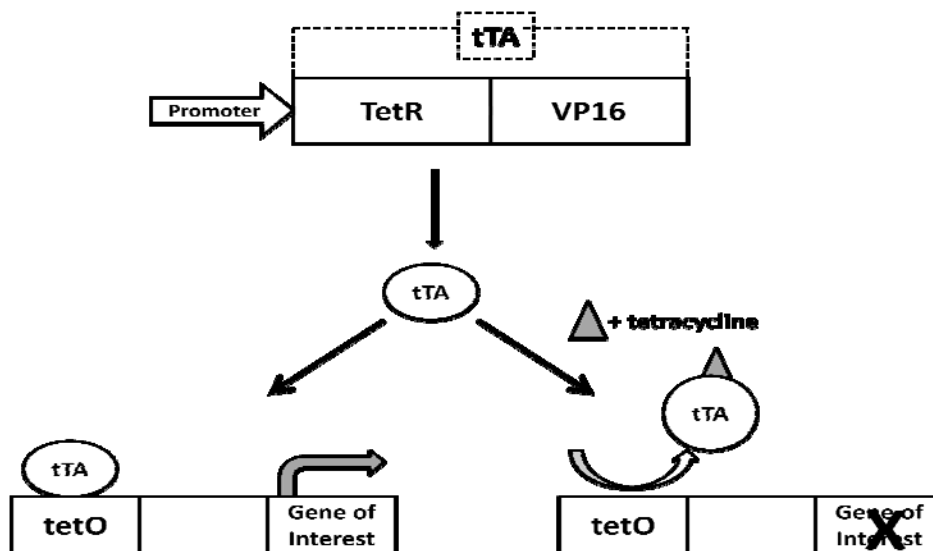


Figure 1.5: “Tet-off”-regulated gene expression system.

Recently, inducer molecules capable of regulating the timing and level of gene expression in specific areas of the body have proven effective in managing therapeutic gene expression. Intrexon Corporation’s RheoSwitch™ inducible gene expression technology system controls gene expression in this manner. This system was first introduced in 2003 and utilizes a modified version of the ecdysone receptor (EcR) and retinoid X receptor (RXR) responsive system that mimics the action of steroidal insect hormone 20-hydroxyecdysone found in *Drosophila melanogaster* [155]. The RheoSwitch system uses hybrid EcR and RXR proteins to regulate gene expression via GAL4 response elements. The transcription factor RheoReceptor-1 is comprised of the ligand-binding domain on EcR fused to the DNA-binding domain of yeast GAL4, and the transcription factor RheoActivator is comprised of the ligand-binding domain of RXR fused to the activation domain of VP16. A synthetic, non-steroidal analog of 20-hydroxyecdysone, RheoSwitch Ligand 1 (RSL1) [N-(2-ethyl-3-methoxybenzoyl)-N’-(3,5-

dimethylbenzoyl)-N'-tert-butylhydrazine] (MW = 382.5), serves as the inducer molecule for this switch. **(Figure 1.6)** The inducer binds tightly and selectively to the chimeric bipartite nuclear

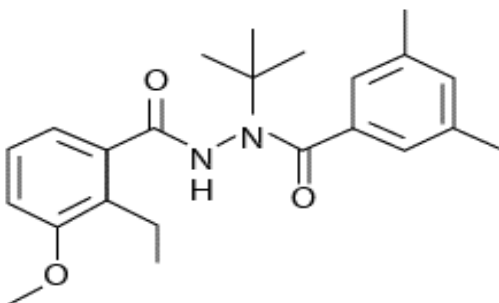


Figure 1.6: RheoSwitch Ligand 1 (RSL1).

receptor (composed of RheoReceptor-1 and RheoActivator), thereby changing the conformation of the receptor protein and activating it so that it releases bound negative regulatory cofactors, resulting in a highly induced transcriptional state. The level of gene expression can be controlled by adjusting the concentration of inducer ligand present in culture medium, and gene expression is repressed in the absence of the inducer [155]. **(Figure 1.7)** This gene-regulating system is commercially available (New England BioLabs, Inc). Furthermore, the synthetic ligand RSL1 shows complete absence of side activity in mammalian cells, and background is virtually nonexistent [151] making this system a superior and attractive choice compared to others.

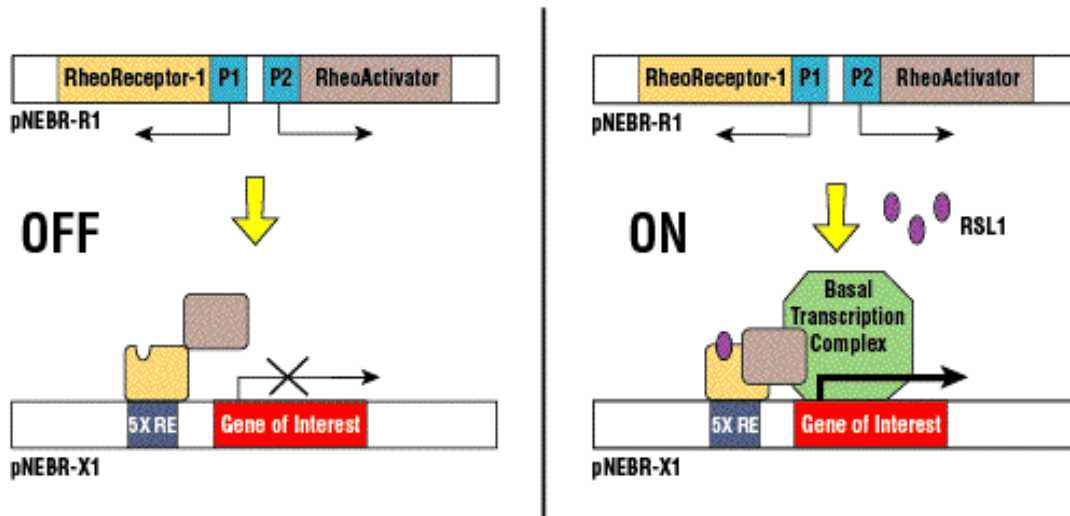


Figure 1.7: Transcriptional control using the RheoSwitch system. (Image from www.neb.com/nebecomm/products/productE3000.asp)

Limitations to the use of these “on-demand” systems include high levels of background expression, the efficiency of gene delivery, and the spatiotemporal control of gene expression [153]. As such, the combination of biomaterial scaffolds and these gene-inducing systems may prove effective in regulating gene expression within a tissue-engineered construct in a spatially- and temporally- defined manner.

1.4 OBJECTIVES

The overarching goal of this research was to develop polymeric controlled release systems for use in cardiovascular regenerative medicine applications. This research effort can be separated into two major components. The first component was to develop a cardiac patch from a biodegradable elastomer capable of delivering growth factors in a sustained and controlled manner to ischemic myocardium for post-MI myocardial repair. The second component was to

develop a biomaterial scaffold throughout which gene expression could be regulated in a spatially-defined manner for successful tissue construct development.

1.4.1 Objective #1: Biodegradable PEUU as a controlled release system

Insulin-like growth factor-1 and hepatocyte growth factor have both been implicated in the intrinsic response of the heart to myocardial infarction [134, 156-158]. Given the inability of the heart to mend itself, it has been postulated that exogenous administration of one or both of these growth factors may enhance myocardial repair and regeneration. While direct injections of soluble IGF-1 or HGF have demonstrated some beneficial effect in ischemic myocardium [159], given the short half-lives of these molecules and their high clearance rates *in vivo*, we hypothesized that a polymeric system capable of delivering IGF-1 or HGF in a sustained and controlled manner over several weeks *in vivo* may prove more effective in myocardial repair and regeneration than administration of soluble factor alone. To this end, we assessed the incorporation of IGF-1 or HGF into a biodegradable PEUU by quantifying the release of growth factor over a predetermined time period *in vitro*. In addition, we verified the bioactivity of released growth factor using *in vitro* cell assays.

Regulation of gene expression via a biomaterial scaffold may alleviate some of the problems associated with gene therapy, such as transfection efficiency, cell survival, and spatiotemporal control of gene expression [141-144]. In addition, we hypothesized that the spatiotemporal control of gene expression within a tissue engineered construct may allow for the development of complex tissues and organs consisting of several cell types. To this end, we assessed the incorporation of a gene-inducer molecule, the synthetic ligand RSL1, into a

biodegradable PEUU by quantifying the release of ligand over a predetermined time period *in vitro*. In addition, we verified the bioactivity of released ligand using an *in vitro* cell assay for gene expression.

1.4.2 Objective #2: A cardiac patch for post-MI myocardial repair

We have previously demonstrated that the application of a biodegradable PEUU patch to ischemic myocardium in a rat subacute infarct model increased LV wall thickness, stemmed LV dilation, and restored some contractile function to the ventricle [3]. For this objective, we hypothesized that a biodegradable PEUU capable of sustained, local delivery of IGF-1 or HGF to ischemic myocardium in a rat subacute infarct model would further improve LV dimension and function due to the therapeutic involvement of IGF-1 and HGF in myogenic and cardiac commitment and repair.

PEUU scaffolds without growth factor or scaffolds containing either IGF-1 or HGF were fabricated by a thermally induced phase separation method. In this objective, we assessed these patches by applying them onto the hearts of rats injured by myocardial infarction. At predetermined time-points post-patch implantation, improvement in LV function was evaluated using echocardiography. Eight weeks post-patch implantation, the animals were sacrificed, the hearts were explanted, and each heart was histologically assessed for restoration of LV wall thickness, muscle mass, and angiogenesis.

1.4.3 Objective #3: Spatial control of gene expression via a polymer scaffold

While tissue engineering aims to repair or regenerate a tissue or organ, researchers often simplify the process by overlooking the inherent complexity associated with a tissue type. Multiple cell types must perform specific functions in synchrony to form a functional tissue or organ structure. Embryogenesis demonstrates the commitment of cells to multiple cell fates in a well-regulated spatial and temporal manner. Growth factor gradients and spatial patterning of gene expression direct cell commitment, wound repair, and vascularization of tissues [104, 160-164]. As such, tissue engineered constructs would ideally provide a dynamic environment for the direction of cell fate in a spatially- and temporally-defined manner in order to accurately mimic natural tissue development.

In this objective, we evaluated the ability of a biodegradable PEUU to deliver inducer molecules to spatially control gene expression throughout a tissue engineered construct. We hypothesized that such a construct would demonstrate the ability to drive sub-populations of precursor cells on a scaffold towards one lineage and others down different pathways in a spatially-defined manner. Polymer films from solvent casting and porous scaffolds from a thermally induced phase separation process were fabricated with and without inducer molecule, as were films and scaffolds with spatially-defined regions containing or omitting inducer molecules. Cells cultured on films and within scaffolds were evaluated for control of gene expression by the polymer, and specifically, for spatial control of gene expression.

2.0 CONTROLLED RELEASE POLYURETHANE SCAFFOLDS FOR SOFT TISSUE ENGINEERING

2.1 INTRODUCTION

Polyurethanes for biomedical applications were first introduced in the 1960s [81]. While their toughness and durability made polyurethanes an attractive choice for application in medical devices, their susceptibility to chemical attack *in vivo* raised concerns about their biostability and safety [165, 166]. Attack by activated macrophages was postulated to lead to formation of toxic degradation products, thereby raising concerns about the safety of polyurethanes for *in vivo* application [165]. Since then, many groups have worked to develop polyurethane elastomers with improved biostability for medical application.

High molecular weight polyurethane elastomers are commonly synthesized by a two-step reaction. In the first step, reaction of a diisocyanate with a long-chain polyester or polyether diol produces a prepolymer with isocyanate functionality. Chain extension by addition of a short-chain diamine or diol in the second step results in the formation of a high molecular weight, segmented polyurethane elastomer, in which the hard segment is comprised of the diisocyanate and the chain extender and the long-chain polyester or polyether comprises the soft segment. Microphase separations between these hard and soft segments lend polyurethanes their attractive mechanical properties [165]. The ability to vary the hard and soft segments of polyurethanes

through the choice of specific diisocyanate, polyol, and chain extender as well as the ability to tailor-make prepolymer intermediates with targeted properties by varying diisocyanate:diol ratio offers great control over the structure and mechanical properties of biodegradable polyurethane elastomers [165]. Diisocyanates commonly used to synthesize biodegradable polyurethanes include: 1,6-diisocyanatohexane (HDI), 1,4-diisocyanatobutane (BDI), lysine methyl ester diisocyanate (LDI), 2,4-toluene diisocyanate (TDI), and 4,4'-diphenylmethane diisocyanate (MDI). Commonly used polyols include: poly(ethylene oxide) (PEO), poly(propylene oxide), poly(ϵ -caprolactone) (PCL), poly(D,L-lactide), and poly(glycolide).

Biodegradable, biocompatible polyurethanes are designed to undergo hydrolytic or enzymatic degradation *in vivo* and to subsequently form nontoxic degradation products. The overall degradation rate of polyurethane elastomers depends on hard and soft segment chemistries. Polyurethane elastomers with degradable hard segments have been synthesized through the incorporation of an enzymatically labile chain extender [167, 168]. Synthesis of polyurethanes with aliphatic diisocyanates facilitates degradation and results in nontoxic degradation products; LDI decomposes to ethanol and L-lysine, while BDI decomposes to putrescine. By contrast, degradation of aromatic diisocyanates, such as TDI and MDI, produces potentially carcinogenic aromatic diamines [166]. As such, the move to biocompatible, biodegradable polyurethanes has led to the use of aliphatic diisocyanates in lieu of aromatic diisocyanates.

In addition to ensuring the absence of toxic degradation products, researchers have focused on matching the mechanical properties of biodegradable elastomeric polyurethanes to those of the target tissue for repair and regeneration. The adverse consequences of tissue-biomaterial mechanical mismatch have been well documented, especially in vascular graft

applications in cardiovascular regenerative medicine [81]. Many of the traditional polyurethanes used in biomedical applications have been stiff with little or no elastomeric properties, rendering these polymers a poor choice for soft tissue engineering applications.

As such, our group has developed a biodegradable, elastomeric polyurethane, a poly(ester urethane)urea, synthesized from polycaprolactone and 1,4-diisocyanatobutane using putrescine as the chain extender [169]. **(Figure 2.1)** This PEUU has mechanical properties that are attractive for soft tissue engineering applications, such as with blood vessels or myocardium, and is amenable to mechanical conditioning regimens that may be desirable during tissue development [169, 170]. This PEUU has been shown to degrade at a potentially clinically relevant rate *in vitro* [169] and *in vivo* [171] and with no adverse effects on cell viability [169-171]. The thermally induced phase separation method used to fabricate constructs allows the PEUU to be processed into porous scaffolds for the incorporation of biomolecules, and previous work in our laboratory has demonstrated the use of this porous polymeric matrix as a controlled release system for bFGF [172]. Furthermore, the tunable chemistry of this synthetic polymer allows for the tailoring of scaffold mechanical properties and release profiles of biomolecules from the polymer.

The objective of this study was to synthesize and process biodegradable, elastomeric PEUU films and scaffolds with the ability to incorporate and release bioactive molecules in a sustained and controlled manner over a predetermined time period *in vitro*. PEUU scaffolds containing IGF-1 or HGF were fabricated in a manner compatible with use as a cardiac patch to repair and regenerate infarcted myocardium (see Chapter 3). The *in vitro* release kinetics of IGF-1 and HGF from scaffolds were investigated. The bioactivity of released growth factor and the cytocompatibility of the scaffolds were confirmed with *in vitro* cell assays. Additionally,

PEUU films and scaffolds containing a ligand designed to induce cellular gene expression were fabricated for studies on the spatial control of gene expression (see Chapter 4). The *in vitro* release kinetics of ligand from films was investigated. The bioactivity of released ligand was confirmed with *in vitro* cell assays. Finally, the mechanical properties of scaffolds with and without factor were examined.

2.2 METHODS

2.2.1 Biodegradable poly(ester urethane)urea synthesis

PEUU based on polycaprolactone diol (MW=2000, Aldrich), 1,4-diisocyanatobutane (Fluka), and putrescine (Aldrich) was synthesized in a two-step solution polymerization [169]. **(Figure 2.1)** Prior to synthesis, PCL was vacuum-dried for 48 hours to remove residual water, and 1,4-diisocyanatobutane and putrescine were vacuum-distilled. Anhydrous dimethyl sulfoxide (DMSO, Sigma) and stannous octoate (Aldrich) were used as received from the supplier.

A 15 wt% solution of PCL in DMSO was stirred with a 5 wt% solution of BDI in DMSO in a 250 mL three-neck round bottom flask under argon gas. Stannous octoate, the catalyst, was added, and the reaction was allowed to continue at 80°C for three hours with constant stirring. After three hours, the prepolymer solution was removed from heat and allowed to cool to room temperature. Putrescine in DMSO was then added dropwise, with constant stirring, to the prepolymer solution, and the reaction was allowed to continue at room temperature for 12-18 hours. The stoichiometry of the reaction was 2:1:1 BDI:PCL:putrescine. After 12-18 hours of reaction at room temperature, PEUU solution was precipitated in distilled

water and immersed in isopropanol to remove unreacted monomers. Finally, polymer was dried under vacuum at 50°C for 24-48 hours.

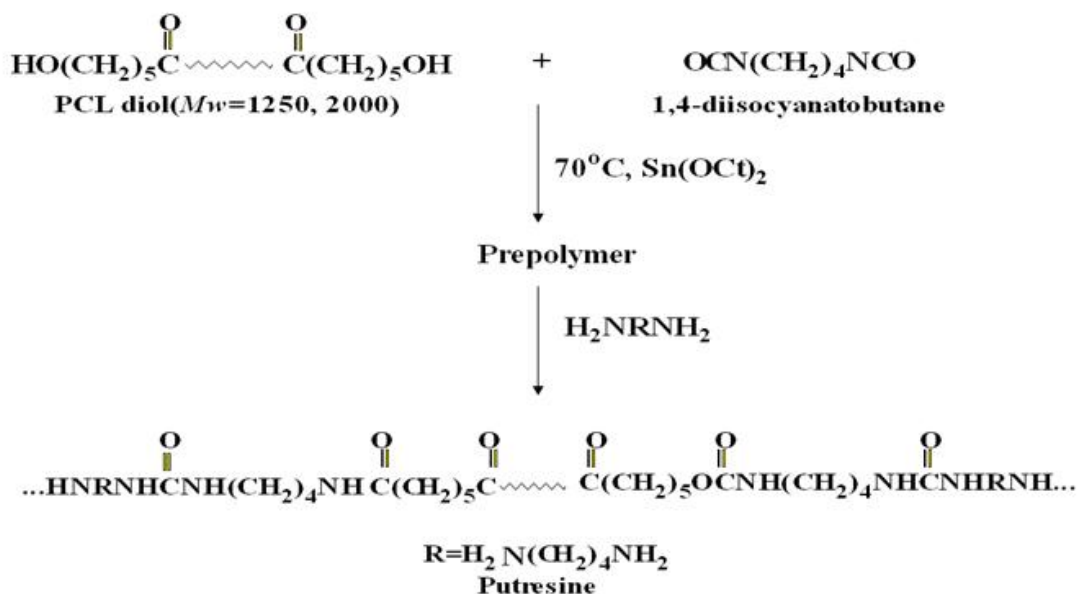


Figure 2.1: Poly(ester urethane)urea synthesis [169].

2.2.2 Fabrication of ligand-loaded PEUU films

After synthesis, PEUU was dissolved in DMSO at 80°C to make a 2 wt% polymer solution. Polymer solution was centrifuged at 250xg to remove any insoluble crosslinked PEUU. PEUU solution was brought to 37°C, and 0.5 mL of polymer solution was cast into each well of 24 well tissue culture polystyrene (TCPS) or glass bottom plates (MatTek Corp). Plates were dried under vacuum at 50°C until solvent was no longer seen evaporating from polymer films. This process resulted in an approximately 50 μm-thick, transparent PEUU film at the bottom of each well of tissue culture or glass bottom plates. For the determination of ligand release kinetics and

cell studies, predetermined amounts of synthetic ligand RSL1 (obtained from Intrexon Corp) were added to polymer solutions after centrifugation and cast into 24 well TCPS or glass bottom plates as described above. Polymer films without ligand served as a negative control for all studies.

2.2.3 Quantification of ligand release from PEUU films

Release kinetics for PEUU films containing RSL1 ligand were determined *in vitro*. Phosphate buffered saline (PBS) was used as release medium. Wells of 24 well TCPS plates cast with PEUU films containing 0-150 μ M ligand were incubated in 1 mL of PBS per well at 37°C. Release media were collected at pre-determined time points over three weeks and replaced with fresh PBS. Release media were kept frozen at -20°C until analyzed. Known concentrations of RSL1 ligand were added to release media collected from polymer films without ligand, and solutions were assayed via UV spectrometry at 250 nm to obtain a ligand standard curve. Release media from polymer films containing ligand were then assayed with UV spectrometry at 250 nm and compared to the ligand standard curve to determine the amount of ligand released over time.

2.2.4 Verification of bioactivity of released ligand

The bioactivity of released RSL1 was determined by the ligand's ability to induce gene expression in B16 cells (a murine melanoma cell line) stably transfected to expressed green

fluorescent protein (GFP) in the presence of ligand. For these studies, B16 cells were plated onto TCPS. 24 well TCPS plates cast with PEUU films containing 1-150 μM RSL1 ligand were incubated in B16 growth medium (see Appendix A) at 37°C. Polymer films without ligand served as a negative control. Growth medium was removed at pre-determined time points from polymer films and transferred to B16 cells on TCPS. Gene expression was visualized 48 hours post-degradation media transfer with fluorescent microscopy using an Olympus Provis light microscope (Center for Biologic Imaging, University of Pittsburgh). Gene expression was quantified using MetaMorph imaging data analysis software (Molecular Devices).

2.2.5 Fabrication of factor-loaded PEUU scaffolds

Three-dimensional, porous PEUU scaffolds were fabricated by a thermally induced phase separation (TIPS) method [170]. Following synthesis, PEUU was dissolved in DMSO at 80°C to make an 8 wt% polymer solution. As with PEUU films, insoluble, crosslinked polymer was removed by centrifugation at 250xg, and PEUU solution was once again heated to 80°C. Hot polymer solution was injected into a cylindrical glass mold (inner diameter 10 mm) capped with rubber stoppers. The mold was immediately placed at -80°C for three hours. Endcaps were then removed, and the mold was transferred to 200-proof ethanol for 3-7 days at 4°C for solvent extraction. Solvent extraction was considered complete once the polymer scaffold was released from (i.e. the scaffold was no longer attached to) the glass mold. Following DMSO removal, scaffolds were placed in water overnight to remove ethanol and reconstitute pore structure. Finally, scaffolds were vacuum-dried for 24 hours.

2.2.5.1 Fabrication of ligand-loaded scaffolds

To fabricate ligand-loaded scaffolds, RSL1 ligand stock solution was made in DMSO. Ligand in DMSO was then added to the 8 wt% polymer solution at 80°C moments before solution was injected into the cylindrical glass mold and transferred to -80°C. Each scaffold contained a 10 µM final ligand concentration. Scaffolds without ligand served as a negative control

2.2.5.2 Fabrication of growth factor-loaded scaffolds

To fabricate IGF-1- or HGF-loaded scaffolds, IGF-1 and HGF (R&D Systems) were first reconstituted in PBS in an excess of bovine serum albumin (BSA) (1:100) to stabilize the protein. Solutions containing growth factor and BSA were then snap-frozen in liquid nitrogen and vacuum-dried for 48 hours. IGF-1 and HGF stock solutions were subsequently made in DMSO. Growth factor in DMSO was added to the 8 wt% polymer solution at 80°C and immediately injected into the cylindrical glass mold and transferred to -80°C. IGF-1-loaded scaffolds contained 2.5 mg of BSA and a final IGF-1 concentration of either 250 or 500 ng/mL of PEUU solution. HGF-loaded scaffolds contained 2.5 mg of BSA and a final HGF concentration of 250 ng/mL of PEUU solution. Scaffolds without growth factor, but with BSA, served as a negative control for all studies.

2.2.6 Mechanical testing of PEUU scaffolds

Scaffolds with and without growth factor or ligand were snap frozen in liquid nitrogen and cut into 500 μm -thick discs. Tensile properties were measured on an MTS TytronTM 250 MicroForce Testing Workstation (10 mm/min crosshead speed) according to ASTM D638-98. Five samples were tested for each scaffold.

2.2.7 Quantification of growth factor release from PEUU scaffolds

Release kinetics for PEUU scaffolds containing IGF-1 or HGF were determined *in vitro*. Phosphate buffered saline (PBS) was used as release medium. Scaffolds were cut into 500 μm -thick discs, weighed, and placed into wells of 24 well tissue culture plates. Scaffolds were incubated in 1 mL of PBS per well at 37°C. Release media were collected at pre-determined time points over three weeks and replaced with fresh PBS. Release media were kept frozen at -20°C until analyzed. An IGF-1 or HGF enzyme-linked immunosorbant assay (ELISA, R&D Systems) was used to quantify growth factor concentration in release media (see Appendices B and C for ELISA protocols.) Degradation solution samples were serially diluted (1:1, 1:5, 1:10, 1:50, and 1:100) and compared to standard curves generated in PBS or in degradation solution from polymer without growth factor. In addition, release media from polymer films omitting growth factor were dosed with known concentrations of IGF-1 and assayed via UV spectrometry at 280 nm to obtain a standard curve for IGF-1 in solution as an alternative means of quantifying growth factor release.

2.2.8 Verification of bioactivity of released growth factor

The bioactivity of released IGF-1 was measured by a cell mitogenic assay. Balb/3T3 cells (a mouse embryonic fibroblast cell line, R&D Systems) and MG-63 cells (a human osteosarcoma cell line, R&D Systems) were selected due to their documented dose-dependent proliferation in response to IGF-1 treatment [138, 173]. Balb/3T3 and MG-63 cells were plated at 2×10^4 cells/mL in each well of 24 well TCPS plates. 500 μm -thick sections of scaffolds with and without IGF-1 were placed into wells of 24 well tissue culture plates in cell basal media (See Appendix D). Media from wells containing scaffolds were collected at predetermined time points over three weeks, sterile-filtered, and kept frozen at -20°C until transfer to cells. Prior to growth media exchange with polymer degradation media, cells were treated overnight with 1 $\mu\text{L}/\text{mL}$ colcemid to synchronize cell cycle. Cells were then washed with PBS to remove traces of colcemid and fed with the appropriate polymer degradation media. 96 hours post-degradation media treatment, cell number was measured using the MTT mitochondrial activity assay. (See Appendix E for MTT protocol.) Data were normalized to cells maintained in growth media.

The bioactivity of released HGF was measured by a cell mitogenic assay. Human umbilical vein endothelial cells (HUVECs) were selected due to their documented mitogenic response to HGF [174]. HUVECs were plated onto a 6 well TCPS plate. 500 μm -thick sections of scaffolds with and without HGF were placed into wells of 24 well TCPS plates in cell basal media. (See Appendix F) Media from wells containing scaffolds were collected at predetermined time points over three weeks, sterile-filtered, and kept frozen at -20°C until being transferred to cells. An *in vitro* wound healing assay was used to confirm the mitogenic effect of HGF on cells [174]. Briefly, once cells had grown to confluence, a cell scraper was used to create a wound down the center of each well of the 6 well plate. Cells were then washed with

PBS to remove cell debris from the wound and treated with polymer degradation solutions. A live-cell imaging system from Automated Cell Technology (ACT) [175] was used to image cells at 10 minute intervals over a four day period. Cell motility was quantified in terms of cell velocity (using ACT software) [175] and cell migration into the wound (using NIH ImageJ software).

2.2.9 Statistical methods

Data are reported as mean \pm standard deviation. All statistical analyses were performed using SPSS software. For controlled release data, scaffolds were compared with repeated measures ANOVA to evaluate the effect of time and loading concentration on ligand release. For cell proliferation studies, statistical analyses of MG-63 and Balb/3T3 cell proliferation were performed using a t-test for evaluation of differences. For cell motility studies, data were analyzed by ANOVA with Tukey post-hoc testing for specific differences between various degradation solutions. Significance was defined at $p < 0.05$ level.

2.3 RESULTS

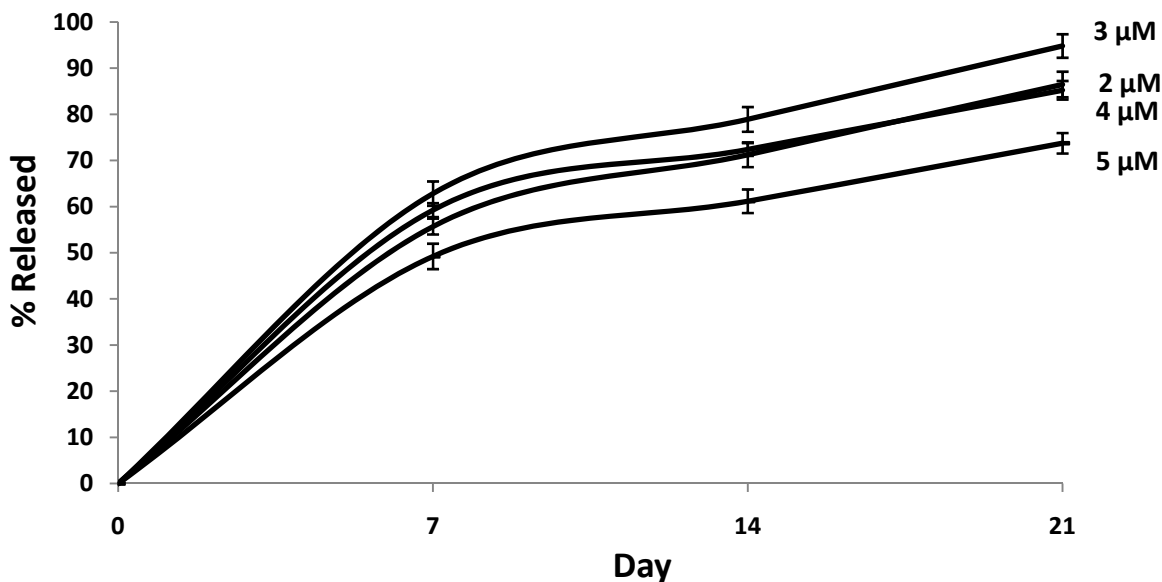


Figure 2.2: Ligand release curves for 2-5 μM loading concentration of RSL1. An initial release of 49%-63% of RSL1 occurred over the first 7 days. This was followed by a slower release of RSL1 over the next two weeks, resulting in 73%-95% of ligand being released over a three week period *in vitro*.

2.3.1 RSL1 release from PEUU films

PEUU films with lower ligand loading concentrations (0-5 μM) exhibited a two-stage release profile; an initial burst release was followed by a slower release over three weeks *in vitro*. A release of 49%-63% of RSL1 occurred over the first 7 days. This was followed by a slower release of RSL1 over the next two weeks, resulting in 73%-95% of loaded RSL1 being released over a three week period *in vitro*. (Figure 2.2) For higher loading concentrations (50-150 μM), a release of 6%-18% occurred over the first 7 days. A total of 20%-60% of loaded RSL1 was released over a four week period *in vitro*. (Figure 2.3) Release profiles (% released) from 50-150 μM RSL1-containing polymers are significantly different between all groups with respect to

both time and loading concentration ($p < 0.00$). However, it should be noted that equal molar amounts of ligand are released from films at each time point, regardless of loading concentration (i.e. $9 \mu\text{M}$ at day 7, $16 \mu\text{M}$ at day 14, $23 \mu\text{M}$ at day 21, and $30 \mu\text{M}$ at day 28). For lower loading concentrations, release profiles are significantly different with respect to both time and concentration between all groups ($p < 0.00$) except the $2 \mu\text{M}$ and $4 \mu\text{M}$ loading concentrations which are significant only with respect to time ($p < 0.00$).

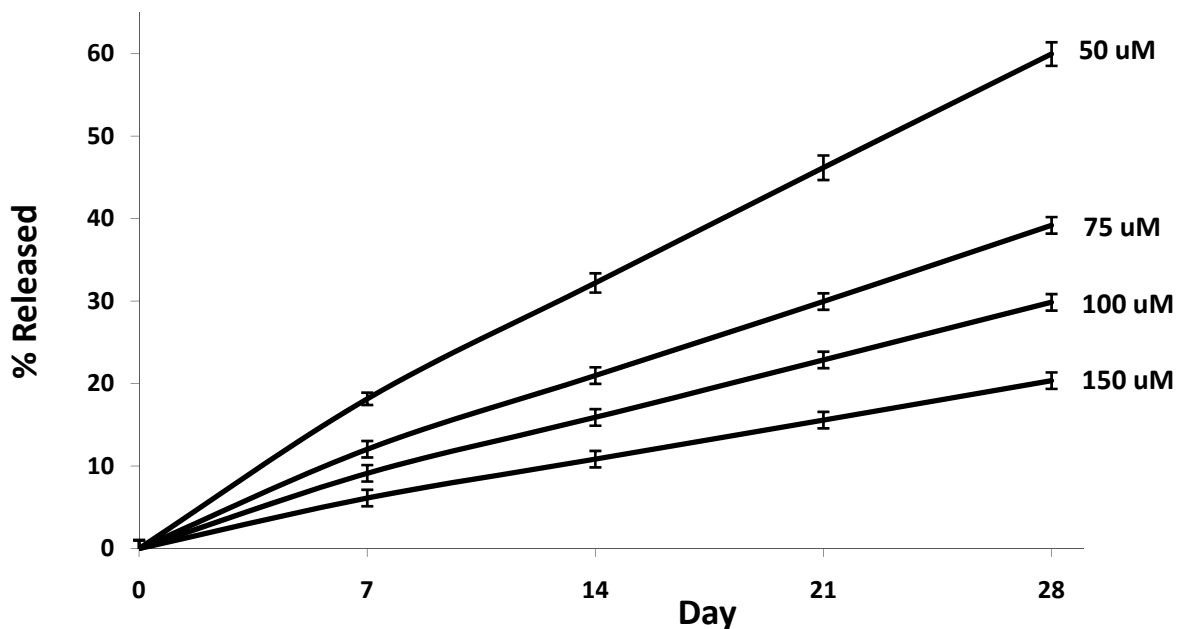


Figure 2.3: Ligand release curves for 50-150 μM loading concentration of RSL1. An initial release of 6%-18% occurred over the first 7 days. A total of 20%-60% of ligand was released over a four week period *in vitro*.

2.3.2 Bioactivity of released RSL1

A simple bioactivity assay for released RSL1 assessed gene expression in B16 cells cultured in release media from PEUU films loaded with 1-10 μM RSL1. Release media from PEUU films

without RSL1 served as negative controls. Cells in release media from all films containing RSL1 expressed GFP 48 hours post-treatment, while cells in release media from films without ligand did not. Gene expression was evident for all time points assayed (0-21 days). **(Figure 2.4)** Furthermore, dose-dependent gene expression was seen in cells in release medium from films containing 0-5 μM RSL1. Increasing ligand concentration from 0-5 μM resulted in an increasing number of GFP⁺ cells. **(Figure 2.5)**

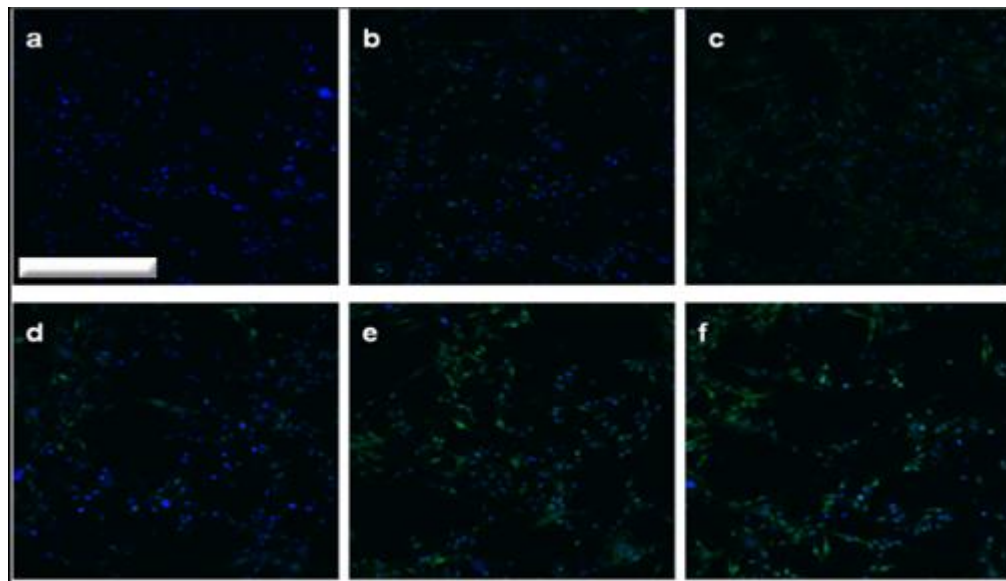


Figure 2.4: Gene expression in cells treated with release medium from PEUU films containing (a) 0 μM , (b) 1 μM , (c) 2 μM , (d) 3 μM , (e) 4 μM , and (f) 5 μM RSL1. Scale bar = 500 μm for all images.

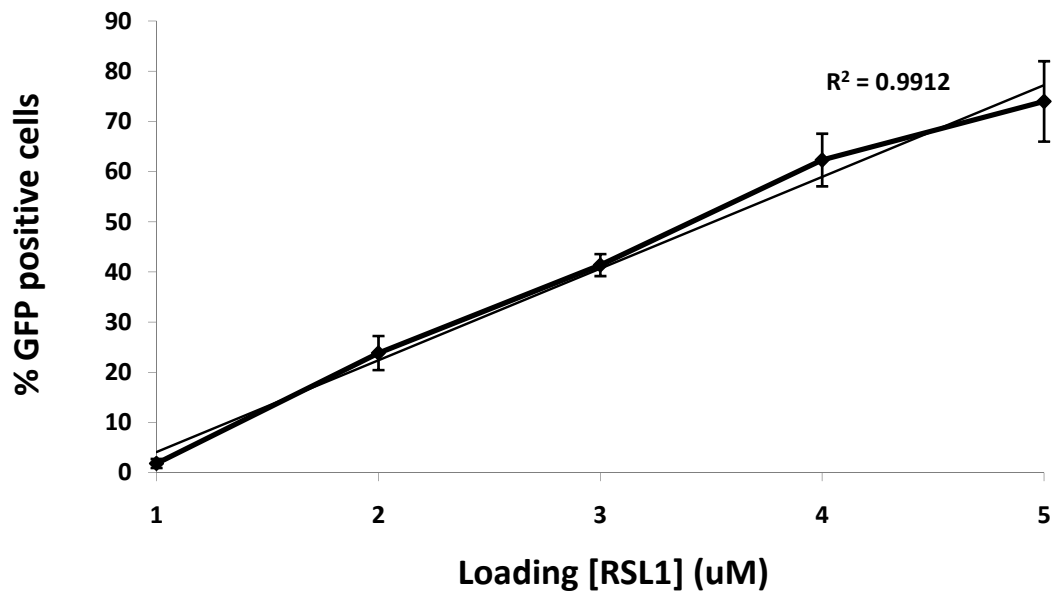


Figure 2.5: Dose-dependent GFP expression in cells in degradation solutions from polymer containing 1-5 μ M RSL1. % GFP positive cells quantified as % of cells visibly positive for green fluorescence.

2.3.3 Mechanical properties of PEUU scaffolds

TIPS scaffolds fabricated without the addition of any biomolecules (BSA, growth factor, or RSL1 ligand) had tensile strengths of 0.61 ± 0.15 MPa. Scaffolds containing BSA alone had tensile strengths of 0.43 ± 0.04 MPa, and scaffolds containing BSA and growth factor (IGF-1 or HGF) had tensile strengths of 0.32 ± 0.18 MPa. Scaffolds containing RSL1 ligand had tensile strengths of 0.48 ± 0.28 MPa.

2.3.4 Growth Factor Release from PEUU scaffolds

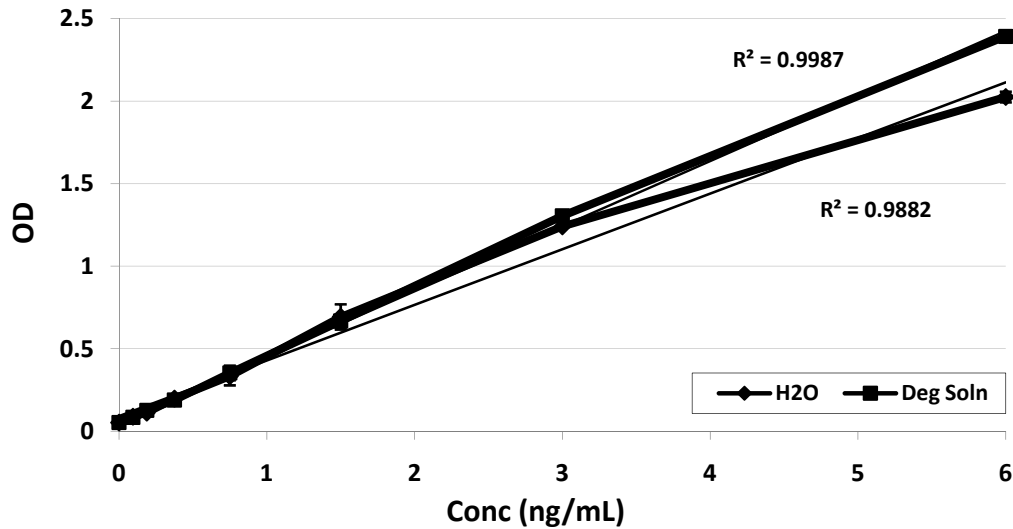


Figure 2.6: IGF-1 ELISA standard curves in distilled water and in degradation solution from scaffolds without growth factor.

Standard curves for IGF-1 and HGF were obtained with protein standards reconstituted in distilled water and in degradation solution from PEUU scaffolds containing BSA alone (i.e. no growth factor). (**Figure 2.6 & Figure 2.7**) All degradation solution samples from scaffolds containing IGF-1 resulted in a zero reading regardless of dilution. All degradation samples from scaffolds containing HGF also resulted in a zero reading regardless of dilution. Additionally, standard curves for IGF-1 generated using UV spectrometry yielded zero readings for all concentrations assayed.

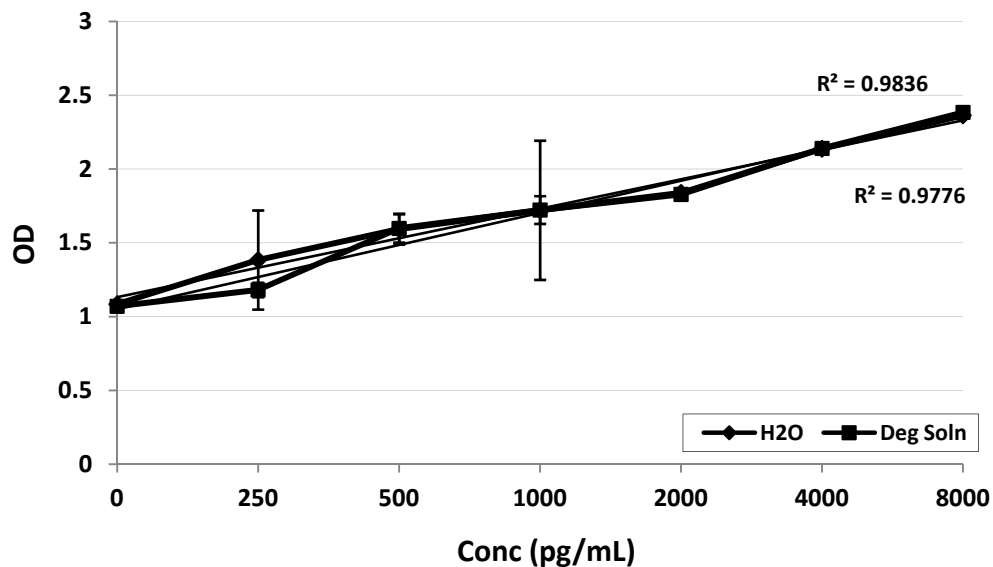


Figure 2.7: HGF ELISA standard curves in distilled water and in degradation solution from polymer without growth factor.

2.3.5 Bioactivity of released IGF-1

MG-63 cells treated with day 7 and day 14 degradation solutions from scaffolds containing IGF-1 exhibited a significant increase in proliferation compared to those in degradation solutions from scaffolds without growth factor ($p < 0.05$). Cells treated with day 7 degradation media from scaffolds containing 500 ng/mL IGF-1 exhibited a 2.0-fold increase in cell number compared to cells treated with degradation media from scaffolds without growth factor. Cells treated with day 14 degradation media from scaffolds containing IGF-1 exhibited a 1.6-fold increase over cells in degradation media from scaffolds without growth factor. No significant difference in cell number was seen between cells treated with degradation media collected at day 21 from either set of scaffolds. (Figure 2.8)

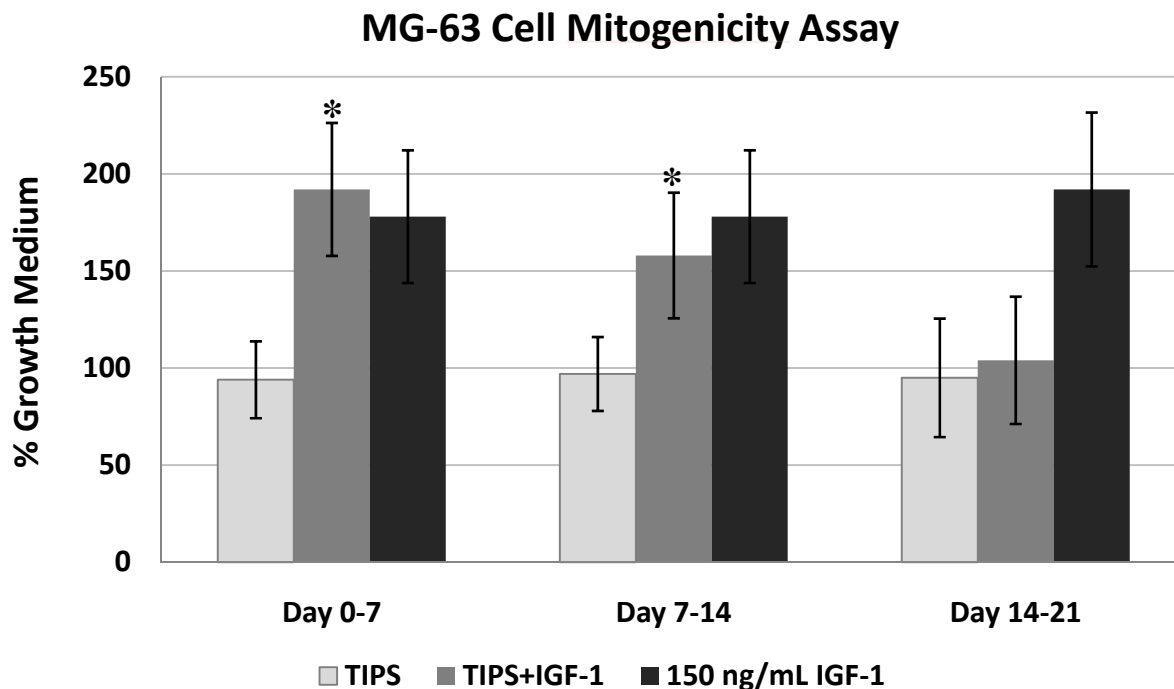


Figure 2.8: MG-63 cell growth in degradation solutions relative to growth medium (* $p < 0.05$).

Balb/3T3 cells treated with day 7 and day 14 degradation solutions from scaffolds containing IGF-1 exhibited a significant increase in proliferation compared to those in degradation solutions from scaffolds without growth factor ($p < 0.05$). Cells treated with day 7 degradation media from scaffolds containing 500 ng/mL IGF-1 exhibited a 2.1-fold increase in cell number compared to cells treated with degradation media from scaffolds without growth factor. Cells treated with day 14 degradation media from scaffolds containing IGF-1 exhibited a 1.7-fold increase over cells in degradation media from scaffolds without growth factor. No significant difference in cell number was seen between cells treated with degradation media collected at day 21 from either set of scaffolds. **(Figure 2.9)**

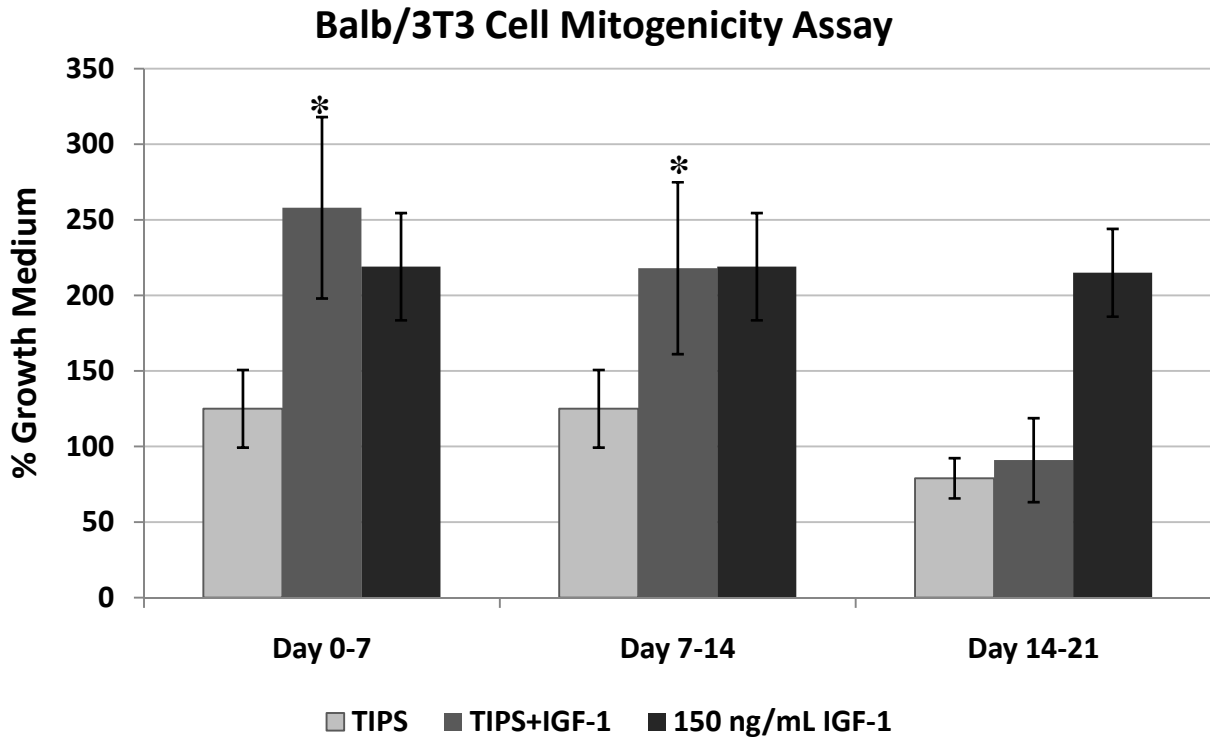


Figure 2.9: Balb/3T3 cell growth in degradation solutions relative to growth medium (* $p < 0.05$).

2.3.6 Bioactivity of released HGF

There was no significant difference in cell velocity between cells maintained in degradation solutions from polymer with HGF and those maintained in degradation solutions from polymer without growth factor. Furthermore, addition of HGF to growth medium had no significant effect on cell velocity. **(Figure 2.10)** 48 hours post-treatment with degradation solutions, growth medium, or medium containing HGF, cells maintained in day 7 and day 21 degradation solutions from scaffolds with HGF more significantly grew into and repopulated the wound than those maintained in growth medium or degradation solutions from scaffolds without growth factor ($p < 0.05$).

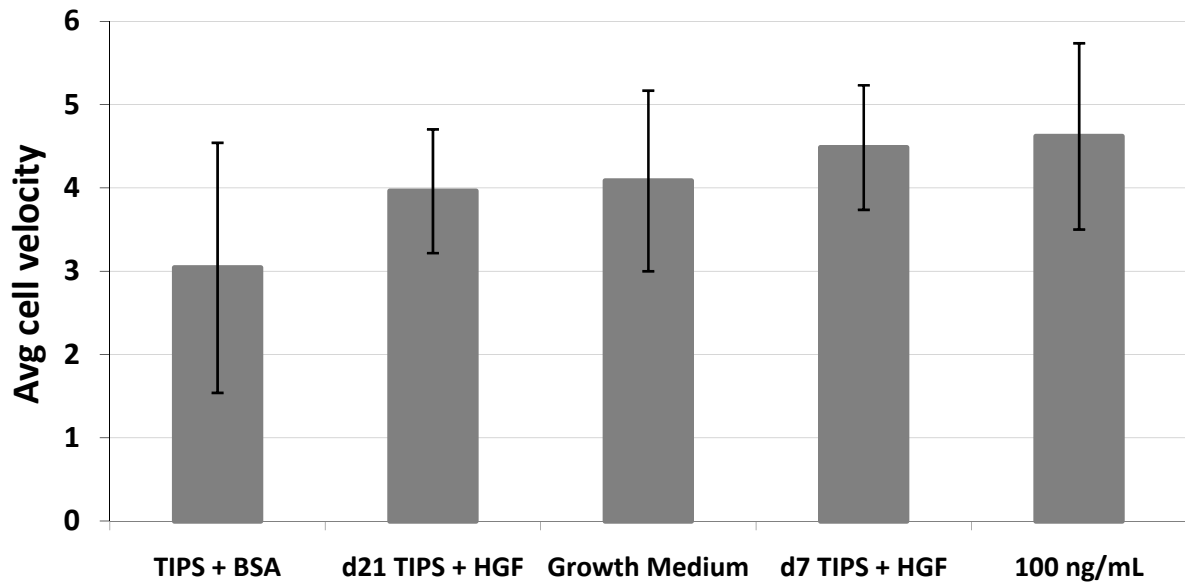


Figure 2.10: HUVEC average cell velocity.

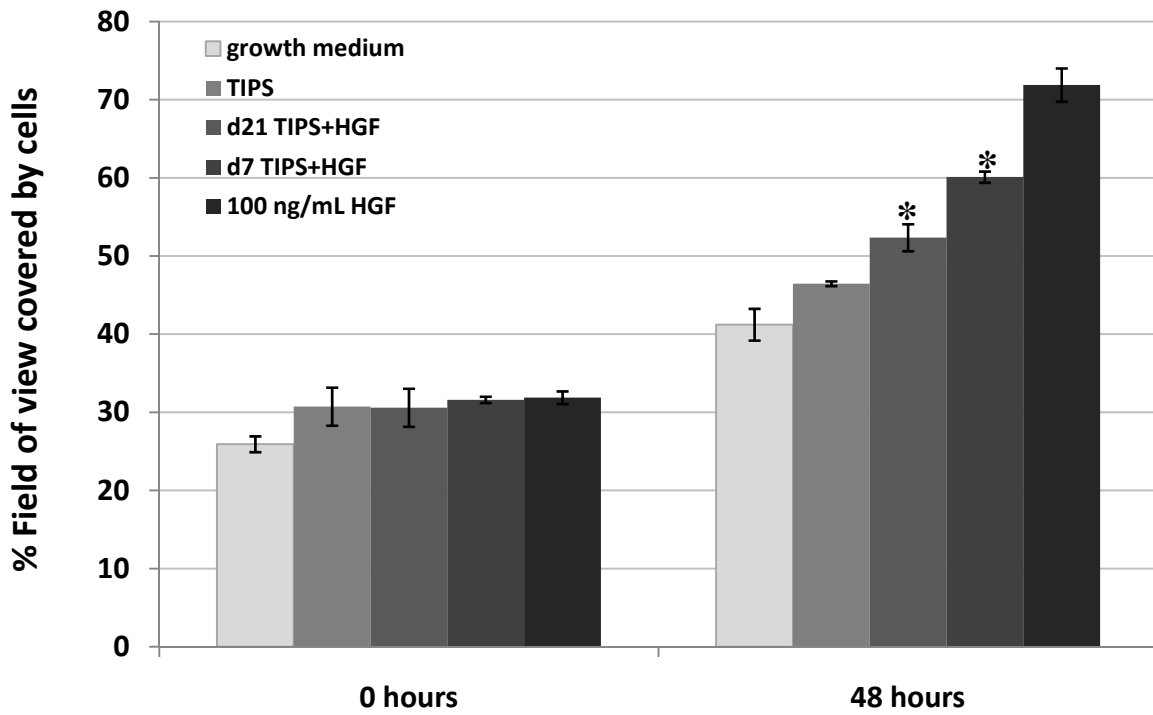


Figure 2.11 Wound infiltration by HUVECs with time (*p<0.05 compared to cells in growth medium and cells in degradation solutions from polymer without growth factor).

2.4 DISCUSSION

Polyurethanes have been widely used in biomedical devices due to their excellent mechanical properties and moderately good blood compatibility [168, 176]. Most commonly, polyurethanes were used in catheters, pacemaker lead coverings, and wound dressings where degradation was not desired [168, 177]. For *in vivo* application, the long-term biostability of polyurethanes due to their inherent biodegradation became cause for some concern [166].

Once implanted, polyurethanes degrade via several mechanisms. Aliphatic ester linkages in poly(ester urethanes) are susceptible to hydrolysis, while poly(ether urethanes) are susceptible to crack formation and propagation. Enzyme-mediated degradation as a part of host inflammatory response is also known to play a role in polyurethane degradation. With *in vivo* application, it was discovered that degradation of polyurethanes synthesized from aromatic diisocyanates such as TDI and MDI lead to the formation of products with putative carcinogenic effects [165, 166]. Therefore, more recent efforts by researchers to design degradable polymers for tissue repair and regeneration has warranted the use of aliphatic diisocyanates such as LDI and BDI. To this end, researchers have investigated a variety of soft segment chemistries using various polyesters with aliphatic diisocyanates to synthesize biocompatible, biodegradable polyurethanes.

Overall polymer degradation rate is controlled by the chemistries of both the hard and soft segments. Several groups have researched the effects of varying the soft segment in polyurethane syntheses for tissue engineering applications. Recently, PEO and PCL have both been investigated, with each imparting different physical and mechanical properties to polymers. Polyurethanes synthesized from PEO using LDI and a phenylalanine-based chain extender were characterized as weak, amorphous materials, while those synthesized using PCL were strong and

elastomeric [168]. Polyurethanes combining PEO and PCL in the soft segment have also been characterized; increasing PEO content resulted in weaker and less extensible materials with faster degradation rates [178, 179]. Our group has synthesized a poly(ether ester urethane)urea with the use of a triblock soft segment consisting of PCL and polyethylene glycol (PEG) using BDI and a putrescine chain extender. Increasing PEG length resulted in faster degradation rates. The strength and flexibility of these polyurethanes were tunable by adjusting chemistry of the triblock soft segment, and these polymers were shown to be cytocompatible when cultured with HUVECs suggesting their potential for cardiovascular tissue engineering applications in which high strength and flexibility are necessary [180].

In addition to soft segment modification, researchers have investigated the inclusion of biodegradable hard segments in polyurethanes. The use of a phenylalanine chain extender, as previously mentioned, accelerated enzyme-mediated degradation in the presence of chymotrypsin and trypsin [168]. Antibacterial drugs have also been incorporated into the hard segment of polyurethanes. These polymers are designed to degrade upon implantation via enzymatic attack by inflammatory cells. While inclusion of the antimicrobial drug enhances enzymatic degradation, the drug itself serves to counter biofilm formation and the development of infection [181, 182].

While these polymers show promise in soft tissue engineering applications, several biodegradable polyurethanes have been investigated *in vitro* and *in vivo* specifically for myocardial repair and regeneration. The aforementioned polyurethane synthesized from PCL and LDI using a phenylalanine chain extender was patterned with laminin lanes. Spatial organization of rat neonatal cardiomyocytes on laminin-patterned polyurethane led to the development of a multilayered, organized tissue construct that may serve as a vehicle for cell

transplantation into ischemic myocardium [100]. Skeletal myoblasts were seeded onto a polycaprolactone-based polyurethane (Artelon) known to degrade by hydrolysis over a five year period. After implantation in ischemic rat myocardium, numerous myoblasts were found throughout the patch, confirming development of a material that allows for the transfer of large numbers of cells to damaged myocardium [176].

Our group has previously reported on the synthesis of a poly(ester urethane)urea based on PCL and putrescine [169]. The tunable chemistry of this polymer allows for the tailoring of scaffold mechanical properties and release profiles of biomolecules from the polymer matrix making it an attractive choice for myocardial repair and regeneration. We have demonstrated that this PEUU degraded at a clinically relevant rate *in vitro* [169] and *in vivo* [171] and with no adverse effects on cell viability [169, 171, 180]. PEUU was electrospun to produce scaffolds with fiber diameters similar to those of native extracellular matrix [97]. Porous scaffolds were also fabricated through a thermally induced phase separation method [170]. Of the two methods, the TIPS method proved advantageous for the fabrication of porous scaffolds as it allowed for the generation of pore sizes and porosities more attractive for cellular ingrowth [170]. In addition to the fabrication of porous scaffolds, we have demonstrated the successful incorporation of biomolecules into a porous PEUU scaffold and have demonstrated the use of this polymeric matrix as a controlled release system for basic fibroblast growth factor [172].

For this research, we incorporated insulin-like growth factor-1 and hepatocyte growth factor (factors implicated in muscle repair and regeneration) into TIPS PEUU scaffolds and evaluated the kinetics of growth factor release as well as the bioactivity of released growth factor. In addition, we incorporated a ligand designed to induce gene expression in cells into

PEUU films and TIPS scaffolds and evaluated the kinetics of ligand release as well as the bioactivity of released ligand.

A biphasic release of RSL1 was observed from PEUU films containing low loading concentrations of inducer ligand over a three week period *in vitro*. The initial burst phase is most likely due to diffusion mechanisms. In the second phase, PEUU degradation is occurring and likely contributing to the diffusion of RSL1 from the polymer. Such release profiles are common for other polymer delivery systems [183] and have been demonstrated with the incorporation of other biomolecules into our polymer matrix [172]. Higher loading concentration resulted in slower %release of RSL1; however, equal molar amounts of ligand were released from polymer films regardless of loading concentration. This could be due to the interactions between highly hydrophobic domains of the ligand molecule and the polymer itself. Further studies are necessary to elucidate the mechanism behind these release profiles, as are studies to determine the optimal RSL1 loading concentration and subsequent release profile for *in vivo* applications.

The bioactivity of RSL1 released from PEUU films was verified over a 21 day period *in vitro* as demonstrated by a simple GFP expression assay in stably transfected B16 cells. GFP expression was observed in cells cultured in all degradation solutions from polymer containing ligand, while cells cultured in degradation solutions from polymer omitting ligand did not express GFP. A dose-dependent response was seen in cells cultured in degradation solutions from polymer loaded with 1-5 μM RSL1, demonstrating a dose-responsive system in this range of ligand concentration.

IGF-1 and HGF release curves could not be obtained via ELISA. While ELISA standard curves were obtained for IGF-1 and HGF using protein reconstituted in both distilled water and polymer degradation solution from polymer omitting growth factor, all degradation solutions

from polymer containing growth factor resulted in a zero reading regardless of dilution factor. However, results from *in vitro* bioactivity assays confirmed the presence of bioactive IGF-1 and HGF in degradation solutions from polymer containing growth factor. Scaffolds without growth factor served as negative controls, and a significant difference in cell proliferation (IGF-1) or motility (HGF) was observed in cells treated with polymer with and without growth factor. From this data, it is reasonable to conclude that IGF-1 and HGF have been successfully incorporated into PEUU scaffolds and that they are bioactive upon release. It is postulated that the scaffold fabrication process, while not denaturing the protein, is altering its conformation, thereby rendering it unrecognizable by the antibody used for the specific ELISA kit in question. While some loss of bioactivity is reasonable to expect in the course of the fabrication process, the bioactivity assays support the conclusion that a significant amount of loaded protein retains its bioactivity, thereby lending to the conclusion that loss of bioactivity and protein denaturation are not the reasons behind failure of the ELISA assays.

Our group has previously demonstrated the successful incorporation and controlled release of bFGF from TIPS scaffolds. Scaffolds were fabricated through the TIPS processing method used for this research, and protein was stabilized by BSA and added to PEUU solution just as with IGF-1 and HGF for this research. An initial burst release of 19% of loaded bFGF was observed over the first 24 hours followed by an additional 11% over the next 24 hours. A slower release of bFGF was observed over the next 3 weeks *in vitro*. For these studies, bFGF was radioactively-tagged and release was quantified using a radioactivity assay. Furthermore, bioactivity of released bFGF was successfully demonstrated using an *in vitro* cell culture assay [172]. Results from this previously published research further support the conclusion that polymer fabrication and processing methods do not denature proteins and cause significant loss

of bioactivity. As such, alternative methods for quantifying IGF-1 and HGF release from PEUU scaffolds must be explored. IGF-1 is a 7.5 kDa protein, while bFGF is a 18 kDa protein. By contrast, HGF is much larger, and is approximately 70 kDa. Considering molecular weight alone, it can be hypothesized that release profiles for IGF-1 should closely resemble those for bFGF. It may be hypothesized that HGF would display a slower release due to its higher molecular weight.

It has been reported in the literature that IGF-1 concentration in solution can be determined via UV spectrometry. To this end, known concentrations of IGF-1 were added to degradation solutions from scaffolds omitting growth factor and assayed via UV spectrometry to obtain a standard curve. All measurements from this assay resulted in zero readings, and it is postulated that the concentrations of IGF-1 used in our studies were too low for detection with this method.

Based on release profiles of ligand from polymer films and *in vitro* bioactivity assays using degradation solutions from polymer containing ligand or polymer containing growth factor, we have successfully demonstrated the fabrication of a biodegradable, elastomeric poly(ester urethane)urea capable of releasing biomolecules in a sustained and controlled manner over a specified time period *in vitro*. Its physical and mechanical properties make this polymeric system an attractive option for soft tissue engineering applications in regenerative medicine.

3.0 IGF-1- AND HGF-LOADED CARDIAC PATCHES FOR MYOCARDIAL REPAIR AND REGENERATION

3.1 INTRODUCTION

Following myocardial infarction, many patients develop heart failure due to the limited regenerative capacity of the heart. While mechanical assist devices, surgical interventions, and pharmaceutical therapies have proven somewhat effective in improving cardiac function, they have failed in preventing mortality in patients with congestive heart failure [4, 5, 171]. As such, researchers have investigated a number of biomaterials, growth factors, and combinations of the two for the repair of ischemic myocardium.

Insulin-like growth factor-1 and hepatocyte growth factor are among growth factors being examined for myocardial repair and regeneration. IGF-1 and HGF have both been implicated in the heart's intrinsic response to myocardial infarction [129, 158]. HGF is a potent angiogenic factor and is known for its anti-apoptotic and motogenic effects on cells [121-123], while IGF-1 has been shown to play a key role in muscle cell commitment and proliferation and to aid in muscle regeneration [2, 128, 129]. As such, it has been postulated that exogenous administration of one or both of these growth factors may enhance myocardial repair and regeneration, and the overexpression of IGF-1 or HGF in ischemic myocardium has been shown to have some beneficial effect on muscle regeneration [125, 184-186].

Among polymers investigated for myocardial repair and regeneration is a class of biodegradable, elastomeric polyurethanes that possess physical and mechanical properties desirable for cardiac tissue engineering [100, 168, 169, 176]. Our group has previously reported on the synthesis of a poly(ester urethane)urea with mechanical properties that are attractive for soft tissue engineering applications, such as with blood vessels or myocardium [169, 170]. We have demonstrated the ability of this polymer to function as a controlled-release system for IGF-1 and HGF *in vitro* (Chapter 2). In addition, our group recently reported that the application of a biodegradable, elastomeric PEUU patch to ischemic myocardium in a rat subacute infarct model promoted smooth muscle formation, stemmed LV dilation, and improved contractile function [3].

For this research, it was hypothesized that PEUU patches loaded with IGF-1 or HGF would more greatly improve LV dimension and function compared to patches without growth factor due to the therapeutic involvement of IGF-1 and HGF in myogenic and cardiac commitment and repair. It is postulated that the sustained and controlled *in vivo* delivery of IGF-1 or HGF may prove more effective in myocardial repair and regeneration than administration of soluble factor alone. As such, the application of controlled release polymer scaffolds in a rat subacute infarct model was investigated. PEUU patches without growth factor and patches containing either IGF-1 or HGF were implanted directly on infarcted LV walls. Eight weeks post-patch implantation, LV function was evaluated using echocardiography. In addition, LV wall thickness, muscle mass, and angiogenesis were examined histologically.

3.2 METHODS

3.2.1 Preparation of cardiac patches from biodegradable, elastomeric PEUU

PEUU was synthesized and processed into porous scaffolds by a thermally induced phase separation method [170]. Scaffolds containing BSA alone or BSA with either IGF-1 or HGF were fabricated as described in Chapter 2. Scaffolds were elastic, and those containing BSA had tensile strengths of 0.43 ± 0.04 MPa, while scaffolds containing BSA and growth factor (IGF-1 or HGF) had tensile strengths of 0.32 ± 0.18 MPa. Prior to implantation, scaffolds were cut into circular patches roughly 6 mm in diameter and 300 μm thick. Scaffolds were immersed in 200-proof ethanol for 30 minutes, transferred to sterile phosphate buffered saline for 30 minutes, and sterilized under UV light for an additional 60 minutes.

3.2.2 Animal model of subacute myocardial infarction

Adult female Lewis rats (Harlan Sprague Daley) weighing 200 to 250 grams were used. All research protocols were approved by the University of Pittsburgh's Institutional Animal Care and Use Committee and the Children's Hospital of Pittsburgh Animal Research Care Committee. All protocols followed the National Institutes of Health animal care guidelines.

Anesthesia was administered using 3.0% isoflurane inhalation. Once anesthesia was induced, rats were intubated and placed on a rodent volume-controlled mechanical ventilator. Electrocardiogram and tail cuff blood pressure were monitored throughout the course of the surgical procedure. The heart was exposed through a left thoracotomy, and the proximal left

anterior descending coronary artery was ligated with 7-0 polypropylene. Regional cyanosis and ST-segment elevation were used to confirm myocardial ischemia. The incision was closed using 4-0 silk continuous sutures.

3.2.3 PEUU patch implantation

Two weeks post-infarction, animals were anesthetized and examined with echocardiography to determine infarct size. Infarct size was calculated as the percentage of scar area (akinetic or dyskinetic regions) to LV free wall area. A total of 45 rats with infarcts greater than 25% of the LV free wall were included in the study and split into five groups: those receiving a patch loaded with 250 ng/mL IGF-1 (low IGF-1 group, n=8), those receiving a patch loaded with 500 ng/mL IGF-1 (high IGF-1 group, n=9), those receiving a patch loaded with HGF (HGF group, n=8), those receiving a patch without growth factor (patch control group, n=8), and sham repair (infarction control group, n=12).

The infarcted anterior wall was once again exposed via a left thoracotomy. The surface of the infarcted area, including the remaining epicardium and some of the integrated fibrous tissue, was scraped and removed prior to patch implantation. Subsequent to scraping, the anterior infarcted region was covered with a PEUU patch using 7-0 polypropylene over-and-over peripheral sutures. For the infarction control group, a thoracotomy was performed two weeks post-infarction, but no scraping or patch placement was performed.

3.2.4 Echocardiography analysis

Echocardiography was performed at the time of patch implantation (0 weeks, 2 weeks post-infarction), 4, and 8 weeks post-patch implantation. Rats were again anesthetized with isoflurane. Standard transthoracic echocardiography was performed using the Acuson Sequoia C256 system with 13-MHz linear ultrasonic transducer (15L8; Acuson Corporation) in a phased-array format. B-mode measurements on the LV short-axis view (papillary muscle level) were performed [3]. The end-diastolic (EDA) and end-systolic (ESA) LV internal cavity areas were measured by tracing the endocardial border. The regional EDA and ESA at the infarcted antero-lateral wall segment were also measured using a floating centroid method [3]. The global and regional LV fractional area change (%FAC) were estimated as:

$$\% \text{ FAC} = \frac{EDA - ESA}{EDA} \times 100$$

All measurements were performed using Scion Image software (Scion Image).

3.2.5 Histological assessment

Eight weeks after patch implantation (10 weeks post-infarction), rats were anesthetized, and the heart was exposed and arrested by apical injection of 2 mL of a hypothermic arresting solution (68 mmol/l NaCl, 60 mmol/l KCl, 36 mmol/l NaHCO₃, 2.0 mmol/l MgCl₂, 1.4 mmol/l Na₂SO₄,

11 mmol/l dextrose, 30 mmol/l butanedione monoxime, 10,000 U/l of heparin). The embedded frozen LV tissues were serially sectioned at 8 μm in the LV transverse direction.

Hematoxylin and eosin (H&E) staining and immunohistochemical staining were performed with antibodies against alpha-smooth muscle actin (α -SMA, Sigma), von Willebrand Factor (vWF, DAKO), and sarcomeric alpha-actinin (EA53, Sigma). Nuclei were stained with Hoechst no. 33258 (Sigma). (See Appendices G & H for staining protocols.) The entire patch implanted region of each heart was photographed with bright-field (H&E staining) and fluorescent microscopy (vWF, α -SMA, and EA53) using an Olympus Provis light microscope (Center for Biologic Imaging, University of Pittsburgh). To observe the pattern of α -SMA⁺ staining across the infarcted wall, 10 different fields at 20x were examined for each heart (n = 4 rats/group). For each LV sample, 4 different microscopic fields at 20x for the wall thickness measurement and 10 different fields at 20x for capillary density were examined for each rat (n = 5 rats/group). The wall thickness of the infarcted anterior wall (patch implanted region) was measured using NIH ImageJ software for all groups. Capillaries were recognized as tubular structures positively stained for vWF, and smooth muscle bundles were recognized as structures positively stained for α -SMA.

3.2.6 Statistical methods

All data are expressed as mean±standard deviation. All analyses utilized SPSS software. The wall thickness in each group was compared by ANOVA with Tukey post-hoc testing. Echocardiography data were compared by 2-way repeated ANOVA with Tukey post-hoc testing. Statistical significance was defined at a value of $p < 0.05$.

3.3 RESULTS

3.3.1 Gross morphology

There were no early or late postoperative deaths in any of the surgical groups. Eight weeks post-patch implantation, none of the PEUU patches had formed strong adhesions to the chest wall, and the surfaces of all patches were covered with fibrous tissue. (**Figure 3.1**)

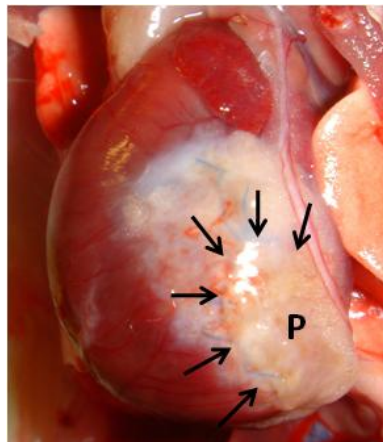


Figure 3.1: Representative image of a patched heart (albumin control) 8 weeks after implantation. Arrows point to the patched region. P = patch.

3.3.2 LV wall thickness, formation of muscle bundles, and capillary density

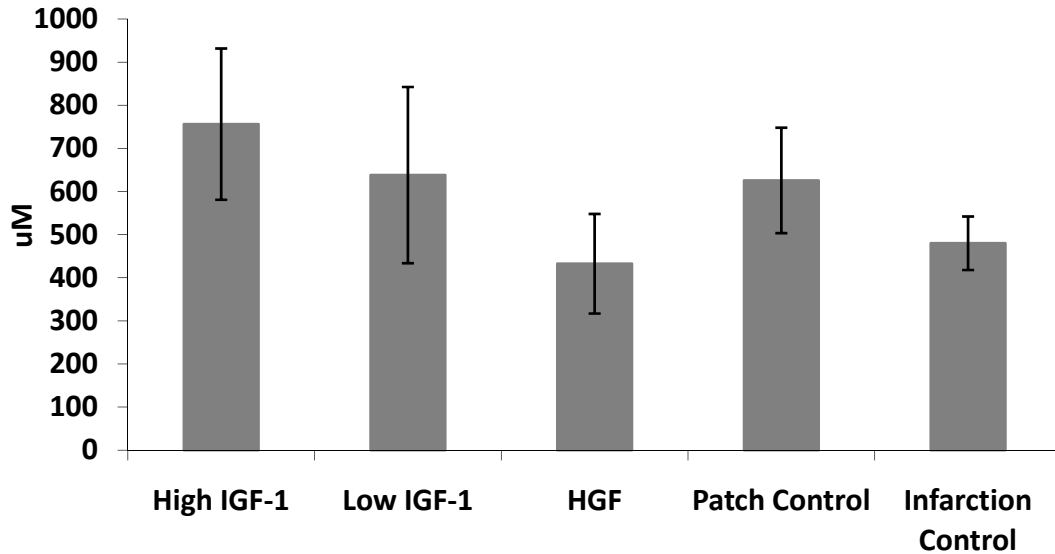


Figure 3.2: LV wall thickness

From analysis of H&E staining, eight weeks post-patch implantation, the majority of all patches were absorbed. Remnant areas of patches appeared to be infiltrated by macrophages and fibroblasts. Examination of H&E stained sections using bright-field microscopy showed no appreciable difference in LV wall thickness in hearts receiving control, low IGF-1, or high IGF-1 patches. In contrast, infarction control and HGF patched hearts appeared to have thinner walls than the other groups. **(Figures 3.2 and 3.3)** From histological section analysis using NIH ImageJ software, the LV wall thickness for each group was found to be as follows: infarction control: $480 \pm 62 \mu\text{m}$, patch control: $626 \pm 122 \mu\text{m}$, low IGF-1: $638 \pm 204 \mu\text{m}$, high IGF-1: $756 \pm 175 \mu\text{m}$, and HGF: $432 \pm 115 \mu\text{m}$. No significant difference was seen in wall thickness between any of the experimental groups or controls.

Immunohistochemical examination of hearts using fluorescent microscopy revealed regions under the patch positively stained for α -SMA in all hearts receiving control, low IGF-1, or high IGF-1 patches. In all three of these groups, α -SMA⁺ cells were seen not only associated with vascular structures, but also throughout tissue underlying the patch. (**Figure 3.4a-c**) Capillaries (vWF⁺ tubular structures) were visible in the region underlying the patch in control, low IGF-1, and high IGF-1 patched hearts. Comparatively, little α -SMA⁺ staining was evident in hearts receiving HGF patches. (**Figure 3.4d**) Furthermore, fewer vascular structures stained positive for vWF in HGF patched hearts compared to the other three groups. No EA53 positive staining was seen in any of the groups.

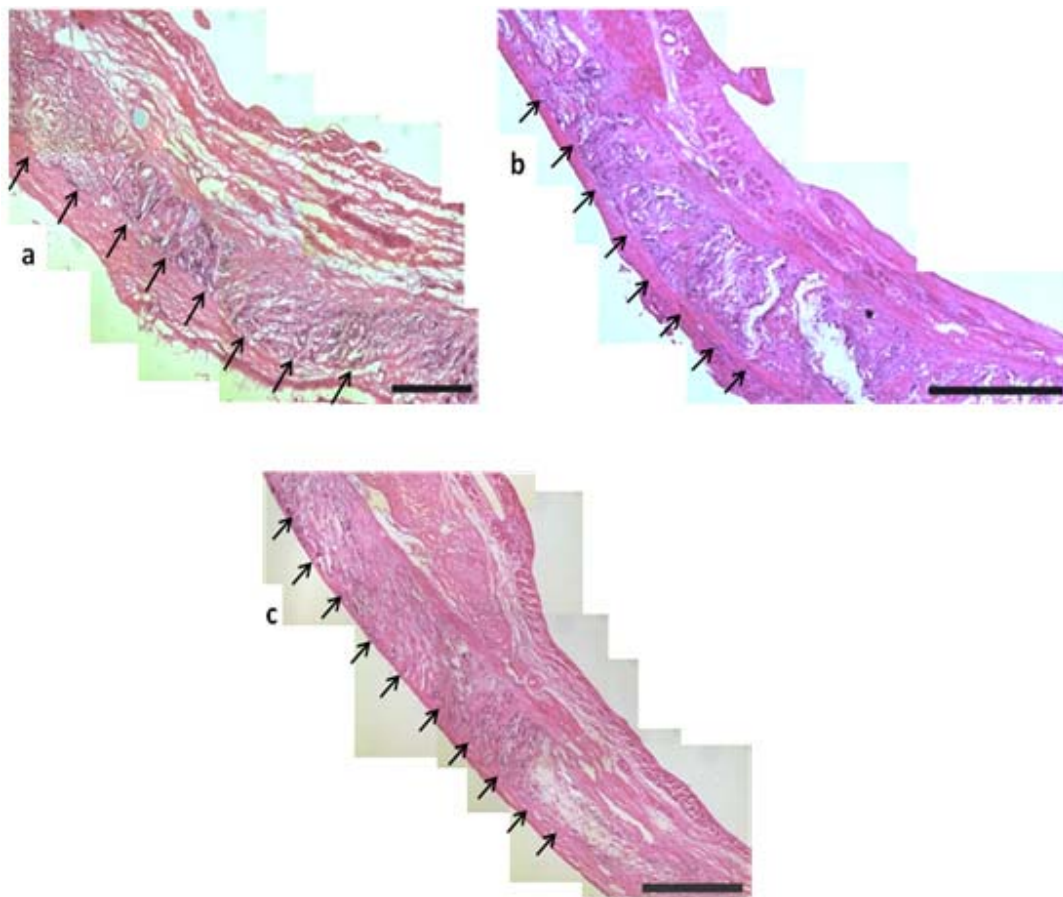


Figure 3.3: Representative histological sections of H&E staining of hearts receiving (a) high IGF-1, (b) control, and (c) HGF patches 8 weeks after implantation. Black arrows indicate patch. Scale bars are 500 μ m in all images.

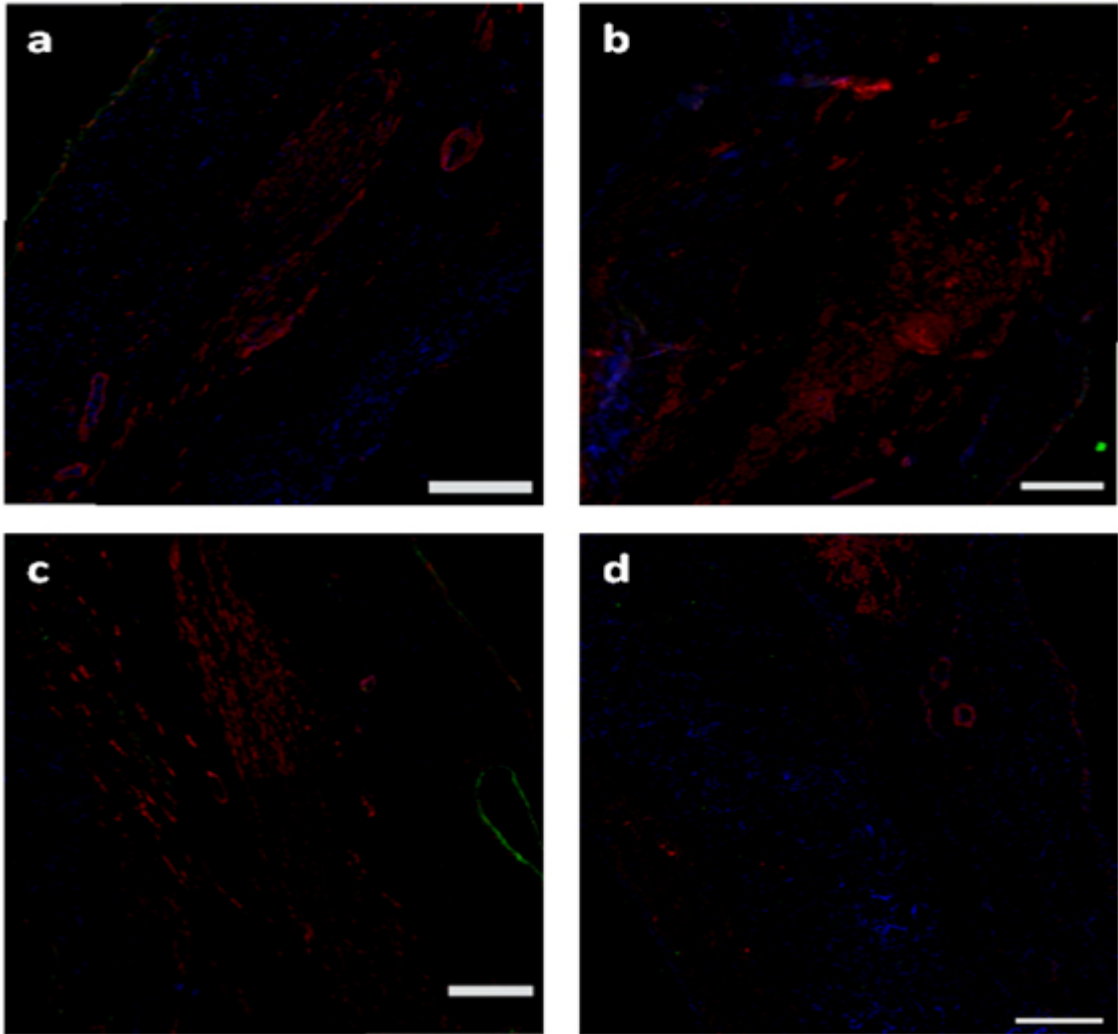


Figure 3.4: Smooth muscle bundles and capillaries in (a) patch control, (b) high IGF-1, (c) low IGF-1, and (d) HGF patched hearts. Red: α -SMA, Green: vWF, Blue: Hoechst dye (nuclear stain). Scale bars are 200 μ m in all images.

3.3.3 LV cavity size and contractile function

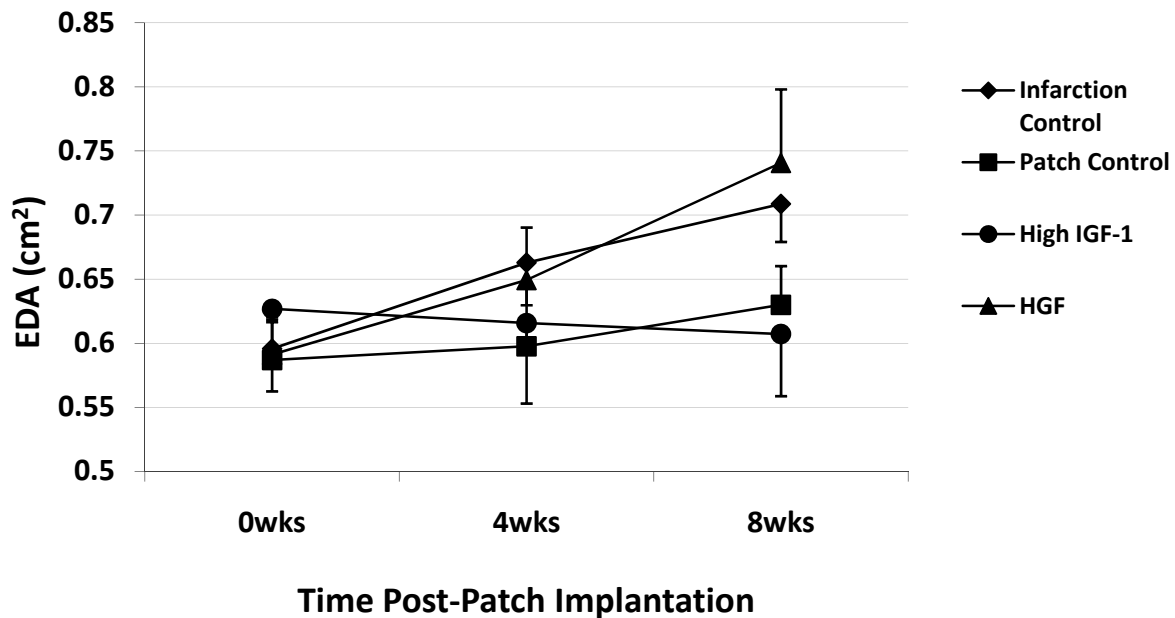


Figure 3.5: LV end-diastolic area (EDA) for infarction control, patch control, IGF-1, and HGF groups. EDA for the infarction control and HGF groups significantly increased at 8 weeks compared to 0 weeks (* $p < 0.05$). No significant difference in EDA was seen between experimental groups.

The patch control and high IGF-1 groups did not experience a significant change in EDA after patch implantation at any of the time points. The EDA of the infarction control and HGF groups were significantly increased at 8 weeks compared to the 0 week time point ($p < 0.05$). However, no significant difference in EDA was seen between the various groups. (**Figure 3.5**)

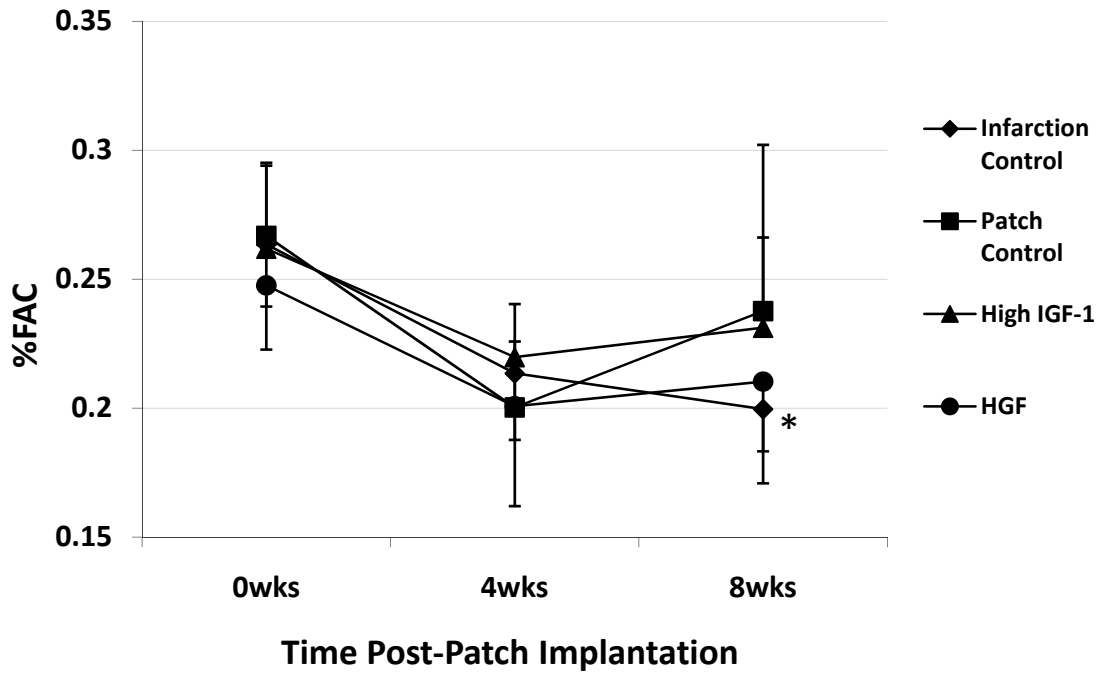


Figure 3.6: Fractional Area Change (%FAC) for infarction control, patch control, IGF-1, and HGF groups. %FAC for the infarction control significantly decreased at 8 weeks compared to 0 weeks (* $p < 0.05$). No significant difference in %FAC was seen between experimental groups.

A significant decrease in %FAC was seen at 8 weeks for the infarction control group compared to the 0 week time point ($p < 0.05$). No significant difference in %FAC was seen at any time points in any of the other groups following patch implantation. No significant difference in %FAC was seen between the various groups. **(Figure 3.6)**

3.4 DISCUSSION

Insulin-like growth factor-1 plays essential roles in embryonic and postnatal development of several organs and tissues [187], and IGF-1 knockout mice have been shown to suffer from severe disruption in skeletal muscle tissue formation [188]. In adults, IGF-1 has been implicated in several pathways in skeletal muscle formation and regeneration [2] and is expressed during the early and middle stages of muscle repair [188]. IGF-1 is involved in muscle regeneration through the inhibition of apoptosis [129, 188], the promotion of skeletal muscle cell proliferation and differentiation [188, 189], and the recruitment of stem cells to the site of injury [129]. In the cardiac milieu, it has been suggested that ventricular dilation following MI can be at least partially attributed to architectural changes in cardiomyocyte arrangement. The underlying mechanism of ventricular dilation can therefore be linked to cardiomyocyte death in the infarct zone [158]. Following MI, IGF-1 has been shown to stimulate hypertrophy and prevent death of cardiomyocytes, thereby attenuating ventricular dilation [158]. Furthermore, studies in patients with advanced chronic heart failure have demonstrated that the local expression of IGF-1 is considerably reduced in skeletal muscle and that this deficiency might contribute to loss of muscle bulk in congestive heart failure [129].

As such, research has focused on the administration of IGF-1 to senescent and injured muscle in order to repair and regenerate it. Experiments with IGF-1 overexpression have demonstrated IGF-1's role in protecting against aging in muscle. Transgenic mice overexpressing a local IGF-1 isoform under the control of strong skeletal-muscle regulator elements (mIGF-1) showed increased muscle mass with augmented muscle force generation compared to age-matched wild-type mice. Additionally, 2-year-old wild-type mice underwent muscle atrophy, while expression of the mIGF-1 transgene protected mice from loss of muscle

mass associated with senescence. Overexpression of the mIGF-1 transgene also preserved the regenerative capability of muscle tissues. [185]. Additionally, increased stem cell recruitment to sites of muscle injury was seen in mIGF-1 transgenic mice, and these cells exhibited increased myogenic differentiation [184]. In a mouse model of Duchenne's muscular dystrophy (*mdx*), supplemental expression of mIGF-1 increased muscle mass and force generation and decreased muscle necrosis in mIGF-1 *mdx* mice as compared to age-matched *mdx* mice [190]. Overexpression of IGF-1 in the heart of transgenic mice increased new cardiomyocyte formation and proliferation and opposed age-related alterations in cardiomyocytes. In addition, IGF-1 overexpression induced division, enhanced telomerase activity, delayed senescence, and preserved the reservoir of functional cardiac stem cells [186]. Finally, transgenic overexpression of IGF-1 was shown to promote engraftment, differentiation, and functional improvement when cells were transplanted into ischemic myocardium following MI [130-134].

Given the aforementioned results, research has emerged focusing on the sustained, local delivery of IGF-1 to ischemic myocardium via biomaterial scaffolds. To this end, biotinylated self-assembling peptide nanofibers have been used to deliver IGF-1 to ischemic myocardium, and in combination with cell therapy. Results suggest decreased apoptosis, increased cell growth, and improved systolic function [135]. IGF-1 has also been successfully incorporated into a number of biomaterials for enhanced bone regeneration [136-140]. These studies suggest that sustained, controlled delivery of IGF-1 may prove useful in a number of tissue engineering applications, including those in the cardiovascular arena. However, research towards the controlled release of IGF-1 in the cardiac arena is currently limited.

While preferential to endothelial and epithelial cells, hepatocyte growth factor is also expressed in normal and regenerating skeletal muscle tissues and plays a key role during the

early stage of muscle regeneration [188]. HGF elicits mitogenic, motogenic, and morphogenic activities during tissue development and regeneration and has been shown to have potent angiogenic and anti-apoptotic actions [121-123, 125]. HGF has been shown to activate quiescent satellite cells in primary culture. However, while leading to increased myoblast proliferation, HGF inhibited differentiation of myoblasts into myotubes, thereby confirming involvement in only the early stages of muscle regeneration [188]. In the cardiac milieu, it has been demonstrated that normal myocardium has low levels of HGF and HGF receptor, c-Met. However, upon isolation and cultivation, cardiomyocytes and cardiac endothelial cells upregulated c-Met mRNA and addition of HGF was shown to have a cytoprotective effect on cultured cardiomyocytes. Following MI, c-Met receptor mRNA and HGF mRNA were shown to increase in the heart. The increase in c-Met and HGF provided protection to cardiomyocytes and played a role in angiogenesis following MI [68, 157, 158]. Furthermore, in a rat model of ischemia-reperfusion injury, endogenous HGF reduced infarct area by suppressing cell death [191], thereby suggesting a therapeutic role of HGF in ischemic heart disease.

As such, research has focused on the administration of HGF to ischemic myocardium for its repair and regeneration. Mesenchymal stem cells have been shown to express HGF and c-Met, and HGF-stimulated chemotaxis in these cells has been shown to play an important role in MSC recruitment to sites of tissue regeneration [192]. In ischemic myocardium, HGF has been implicated in stem cell recruitment as well as in the differentiation of these stem cells to the cardiac lineage [124]. Local overexpression of adenovirus-encoded HGF in ischemic myocardium had anti-apoptotic effects on cardiomyocytes and induced angiogenesis. Furthermore, preservation of cardiac function and LV wall dimension along with improved LV wall thickness were demonstrated with local HGF overexpression [125]. Implantation of MSCs

overexpressing HGF into ischemic myocardium improved function, decreased scar size, and increased capillary number [68]. Furthermore, intravenous administration of soluble HGF following ischemia-reperfusion injury resulted in improved cardiac performance 8 weeks post-MI [157].

Given the aforementioned results, research has emerged focusing on the sustained, local delivery of HGF to ischemic myocardium. Following MI in a rat heart, the application of a gelatin sheet containing HGF over infarcts injected with skeletal muscle cells resulted in increased angiogenesis, decreased fibrotic area, and attenuation of LV dilation compared to controls [126]. Application of a polymer saturated with HGF to the infarcted anterior wall following MI in a rat model resulted in decreased scar size, decreased LV dimension, increased ejection fraction, and increased contractility [127]. These preliminary results suggest that a polymeric delivery system for HGF may prove successful in myocardial repair and regeneration. However, as with IGF-1 controlled release systems, research in this area is limited.

For this study, we implanted PEUU scaffolds containing IGF-1, HGF, or no growth factor into ischemic myocardium in order to repair and regenerate the myocardium following MI. Eight weeks post-patch implantation, LV wall thickness was evaluated through hematoxylin and eosin staining. The formation of smooth muscle bundles and capillaries was assessed histologically through α -SMA and vWF staining. Additionally, LV function was evaluated with echocardiography 4 weeks and 8 weeks post-patch implantation.

Implantation of cardiac patches containing IGF-1 showed no significant increase in LV wall thickness, formation of smooth muscle bundles, or capillary formation compared to patches without growth factor. Additionally, decrease in EDA due to IGF-1-loaded cardiac patches was not significant compared to control patches. Implantation of HGF-loaded cardiac patches

resulted in significantly decreased LV wall thickness compared to control and IGF-1 loaded patches; wall thickness in the HGF group was comparable to that of non-patched hearts (infarction control). Furthermore, HGF-patched hearts had significantly greater EDA at 8 weeks compared to the time of patch implantation, although this increase in EDA was not significant compared to IGF-1-loaded patches or control patches. No significant difference in %FAC was evident among any of the groups.

While significant differences in EDA were not seen between groups, IGF-1-loaded patches exhibited a trend towards improved EDA at 8 weeks post-patch implantation compared to control and HGF patches. HGF-loaded patches exhibited a trend towards increased EDA and decreased %FAC at 8 weeks post-patch implantation, although these results were also not statistically significant. Bearing in mind the small sample size (n=8 or n=9 per group), increasing the number of animals included in these studies would increase the power of the test and may yield a statistically significant result. Therefore, although the results of this study contradict our initial hypothesis, they should not be discounted. Trends towards improved EDA with IGF-1-loaded patches and trends towards worsened EDA and %FAC with HGF-loaded patches may warrant additional investigation.

Following failure of methods to quantify the release of growth factor from PEUU scaffolds *in vitro*, it was conjectured in Chapter 2 of this dissertation that the scaffold fabrication process may be altering protein conformation. As such, the *in vivo* efficacy of released growth factors may be diminished. Furthermore, IGF-1 and HGF have both been shown to have short half-lives and high clearance rates *in vivo* [126, 127, 138]. Therefore, increasing IGF-1 and HGF loading concentration in PEUU scaffolds may produce statistically significant results compared to control scaffolds and the growth factor-loaded scaffolds investigated in this study. However,

it should be noted that doubling IGF-1 concentration from 250 ng/mL to 500 ng/mL for this study showed no appreciable effect on LV wall thickness or smooth muscle and capillary formation.

Additionally, it has been suggested that the specific local isoform of IGF-1 used for myogenic repair plays a significant role in this repair (for example, using cIGF-1 instead of mIGF-1 proved detrimental) [2, 129]. As such, the possibility exists that the isoform of IGF-1 used in this study was not the optimal one for use in a rat model of MI. Further investigation into and understanding of the mechanistic actions of various IGF-1 isoforms, and more specifically, those implicated in myogenic repair in humans may provide insight into the development of a successful IGF-1-loaded cardiac patch.

Especially intriguing results of this study were the trends towards negative LV remodeling and function following the application of a HGF-loaded cardiac patch. Since HGF plays a key role in muscle regeneration at the early stage of repair and has been shown to inhibit differentiation of muscle cells to myotubes [188], a possible explanation could be that, in a subacute model of MI, HGF inhibits muscle repair. Additionally, it has been suggested that HGF is upregulated in response to acute inflammation following MI [193, 194]. As such, earlier administration of HGF following MI may prove beneficial compared to HGF administration in a chronic model of heart failure. While HGF is known to be a potent mediator of inflammation following MI [195], some inflammation in chronic heart failure may be beneficial in myocardial remodeling and repair. As such, over-suppression of this inflammatory response by the exogenous administration of HGF in the subacute phase may hinder the regeneration process. Therefore, rather than increasing concentration, decreasing HGF loading in cardiac patches may prove beneficial for myocardial repair and regeneration.

Although the results of this study disproved our initial hypothesis, the trends seen with various patch groups may warrant future investigation. Quantifying the *in vitro* controlled release of IGF-1 and HGF from PEUU scaffolds and verifying subsequent bioactivity of released protein (Chapter 2) will help direct efforts to determine optimal loading concentrations for *in vivo* application. Investigation into alternative methods for protein incorporation (such as chemical crosslinking of protein to the polymer matrix or dispersion of microspheres containing protein within the matrix) may prove beneficial in extending protein bioactivity upon release *in vivo*. Furthermore, elucidation of the mechanisms of action of these proteins and their various isoforms coupled with knowledge about optimal loading concentrations and conditions may shed light on the ideal formulation for a cardiac patch.

4.0 SPATIAL CONTROL OF GENE EXPRESSION VIA A BIODEGRADABLE POLYURETHANE

4.1 INTRODUCTION

In the last decade, the field of tissue engineering has emerged as an alternative to organ transplantation. Given the shortage of donor organs available and the number of patients awaiting transplant, researchers have turned to the use of cells and/or natural and synthetic biomaterials to repair and regenerate tissues and organs. Historically, materials used for this purpose have been inert structures aimed at promoting cell attachment for tissue repair [196]. Recently, however, matrices are being engineered to no longer be passive structures, but rather, scaffolds that actively promote tissue growth and development. Tissue engineered scaffolds are currently being employed to deliver growth factors, cytokines, and other signaling molecules to cells and as gene- and drug-delivery vehicles [197-203].

While tissue engineering aims to repair or regenerate a tissue or organ, researchers often simplify the process by overlooking the inherent complexity associated with a tissue type. Multiple cell types must perform specific functions in synchrony to form a functional tissue or organ structure. Embryogenesis demonstrates the commitment of cells to multiple cell fates in a well-regulated spatial and temporal manner. Growth factor gradients and spatial patterning of gene expression direct cell commitment, wound repair, and vascularization of tissues [104, 160-

164]. As such, tissue engineered constructs must provide a dynamic environment for the direction of cell fate in a spatially- and temporally-defined manner in order to most accurately mimic natural tissue development.

To this end, research is focusing on delivering signals to cells via tissue engineered constructs. Natural and synthetic scaffolds are being used for delivery of numerous growth factors including vascular endothelial growth factor (VEGF) and platelet-derived growth factor (PDGF) for pro- and anti-angiogenic therapies [30, 103, 104, 106]. Processes such as inkjet bioprinting allow for the spatial organization of growth factors on substrates like fibrin [204]. Alternatively, in lieu of growth factor presentation, polymers are being used for non-viral gene delivery, thereby allowing cells themselves to produce and deliver growth factors to the site of injury. Naturally-derived polymers such as collagen, its derivatives, and fibrin have been used for this purpose, as have synthetic polymers such as poly(ethylene imine) (PEI) [143, 145].

However, major limitations to the use of gene therapies are the efficiency of gene delivery and the spatial, as well as temporal, control of gene expression. Recently, inducer molecules capable of regulating the timing and level of gene expression in specific areas of the body have proven effective in managing therapeutic gene expression. Intrexon Corporation's RheoSwitch™ inducible gene expression technology system controls gene expression in this manner. By combining unique inducer and receptor molecules, this system allows the induction and adjustable control of gene expression in mammalian cells [151, 205].

The objective of this work was to develop a biodegradable, elastomeric poly(ester urethane) urea (PEUU) scaffold capable of releasing inducer molecules over a period of time, and in a spatially-defined manner, to control gene expression in a tissue engineered construct. Such a construct would demonstrate the ability to drive sub-populations of precursor cells on a

scaffold towards one lineage and others down different pathways in a spatially-defined manner and would be attractive for use in soft tissue applications due to its tunable mechanical properties. Polymer films from solvent casting and porous scaffolds from a thermally induced phase separation process were fabricated with and without inducer molecule, as were films and scaffolds with spatially-defined regions containing or omitting inducer molecule. Cells cultured on films and within scaffolds were evaluated for control of gene expression via the polymer, and specifically, for spatial control of gene expression.

4.2 METHODS

4.2.1 Cells

A single-vector RheoSwitch® for hrGFP (humanized Renilla GFP) expression with a neomycin (Neo) selection marker and insulators flanking the whole cassette of switch components and Neo was tested in transient transfections in B16 cells (melanoma cell line derived from C57BL/6 mice). Stable clones of B16-hrGFP cells were obtained by selection in medium containing 400 ug/mL G418 sulfate. These clones have been tested for induction of hrGFP by treatment with the RheoSwitch® ligand RSL1. The vector used for this purpose was built on pRG-1012b, and is named pRG-1012b-hrGFP. **(Figure 4.1)**

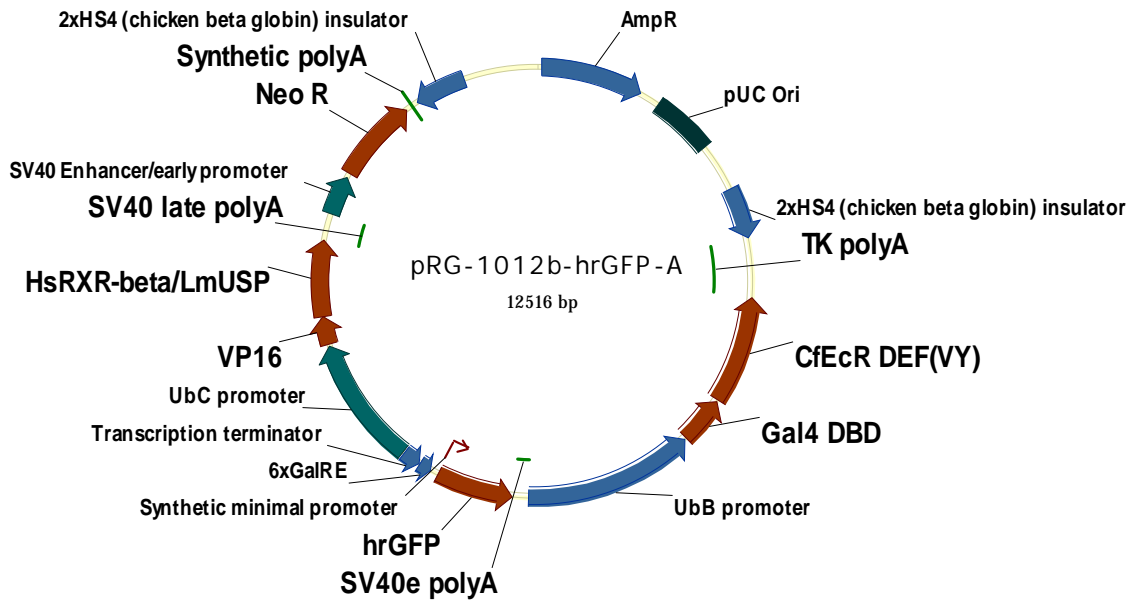


Figure 4.1. Vector map for pRG-1012b-hrGFP.

B16 cells were maintained in growth medium, RPMI-1640 supplemented with FBS, gentamycin, G418 sulfate, non-essential amino acids, and beta-mercaptoethanol. To induce gene expression, varying concentrations of ligand were added directly to growth medium. Gene expression was visualized using fluorescent microscopy.

4.2.2 Polyurethane synthesis

Poly(ester urethane) urea based on polycaprolactone diol (MW 2000, Aldrich), butane diisocyanate (Fluka), and putrescine (Aldrich) was synthesized in a two-step solution polymerization as previously reported [169]. The stoichiometry of the reaction was 2:1:1 BDI:PCL:putrescine. (See Chapter 2 for details on polymer synthesis.)

4.2.3 Preparation of RSL1-loaded PEUU films

PEUU was dissolved in DMSO at 80°C to make a 2 wt% polymer solution. RSL1 ligand stock solution was made in DMSO. Predetermined amounts of ligand (0-150 μM) were added to polymer solutions and cast into 24 well tissue culture or glass bottom plates (MatTek Corp). (See Chapter 2 for details on the fabrication of ligand-loaded polymer films.)

4.2.4 Gene expression via PEUU films

B16 cells were plated directly onto polymer films containing varying concentrations of RSL1 ligand (1-10 μM) on glass bottom plates with culture media exchange every 3-4 days. PEUU films without ligand served as a negative control. Gene expression was visualized with fluorescent microscopy using an Olympus Fluoview 1000 inverted confocal microscope (Center for Biologic Imaging, University of Pittsburgh) and quantified with the use of MetaMorph imaging data analysis software.

4.2.5 Preparation of RSL1 loaded PEUU scaffolds

Three-dimensional scaffolds were fabricated by a thermally-induced phase separation method as previously described [170]. To fabricate ligand-loaded scaffolds, RSL1 ligand in DMSO was added to the 8 wt% polymer solution at 80°C to yield a 10 µM final ligand concentration. Scaffolds without ligand served as a negative control. (See Chapter 2 for details on scaffold fabrication.)

4.2.6 Seeding PEUU scaffolds with B16 cells

B16 cells were seeded onto PEUU scaffolds fabricated with and without RSL1 ligand to demonstrate the ability of the constructs to elicit gene expression. Cylindrical constructs were cut to produce discs 0.5 mm in thickness. Scaffolds were sterilized under UV light for 20 minutes in a biological cabinet. Cells were seeded onto scaffolds at a density of $\sim 5 \times 10^6$ cells/scaffold using a filtration seeding method [206]. Cell-seeded scaffolds were then placed in spinner flask cultures containing B16 growth medium for up to 7 days. At predetermined time points, scaffolds were fixed with 10% formalin, incubated in sucrose, sectioned at 12 µm, stained with a nuclear dye (Hoechst no. 33258, Sigma), and mounted onto slides. Cells and GFP expression were visualized with fluorescent microscopy using an Olympus Fluoview 1000 inverted confocal microscope (Center for Biologic Imaging, University of Pittsburgh), and gene expression was quantified using MetaMorph imaging data analysis software.

4.2.7 Spatial control of gene expression on PEUU films

A 2 wt% PEUU solution in DMSO was obtained as described in Chapter 2. RSL1 ligand in DMSO was added to half of the polymer solution to yield a 10 μM final ligand concentration. Polymer solution without ligand served as a negative control. Droplets (20 μL s each) of PEUU with RSL1 and PEUU without RSL1 were pipetted onto glass microscope slides in a spatially-defined pattern (**Figure 4.2**) and allowed to dry under vacuum. Once solvent was evaporated, another droplet was placed on top of the existing one. In total, five droplets of polymer solution (i.e. 5 x 20 μL s) were placed at each predetermined spot on each microscope slide. Slides were incubated overnight in PBS to remove surface-bound ligand and then sterilized under UV light for 20 minutes. B16 cells were plated onto slides and cultured in Petri dishes for up to 72 hours with culture medium exchange every 24 hours. At predetermined time points, slides were fixed with 2% paraformaldehyde and stained with Hoechst no. 33258 to visualize cell nuclei. Gene expression was visualized with fluorescent microscopy and quantified using MetaMorph imaging data analysis software.

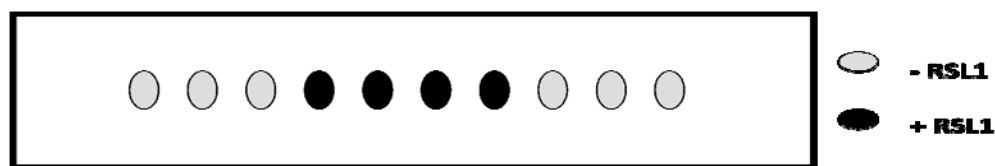


Figure 4.2: Typical slide layout for 2-dimensional spatial control experiments.

4.2.8 Spatial control of gene expression in PEUU scaffolds

An 8 wt% PEUU solution containing RSL1 was obtained as described in Chapter 2. A cylindrical glass mold consisting of an outer glass tube (inner diameter 10 mm) and an inner glass cylinder (outer diameter 4.5 mm) coaxially fixed with rubber stoppers was used. PEUU solution was injected into the space between the two glass cylinders, and immediately subjected to the TIPS method. Once the scaffold was vacuum-dried, it was placed back into the outer cylindrical glass mold. An 8 wt% PEUU solution containing 10 μ M RSL1 was injected into the hollow center of the scaffold, and the TIPS method was repeated. The final scaffold was comprised of a PEUU center with 10 μ M RSL1 and a PEUU outer ring without RSL1. B16 cells were filtration seeded onto the scaffold and cultured as described above.

4.3 RESULTS

4.3.1 Gene expression via media manipulation

B16 cells cultured in growth medium without RSL1 ligand exhibited no GFP expression. GFP expression was evident in all cells cultured in growth medium containing varying concentrations of ligand (1-150 μ M) 48 hours post-RSL1 administration. **(Figure 4.3)**

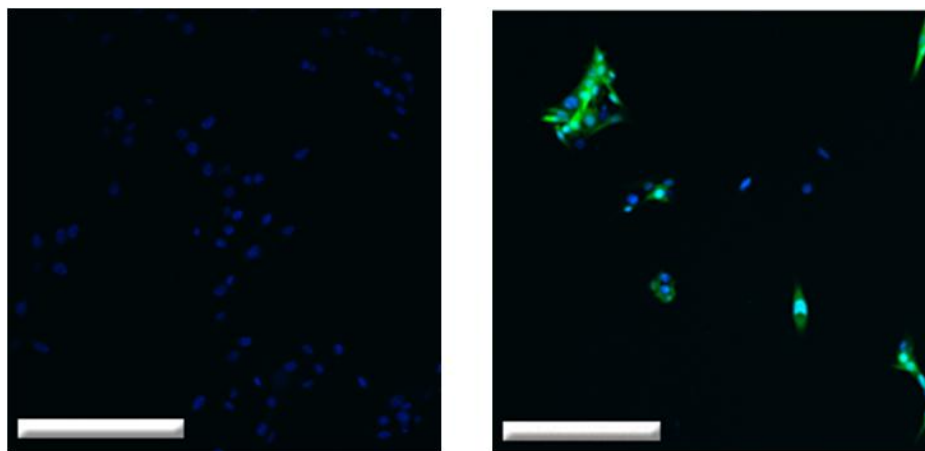


Figure 4.3: Gene expression via media manipulation. 48 hours post-RSL1 administration, cells in growth medium without ligand did not express GFP (left), while cells in growth medium containing 1-5 μM ligand expressed GFP (5 μM concentration shown on right). Scale bars = 500 μm .

4.3.2 Gene expression via PEUU films

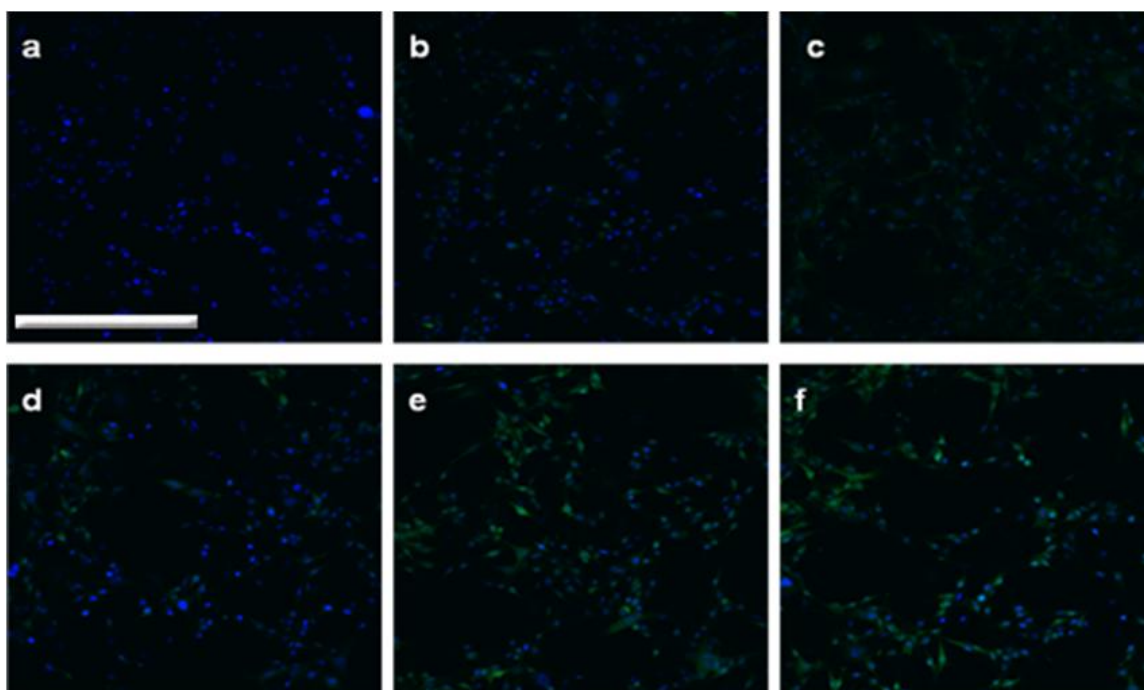


Figure 4.4: Gene expression on PEUU films containing (a) 0 μM , (b) 1 μM , (c) 2 μM , (d) 3 μM , (e) 4 μM , and (f) 5 μM RSL1. Blue: nuclear stain, Green: GFP. Scale bar = 500 μm for all images.

B16 cells cultured directly on PEUU films containing 1-10 μM RSL1 expressed GFP for up to 21 days *in vitro*, while cells cultured on films without ligand did not express GFP. (**Figures 4.4 and 4.5**) Furthermore, cells cultured on films containing 0-5 μM RSL1 demonstrated dose-dependent GFP expression over this time. MetaMorph analysis confirmed a dose-dependent response in these cells. (**Figures 4.6 and 4.7**)

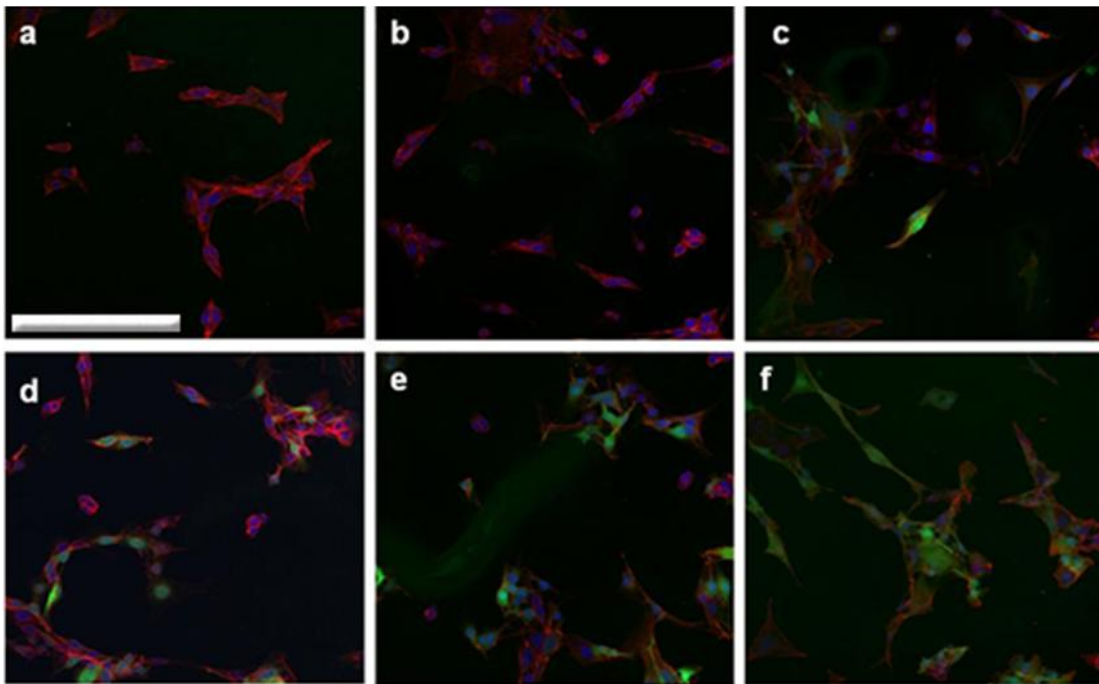


Figure 4.5: Gene expression on PEUU films containing (a) 0 μM , (b) 1 μM , (c) 3 μM , (d) 5 μM , (e) 7 μM , and (f) 10 μM RSL1. Blue: nuclear stain, Red: phalloidin, Green: GFP. Scale bar = 250 μm for all images.

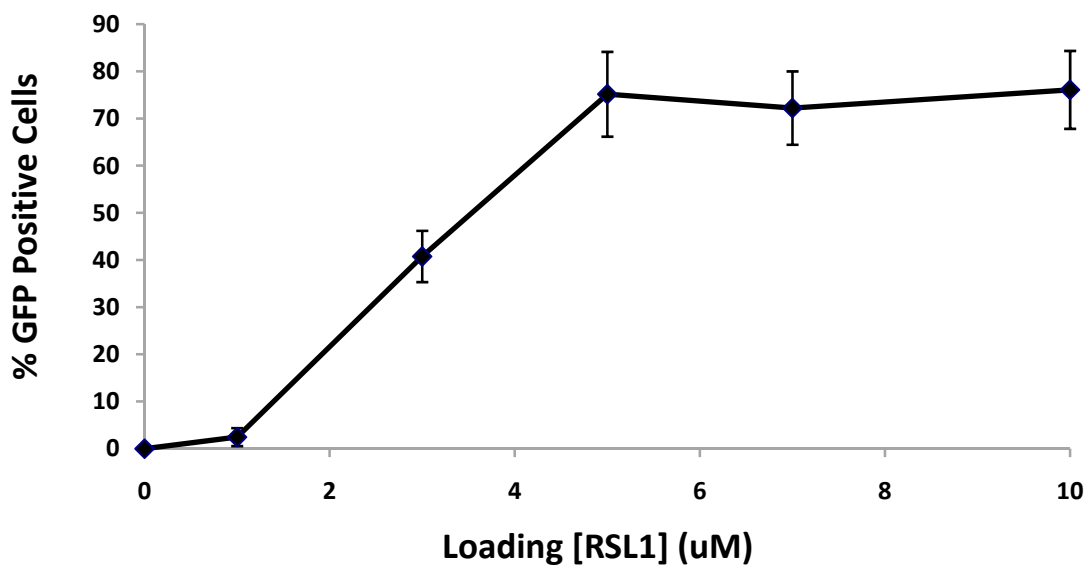


Figure 4.6: Dose-dependent GFP expression in cells on PEUU films containing 0-10 μM RSL1.

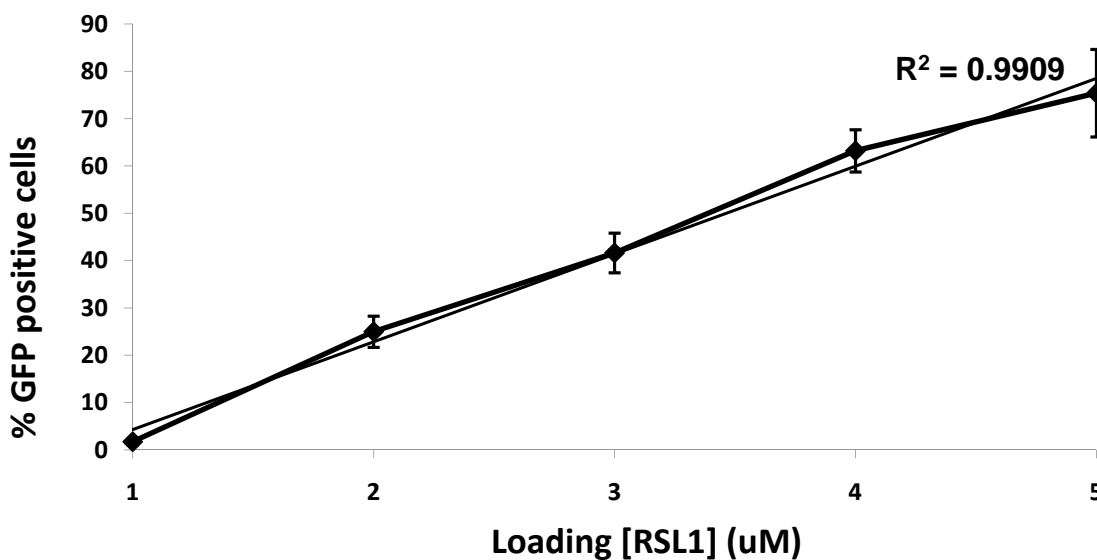


Figure 4.7: Dose-dependent GFP expression in cells on PEUU films containing 1-5 μM RSL1.

4.3.3 Gene expression in TIPS scaffolds

48 hours after cell seeding, cells were found on the surface and interior of PEUU scaffolds and PEUU scaffolds containing RSL1 ligand. Fluorescent microscopy confirmed the presence of cells throughout scaffolds. Cells cultured in scaffolds without RSL1 did not express GFP, while cells cultured in scaffolds with ligand expressed GFP. **(Figure 4.8)**

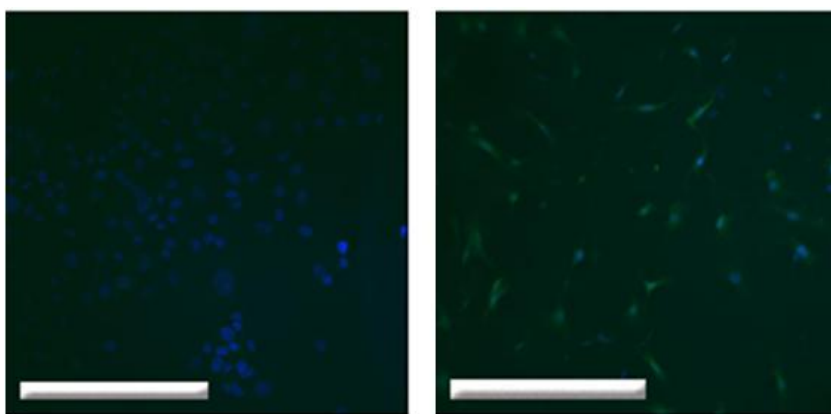


Figure 4.8: Cells within TIPS scaffolds without RSL1 did not express GFP (left), while cells within scaffolds containing RSL1 expressed GFP. Scale bars = 500 μm .

4.3.4 Spatial Control of gene expression on PEUU films

24 hours after cells were plated onto microscope slides containing distinct regions of polymer with and without RSL1, all cells expressed GFP. 48 and 72 hours after cell seeding, however, cells in regions where polymer contained ligand expressed GFP, whereas cells in regions where ligand was omitted from polymer did not express GFP. **(Figure 4.9)** Varying the spatial

patterning of droplets on microscope slides had no effect on this spatially-defined gene expression; regardless of proximity of droplets, and the number of concurrent droplets with or without RSL1, a distinct difference was maintained in whether cells expressed GFP or not following the initial burst phase of ligand release. However, while proximity of droplets did not affect gene expression, it is important to note that droplets had to be distinct from one another. When droplets with and without RSL1 bled into one another, distinct regions of gene expression were no longer detected, and all cells expressed GFP.

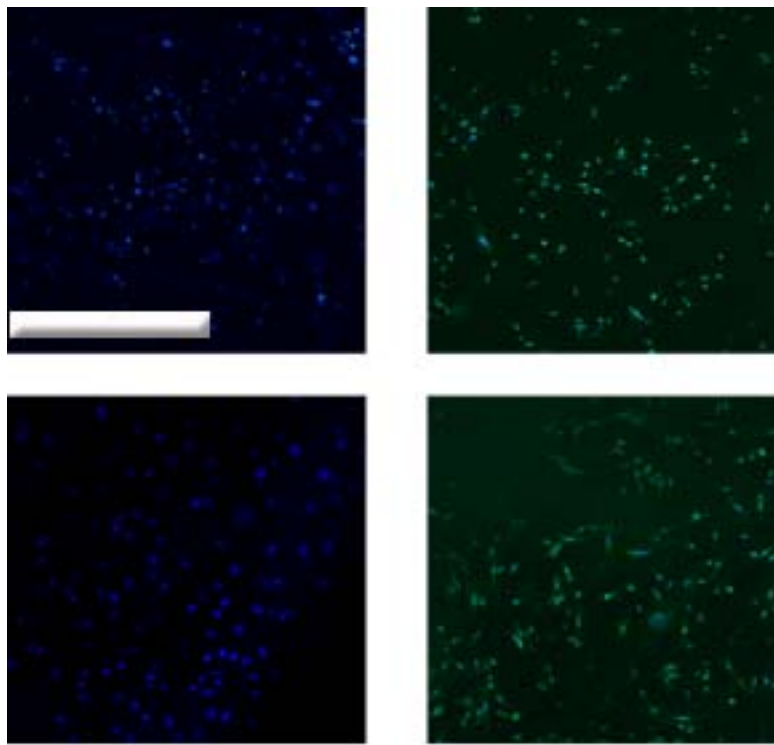


Figure 4.9: Cells on sections of slides containing PEUU without ligand did not express GFP (left), whereas cells on sections of slides containing PEUU loaded with RSL1 clearly expressed GFP (right), thereby demonstrating spatial control of gene expression via 2-dimensional PEUU films. Scale bar = 500 μm for all images.

4.3.5 Spatial control of gene expression in TIPS scaffolds

24 hours, 48 hours, and 5 days after cells were seeded onto TIPS scaffolds with spatially-defined regions containing and omitting RSL1, cells were seen throughout scaffolds using fluorescent microscopy. Cells in the center of the scaffold (containing ligand) expressed GFP, whereas cells in the outer ring (without RSL1) did not express GFP. (**Figure 4.10**)

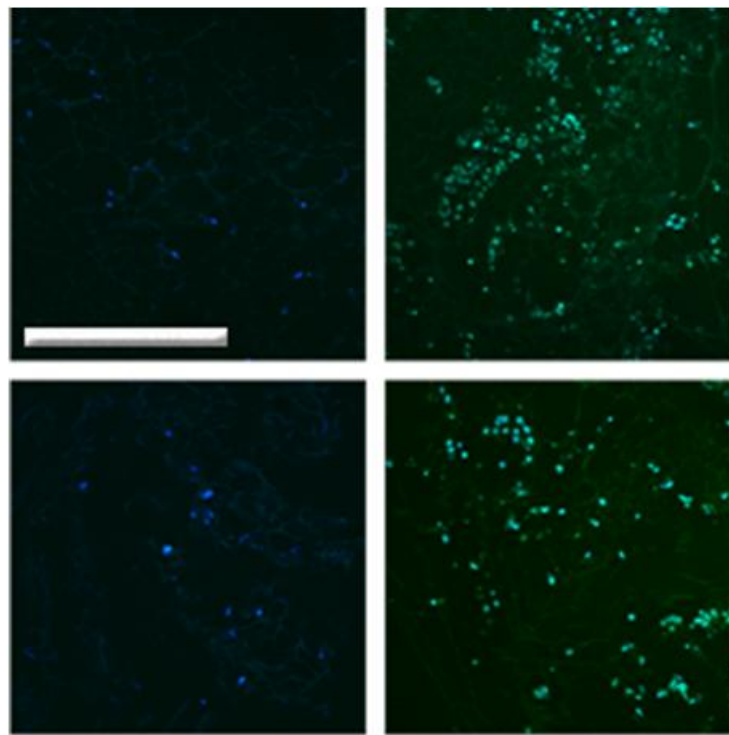


Figure 4.10: Spatial control of gene expression within 3D PEUU scaffolds. Cells in the outer ring of the scaffold, where ligand was omitted, did not express GFP (left), whereas cells in the center of the scaffold, which contained RSL1, clearly expressed GFP (right), thereby demonstrating spatial control of gene expression within a 3-dimensional PEUU scaffold. Scale bar = 500 μm for all images.

4.4 DISCUSSION

Spatial patterning of growth factors and transcription factors is known to determine cell fate during embryogenesis and throughout life. Early patterning of regulatory proteins has been implicated in animal pole determination in the oocyte and definition of the inner cell mass and trophoblast in the early embryo [207]. Subsequent dorso-ventral patterning in the embryo leads to stripe-shaped territories that will later become distinct tissues [208, 209]. Epithelial-to-mesenchymal transitions resulting in migration of cells to new areas of the embryo and their differentiation to new tissues are governed by a host of morphogens, their transcription factors, and interconnecting signaling pathways [210]. Furthermore, spatial patterning of factors is known to play a key role in wound healing [211, 212] and in epithelial-to-mesenchymal and mesenchymal-to-epithelial transitions in cancer and fibrotic disease [210]. As such, a tissue engineered construct capable of directing cell differentiation and behavior on a scaffold, in a spatially-defined manner, would most precisely mimic native tissue development.

An emerging technology to spatially control cell behavior is bioprinting, a range of deposition processes for two- and three-dimensional patterning of biomaterials and/or biologic molecules onto surfaces [213]. Growth factors, such as bone morphogenetic protein-2 and fibroblast growth factor-2 have been successfully inkjet printed onto fibrin substrates to spatially direct cell differentiation, proliferation, and migration [101, 204, 214]. Furthermore, researchers have demonstrated micropatterning of proteins and cells onto biomaterial surfaces using photolithography and other techniques [215-217]. One such example is the patterning of laminin lanes onto elastomeric polyurethanes and PLGA to control the three-dimensional spatial organization of layers of cardiomyocytes *in vitro* [99, 100]. Other approaches to spatially control growth factor presentation within a tissue-engineered construct have included attempts to

regulate the spatiotemporal availability of pro- and anti-angiogenic factors such as VEGF, PDGF, basic fibroblast growth factor, angiopoietin-1 & 2, and thrombospondin in order to control vessel density, size, and maturity [104]. Natural materials such as collagen, hyaluronic acid, fibrin, and alginate have been used for this purpose [218], as have synthetic polymers such as poly(lactic acid) (PLA), poly(glycolic acid) (PGA), and their copolymers (PLGA) [104, 218].

In lieu of growth factor presentation via a tissue-engineered construct, the use of polymers for non-viral gene delivery has been demonstrated. This approach allows cells themselves to produce the gene(s) of interest, thereby driving cell differentiation and proliferation *in vivo*. Synthetic polymers such as poly(ethylene imine) (PEI) [143, 145] and copolymers of PEI with poly(ethylene glycol) (PEG) [147] and poly(N-isopropylacrylamide) (PNIPAm) [146] have been used as delivery vehicles for plasmid DNA. Limitations to the use of these systems include plasmid degradation upon *in vivo* delivery and precise control over localized cellular protein production *in vivo*.

Alternatively, gene-regulating systems such as the tetracycline-dependent system have proven effective in the control of gene expression in cells, and the use of tetracycline-dependent molecular switches to regulate transcription has become popular in control of mammalian gene expression [153]. However, limitations to the use of these systems include the efficiency of gene delivery, the spatiotemporal control of gene expression, high background gene expression due to leaky switches, and the immunogenicity and side effects of molecules used as inducers [153]. Recently, Intrexon Corporation's RheoSwitchTM inducible gene expression technology system has emerged as a means of controlling gene expression through inducer molecules capable of regulating the timing and level of gene expression. The system is built on a synthetic receptor composed of two proteins, RheoReceptor-1 and RheoActivtor that dimerize. In the absence of

inducer molecule, RheoSwitch Ligand RSL1, the receptor represses transcription. When RSL1 ligand is added to the system, it binds to RheoReceptor-1, thereby changing its conformation, releasing bound negative regulatory cofactors, and stabilizing the heterodimer, resulting in a highly induced transcriptional state [151, 155, 205].

High induction coupled with very low basal expression make this system superior to others, such as the tetracycline-regulated gene expression system. RSL1 induces gene expression over a broad range of concentrations in a dose-dependent manner similar to a rheostat device, thereby granting more precise control over expression levels when compared with other systems. Additionally, since RSL1 and the engineered receptor proteins are synthetic and non-steroidal, they cannot be detected by mammalian nuclear receptors, rendering the molecules inert and without side effects in host cells [151, 155, 205]. Furthermore, the ability to transfect cells for use with this system affords researchers great flexibility. Depending on the tissue engineering application at hand, researchers can determine the ideal cell source for tissue repair and regeneration, obtain cells from the patient, a donor, or off-the-shelf, transfect them to express the gene of interest, and then use the RheoSwitchTM system to control levels of gene expression *in vivo* for tissue repair and regeneration. This strategy proves especially attractive for embryonic and other stem cell applications given the multipotentiality of these cells. The RheoSwitchTM system provides a possible means to drive subpopulations of cells to multiple lineages within a single tissue by spatially and temporally controlling gene expression in these cells. Therefore, the combination of this system with a biomaterial scaffold to spatially and temporally control gene expression *in vivo* may prove attractive for tissue engineering applications compared to the local delivery of plasmid or cells alone. Given the aforementioned advantages of this system over others for the control of gene expression, the present study

focused on the use of a biodegradable, elastomeric polyurethane scaffold as a controlled-release system for the delivery of RSL1 inducer molecule for the spatiotemporal regulation of gene expression *in vitro*.

Direct culture of B16 cells on the surface of PEUU films and within three-dimensional PEUU scaffolds confirmed the ability to control gene expression via controlled release from the polymer. Gene expression on PEUU films containing varying concentrations of RSL1 demonstrated a dose-responsive system on which cells could be directly cultured. Spatial control of ligand presentation, and subsequent spatially-organized gene expression, were achieved in PEUU films and three-dimensional scaffolds by selectively incorporating and omitting RSL1 from regions of polymer. After 48 hours in culture, B16 cells plated on regions of microscope slides with PEUU loaded with RSL1 expressed GFP, whereas B16 cells on regions with PEUU alone clearly did not. It is important to note that spatial control of gene expression could be achieved only during the second phase of ligand release in static culture; the initial burst likely saturated culture supernates and resulted in GFP expression in all cells. This limitation was not evident with three-dimensional scaffolds in dynamic culture. Even at 24 hours post-cell seeding, cells in the center of the scaffold, containing RSL1, expressed GFP, whereas cells in the outer ring, without ligand, did not. This spatial control of gene expression was evident out to five days in culture. It is hypothesized that dynamic culture of these cells in a spinner flask results in a large enough sink to eliminate the effects of diffusion of RSL1 from regions of polymer containing RSL1 to regions omitting it.

A spatially-controlled dose-dependent response in PEUU films and scaffolds was not investigated for these studies. Incorporating varying amounts of ligand in spatially-defined regions of polymer films and scaffolds and subsequently demonstrating not only spatial, but also

dose-dependent response in cells would demonstrate development of a highly sophisticated system for the control of gene expression. Such a polymeric controlled release system may have application *in vivo* for the development of complex tissue architectures with highly defined spatial and temporal control over gene expression.

Further studies are needed to determine optimal loading concentration of RSL1 ligand and subsequent release profiles for *in vivo* application. Studies evaluating *in vivo* functionality of this polymeric inducible gene expression system are also necessary. However, we have successfully demonstrated the development of a 3-dimensional polymer scaffold capable of spatially-controlling gene expression in cells *in vitro*. These scaffolds have mechanical properties desirable for soft tissue engineering applications and may provide a means to control progenitor cell commitment in a spatially-defined manner *in vivo* for soft tissue repair and regeneration.

5.0 CONCLUSIONS

The overarching goal of this research was to develop polymeric controlled release systems for use in cardiovascular regenerative medicine applications. A biodegradable, elastomeric poly(ester urethane)urea was investigated *in vivo* as a cardiac patch capable of the sustained and controlled delivery of insulin-like growth factor-1 and hepatocyte growth factor to ischemic myocardium for its repair and regeneration following myocardial infarction. This biodegradable elastomer was further investigated *in vitro* for the spatially-defined, sustained and controlled delivery of molecules designed to induce cellular gene expression.

A biodegradable, elastomeric PEUU with physical and mechanical properties appropriate for the repair and regeneration of the myocardium and other soft tissues was successfully synthesized for this research. This polymer was fabricated into 2-dimensional films and porous 3-dimensional scaffolds incorporating RheoSwitch Ligand RSL1, IGF-1, and HGF. The sustained and controlled release of RSL1 from PEUU was successfully quantified *in vitro*, thereby demonstrating the successful development of a controlled release system for molecules designed to elicit gene expression. Methods used to quantify IGF-1 and HGF release from scaffolds proved ineffective. However, experiments utilizing degradation solutions from polymer containing each of these growth factors elicited positive cellular responses when

transferred from films and scaffolds to cells in culture, thereby demonstrating the successful incorporation of these factors into the polymer matrix and their bioactivity upon release from the polymer (Chapter 2).

IGF-1 and HGF have both been implicated in the heart's intrinsic response to MI [129, 158]. IGF-1 plays a key role in muscle cell commitment, cell proliferation, and regeneration following injury [2, 128, 129], and HGF is a potent angiogenic and anti-apoptotic factor that plays a key role in the regulation of inflammation following MI [121-123]. It was thus postulated that the application of a PEUU scaffold containing either IGF-1 or HGF to the left ventricle following MI would stem LV dilation and restore contractile function more effectively than the application of a scaffold without growth factor. While *in vitro* assays confirmed the bioactivity of both growth factors upon release from scaffolds, PEUU scaffolds containing growth factor showed no significant benefit over scaffolds without growth factor *in vivo*. While these results do not support our initial hypothesis, they should not be ignored or discarded (Chapter 3). It is the hope of the author that these findings will provide the basis for future research on controlled release cardiac patches for myocardial repair and regeneration and provide a means for the successful treatment of ischemic heart disease.

In addition to the aforementioned *in vivo* investigations, the delivery of RSL1, a ligand designed to induce cellular gene expression, to cells in a spatially-defined manner via polymer constructs in order to spatially control gene expression *in vitro* was investigated. We successfully demonstrated the spatial control of gene expression on 2-dimensional PEUU films and within 3-dimensional PEUU scaffolds through the deliberate inclusion and omission of inducer molecule from regions of the polymer (Chapter 4). This research may provide significant contributions to the use of controlled release PEUU scaffolds to regulate

spatiotemporal control of gene expression for gene therapies and may provide a means for directing a population of precursor cells within a single construct to multiple lineages for the successful engineering of complex tissues.

5.1 FUTURE DIRECTIONS

5.1.1 Quantification of the *in vitro* release kinetics of IGF-1 and HGF

While *in vitro* bioactivity assays support the conclusion that IGF-1 and HGF are released in a sustained and controlled manner from PEUU scaffolds, elucidation of the kinetics of growth factor release may prove useful in the successful design of these controlled release systems for *in vivo* tissue engineering applications. Since it is the author's belief that the polymer fabrication process is altering the conformation of IGF-1 and HGF, thereby rendering the proteins unrecognizable by the antibodies used in the commercially-obtained ELISA kits, a panel of antibodies could be examined for their recognition of released IGF-1 and HGF through Western analysis. Once antibodies specific to released protein are identified, they could be used to develop custom ELISAs for the quantification of released IGF-1 and HGF. Alternatively, IGF-1 and HGF could be radiolabeled with ^{125}I prior to incorporation into the polymer matrix. A β counter could be used to quantify radioactivity of degradation solutions, thereby quantifying ^{125}I -IGF-1 and ^{125}I -HGF content in degradation solutions. Since the second method will most likely prove more time-efficient, our group is currently taking steps to obtain radiolabeled protein.

Additionally, investigation into scaffold fabrication and the subsequent development of a method to avoid addition of growth factor while polymer solution is at a high temperature may yield better results both *in vitro* and *in vivo*. Chemical crosslinking of proteins to the polymer or microencapsulation of proteins within the polymer matrix may better protect protein, not only yielding *in vitro* release data, but also improving growth factor bioactivity *in vitro* and *in vivo*.

5.1.2 Development of IGF-1- and HGF-loaded PEUU patches for myocardial repair

Better understanding of the *in vivo* results from investigations with IGF-1- and HGF-loaded patches would help in successfully designing a controlled release cardiac patch for myocardial repair and regeneration. While no significant differences were noted between patched groups, a trend towards improved LV EDA was seen with IGF-1-loaded patches versus patches without growth factor. Trends towards worsened LV EDA and decreased %FAC were observed for HGF-loaded patches versus IGF-1-loaded patches and patches without growth factor. As an initial step, increasing the number of animals used for these studies would improve the power of the test and may yield statistically significant results.

Further investigations into optimal loading concentrations of IGF-1 and HGF may also lend insight into the successful use of this controlled release system for myocardial repair and regeneration. While the concentrations of IGF-1 and HGF used in these studies were selected based on previously published studies, the *in vitro* results suggest that a change in protein conformation may be occurring during the scaffold fabrication process. While a loss in bioactivity is not evident *in vitro*, these changes may affect *in vivo* efficacy of the proteins. It is hypothesized that increasing IGF-1 loading concentration in scaffolds may prove more effective

through increased muscle cell commitment and proliferation. Conversely, it is hypothesized that decreasing HGF loading concentration in scaffolds may prove more effective through attenuation of suppression of inflammation, as inflammation may play a crucial role in myocardial repair. *In vivo* studies evaluating various loading concentrations of IGF-1 and HGF will be useful in determining whether loading concentration impacts myocardial repair and regeneration. In addition, it has been suggested that the specific isoform of IGF-1 used *in vivo* plays a crucial role in the effectiveness of this growth factor. As such, the *in vivo* investigation of the controlled release of various isoforms of IGF-1 and HGF may prove successful in development of an IGF-1- or HGF-loaded cardiac patch.

Furthermore, studies combining IGF-1 and HGF within a single patch may shed light on the synergistic effects of these growth factors and prove more successful for myocardial repair than the application of each growth factor alone. The controlled release of growth factors implicated in muscle repair and regeneration, progenitor cell commitment to the cardiac lineage, regulation of inflammation, or angiogenesis may also prove effective for myocardial repair. A plethora of growth factors exists for investigation with a controlled release cardiac patch. Synergistic effects between several of these factors may also prove more effective than release of any one factor alone.

Finally, the combination of mechanical support from the polymer, biomolecules to direct cell behavior, and any of the cell populations shown to improve myocardial function through direct injection (Chapter 1) may prove more beneficial than the application of any of these alone. Skeletal muscle precursor cells (skeletal myoblasts and muscle-derived stem cells) may respond preferentially to IGF-1 due to its role in muscle cell commitment, proliferation, and repair following injury, and endothelial cell populations may respond preferentially to HGF due to its

role in angiogenesis. As such, a cardiac patch containing IGF-1 and skeletal muscle precursor cells, a patch containing HGF and endothelial cells, or a patch containing both factors and several cell populations may more effectively repair ischemic myocardium when compared to the IGF-1- and HGF-loaded patches examined for this research.

5.1.3 Development of angiogenic and myogenic growth factor-loaded PEUU patches for myocardial repair

Efforts to repair infarcted myocardium have examined the delivery of various angiogenic and myogenic growth factors following MI. VEGF serum levels have been shown to increase following MI and decrease following reperfusion therapy, indicating VEGF's involvement in the heart's healing process [219]. VEGF is known to be a potent angiogenic factor, and its beneficial effects following MI have been demonstrated [32]. Administration of VEGF and its isoform VEGF-165 have been shown in animal models of acute MI to decrease infarct size, increase hyperplasia and mitotic activity in myocardial cells, and increase angiogenesis [32, 219]. It has further been postulated that VEGF recruits hematopoietic and endothelial cells to sites of myocardial injury, thereby accelerating healing by promoting cardiomyogenesis [219]. *In vitro*, VEGF-165 has been shown to induce angiogenic sprouting in murine aortic ring cells cultured on matrigel [220] and human myocardial endothelial cells cultured on fibrin [221].

In addition to VEGF, a number of other growth factors have been evaluated for their potential role in myocardial repair following MI. The *in vitro* effects of erythropoietin on the angiogenic sprouting of the murine aortic ring and human myocardial endothelial cells have been shown to be comparable to that of VEGF [220, 221]. FGF2, another potent angiogenic factor,

has been implicated in increased fibroblast, endothelial, and smooth muscle cell proliferation, collagen deposition, enhanced cardiomyocyte hypertrophy, and improved LV function following infarction [222, 223]. Granulocyte colony-stimulating factor has been postulated to recruit bone marrow cells to sites of myocardial injury [224] and to stimulate neovascularization through modulation of vascular growth factors [225]. Recently, periostin has been shown to induce cardiomyocyte re-entry into the cell cycle and mitosis leading to improved myocardial function, increased angiogenesis, and decreased infarct size [226]. Furthermore, periostin has been implicated in the recruitment of activated fibroblasts to infarcted myocardium and their collagen fibril formation, thereby aiding in the healing process following acute MI [227]. Given the potent angiogenic and myogenic effects of the aforementioned growth factors, a cardiac patch containing one or several of these growth factors may prove successful in myocardial repair and regeneration following MI, and it is the belief of the author that research into such a growth factor-loaded PEUU patch will prove beneficial.

5.1.4 *In vivo* evaluation of PEUU scaffolds for spatial control of gene expression

While the spatial control of gene expression within a PEUU scaffold has been successfully demonstrated *in vitro*, the *in vivo* efficacy of this system remains to be determined. Experiments to determine optimal ligand loading concentration for the successful *in vivo* use of this controlled release system are necessary. Furthermore, GFP was used as a reporter gene in the experiments performed for this research. While this demonstrates that the spatial control of gene expression within a scaffold is possible, experiments using genes of interest for specific tissue engineering applications are necessary before this strategy can gain clinical application.

Additionally, strategies to more precisely control spatial gene expression via the polymer may prove more effective for *in vivo* application of this system. Patterning processes such as inkjet bioprinting and photolithography may yield more highly defined and distinct regions of gene expression than those used in this research. Achievement of spatially-defined dose-dependent gene expression via the polymer would demonstrate development of a highly sophisticated system for control of gene expression and may have application in development of complex tissue architectures *in vivo*. Furthermore, spatially-varied inclusion of multiple gene inducing ligands and subsequent spatial control over the expression of multiple genes via the polymer construct may lend to development of a system that can drive populations of progenitor cells to multiple lineages within a single tissue engineered construct.

APPENDIX A

B16 CELL SUBCULTURING METHOD

Growth Medium:

500 mLs RPMI-1640
50 mLs FBS
5 mLs 10x Non-essential amino acids
5 μ Ls β -mercaptoethanol
100 mg Gentamycin sulfate

Thawing & Plating Protocol:

1. Sterile filter growth medium
2. Thaw cells from LN₂ or -80°C freezer
3. Plate cells onto T-175 flasks (1 vial/flask) in 20 mLs growth medium per flask
4. When cells ~60%-70% confluent, passage as follows

Passaging Protocol:

1. Remove growth medium
2. Wash flasks with PBS to remove traces of serum
3. Add 3 mLs 0.25% trypsin-EDTA to each flask and incubate at 37°C for 2-4 minutes
4. When ~80%-90% of cells detached from plate, add 5 mLs growth medium to each flask
5. Wash flasks with medium, & collect cells in conical tube(s)
6. Redistribute cells 1:6 (i.e. 1 flask passaged to 6 flasks)

Freezing Protocol:

1. Follow passaging protocol through step 5
2. Once cells collected, count cells with hemacytometer
3. Centrifuge at 1000 rpm for 10 minutes
4. While cells in centrifuge, make cryomedium: 10% DMSO + 90% growth medium
5. Discard supernatant and resuspend cells in cryomedium (final concentration: 5×10^5 cells/mL)
6. Aliquot into cryovials and place in isopropanol for slow cooling to -80°C
7. After 24 hours, transfer cells to LN₂

APPENDIX B

IGF-1 ELISA PROTOCOL

1. Prepare all reagents, standards, and samples as per kit instructions.
2. Bring all reagents (except IGF-1 conjugate) to room temperature.
3. Add 150 μL of Assay Diluent RD1-53 to each well of kit microplate.
4. Add 50 μL of standard, control, or sample to each well (in duplicate). Cover plate with adhesive strip, and incubate at 2-8°C for 2 hours.
5. Aspirate each well and wash four times with 400 μL of wash buffer each time. Aspirate wells fully between washes. After the last wash, invert the plate and blot against clean towels.
6. Add 200 μL cold IGF-1 conjugate to each well. Cover plate with new adhesive strip, and incubate at 2-8°C for 1 hour.
7. Repeat the wash in step 5.
8. Add 200 μL of Substrate Solution to each well, protect the plate from light, and incubate at room temperature for 30 minutes.
9. Add 50 μL of Stop Solution to each well.
10. Determine the optical density of each well within 30 minutes using a microplate reader set to 450 nm with wavelength correction set to 570 nm.

APPENDIX C

HGF ELISA PROTOCOL

1. Prepare all reagents, standards, and samples as per kit instructions.
2. Bring all reagents to room temperature.
3. Add 150 μ L of Assay Diluent RD1W to each well of kit microplate.
4. Add 50 μ L of standard, control, or sample to each well (in duplicate). Cover plate with adhesive strip, and incubate at room temperature for 2 hours.
5. Aspirate each well and wash four times with 400 μ L of wash buffer each time. Aspirate wells fully between washes. After the last wash, invert the plate and blot against clean towels.
6. Add 200 μ L HGF conjugate to each well. Cover plate with new adhesive strip and incubate at room temperature for 1.75 hours.
7. Repeat wash in step 5.
8. Add 200 μ L of Substrate Solution to each well, protect plate from light, and incubate at room temperature for 30 minutes.
9. Add 50 μ L of Stop Solution to each well.
10. Determine the optical density of each well within 30 minutes using a microplate reader set to 450 nm with wavelength correction set to 570 nm.

APPENDIX D

MG-63 & BALB/3T3 CELL SUBCULTURING METHOD

MG-63 Growth Medium:

500 mLs MEM
50 mLs FBS
5 mLs 1000 u/u Pen-strep

Balb/3T3 Growth Medium:

500 mLs DMEM
50 mLs FBS
5 mLs 1000 u/u Pen-strep

Thawing & Plating Protocol:

1. Thaw cells from LN₂ or -80°C freezer
2. Plate cells onto T-175 flasks (1 vial/flask) in 20 mLs growth medium per flask
3. When cells ~60%-70% confluent, passage as follows

Passaging Protocol:

1. Remove growth medium
2. Wash flasks with PBS to remove traces of serum
3. Add 3 mLs 0.25% trypsin-EDTA to each flask and incubate at 37°C for 2-4 minutes
4. When ~80%-90% of cells detached from plate, add 5 mLs growth medium to each flask
5. Wash flasks with medium, & collect cells in conical tube(s)
6. Redistribute cells 1:4 (i.e. 1 flask passaged to 4 flasks)

Freezing Protocol:

1. Follow passaging protocol through step 5
2. Once cells collected, count cells with hemacytometer
3. Centrifuge at 1000 rpm for 10 minutes
4. While cells in centrifuge, make cryomedium: 10% DMSO + 90% growth medium
5. Discard supernatant and resuspend cells in cryomedium (final concentration: 5x10⁵ cells/mL)
6. Aliquot into cryovials and place in isopropanol for slow cooling to -80°C
7. After 24 hours, transfer cells to LN₂

APPENDIX E

MTT PROTOCOL

Materials:

MTT (thiazoyl blue, Sigma)
PBS
isopropanol
10 M HCl

Protocol:

1. Make a 5 mg/mL stock solution of MTT in PBS.
2. Add MTT to cells in culture so that MTT final volume is 10% of culture medium volume.
(e.g. 50 μ Ls MTT in 500 μ Ls culture medium in each well of a 24 well plate)
3. Place plate back at 37°C for 4 hours.
4. Remove media and MTT solution and dispose of in proper container.
5. Add 0.04 N HCl in isopropanol to each well to bring volume to initial culture medium volume.
(e.g. 500 μ Ls 0.04 N HCl to each well of a 24 well plate)
6. Cover plate and place at 2-4°C overnight.
7. Measure optical density of solutions using a microplate reader set at 570 nm with reference at 650 nm.

APPENDIX F

HUVEC SUBCULTURING PROTOCOL

HUVEC Growth Medium:

Endothelial Basal Medium-2 (EBM-2, Lonza)

EBM bullet-kit (Lonza)

HUVEC Passaging Reagents:

Hepes-buffered saline solution (HBSS, Lonza)

0.25% Trypsin-EDTA (T-E, Lonza)

Trypsin neutralizing solution (TNS, Lonza)

Thawing & Plating Protocol:

1. Thaw cells from LN₂ or -80°C freezer
2. Plate cells onto T-175 flasks (1 vial/flask) in 20 mLs growth medium per flask
3. When cells ~60%-70% confluent, passage as follows

Passaging Protocol:

1. Remove growth medium
2. Wash flasks with HBSS to remove traces of serum
3. Add 3 mLs T-E to each flask and incubate at 37°C for 2-4 minutes
4. When ~80%-90% of cells detached from plate, add 3 mLs TNS to each flask
5. Wash flasks with TNS, & collect cells in conical tube(s)
6. Redistribute cells 1:4 (i.e. 1 flask passaged to 4 flasks)

Freezing Protocol:

1. Follow passaging protocol through step 5
2. Once cells collected, count cells with hemacytometer
3. Centrifuge at 1000 rpm for 10 minutes
4. While cells in centrifuge, make cryomedium: 10% DMSO + 90% growth medium
5. Discard supernatant and resuspend cells in cryomedium (final concentration: 5×10^5 cells/mL)
6. Aliquot into cryovials and place in isopropanol for slow cooling to -80°C
7. After 24 hours, transfer cells to LN₂

APPENDIX G

VWF AND α -SMA STAINING PROTOCOL

Prior to starting staining protocol, make BSA solution as follows: 0.3g Glycine (SIGMA G-8898) + 1g bovine serum albumin (SIGMA A2503-50g) + 200 ml PBS.

Staining Protocol:

1. Fix sections with 2% PFA for 5 min
2. Wash with PBS
3. Wash with BSA
4. Block with 5% Goat Serum (SIGMA G-9023) in PBS for 1 hour
5. Wash with BSA
6. Stain with 1° Ab: rabbit anti-vWF (DAKO A0082) 1:100 in BSA overnight at 4°C
7. Wash with BSA
8. Wash with PBS
9. Stain with 2° Ab: anti-rabbit Alexa 488 (Molecular Probes A11034) 1:250 in PBS for 1 hr
10. Wash with PBS
11. Wash with BSA
12. Stain with 1° Ab: mouse anti- α -SMA (Chemicon CBL 171) 1:100 in BSA overnight at 4°C
13. Wash with BSA
14. Wash with PBS
15. Stain with 2° Ab: goat anti-mouse cy3 (Jackson #115-165-166) 1:300 in PBS for 1 hr
16. Wash with BSA
17. Wash with PBS
18. Stain nuclei with Hoechst no.33258 (SIGMA B-2883) 1mg/100ml in PBS for 1 min
19. Wash with PBS
20. Mount slides with coverslip using gelvetol (Center for Biologic Imaging)

APPENDIX H

EA53 STAINING PROTOCOL

Prior to starting staining protocol, make BSA solution as follows: 0.3g Glycine (SIGMA G-8898) + 1g bovine serum albumin (SIGMA A2503-50g) + 200 ml PBS.

Staining Protocol:

1. Fix sections with 2% PFA for 5 min
2. Wash with PBS
3. Wash with BSA
4. Block with 5% Goat Serum (SIGMA G-9023) in PBS for 1 hour
5. Wash with BSA
6. Stain with 1° Ab: mouse anti- α -sarcomeric actinin (EA53, Sigma A-7811) 1:200 in BSA overnight at 4°C
7. Wash with BSA
8. Wash with PBS
9. Stain with 2° Ab: goat anti-mouse cy3 (Jackson #115-165-166) 1:300 in PBS for 1 hr
10. Wash with BSA
11. Wash with PBS
12. Stain nuclei with Hoechst no.33258 (SIGMA B-2883) 1mg/100ml in PBS for 1 min
13. Wash with PBS
14. Mount slides with coverslip using gelvetol (Center for Biologic Imaging)

BIBLIOGRAPHY

1. *Heart Disease and Stroke Statistics - 2005 Update*. 2005, American Heart Association: Dallas, Texas.
2. Rosenthal, N. and A. Musaro, *Gene therapy for cardiac cachexia?* Int J Cardiol, 2002. **85**(1): p. 185-91.
3. Fujimoto, K.L., et al., *An elastic, biodegradable cardiac patch induces contractile smooth muscle and improves cardiac remodeling and function in subacute myocardial infarction*. J Am Coll Cardiol, 2007. **49**(23): p. 2292-300.
4. Ott, H.C., J. McCue, and D.A. Taylor, *Cell-based cardiovascular repair--the hurdles and the opportunities*. Basic Res Cardiol, 2005. **100**(6): p. 504-17.
5. Lietz, K. and L.W. Miller, *Will left-ventricular assist device therapy replace heart transplantation in the foreseeable future?* Curr Opin Cardiol, 2005. **20**(2): p. 132-7.
6. Taylor, D.A., *Cell-based myocardial repair: how should we proceed?* Int J Cardiol, 2004. **95 Suppl 1**: p. S8-12.
7. Chachques, J.C., et al., *Myocardial Assistance by Grafting a New Bioartificial Upgraded Myocardium (MAGNUM trial): clinical feasibility study*. Ann Thorac Surg, 2008. **85**(3): p. 901-8.
8. de la Fuente, L.M., et al., *Transendocardial autologous bone marrow in chronic myocardial infarction using a helical needle catheter: 1-year follow-up in an open-label, nonrandomized, single-center pilot study (the TABMMI study)*. Am Heart J, 2007. **154**(1): p. 79 e1-7.
9. Lunde, K., et al., *Autologous stem cell transplantation in acute myocardial infarction: The ASTAMI randomized controlled trial. Intracoronary transplantation of autologous mononuclear bone marrow cells, study design and safety aspects*. Scand Cardiovasc J, 2005. **39**(3): p. 150-8.
10. Lunde, K., et al., *Exercise capacity and quality of life after intracoronary injection of autologous mononuclear bone marrow cells in acute myocardial infarction: results from the Autologous Stem cell Transplantation in Acute Myocardial Infarction (ASTAMI) randomized controlled trial*. Am Heart J, 2007. **154**(4): p. 710 e1-8.

11. Ripa, R.S., et al., *Bone marrow derived mesenchymal cell mobilization by granulocyte-colony stimulating factor after acute myocardial infarction: results from the Stem Cells in Myocardial Infarction (STEMMI) trial*. *Circulation*, 2007. **116**(11 Suppl): p. I24-30.
12. Schachinger, V., et al., *Transplantation of progenitor cells and regeneration enhancement in acute myocardial infarction: final one-year results of the TOPCARE-AMI Trial*. *J Am Coll Cardiol*, 2004. **44**(8): p. 1690-9.
13. Wollert, K.C., et al., *Intracoronary autologous bone-marrow cell transfer after myocardial infarction: the BOOST randomised controlled clinical trial*. *Lancet*, 2004. **364**(9429): p. 141-8.
14. Taylor, D.A., et al., *Regenerating functional myocardium: improved performance after skeletal myoblast transplantation*. *Nat Med*, 1998. **4**(8): p. 929-33.
15. Dib, N., et al., *Safety and feasibility of autologous myoblast transplantation in patients with ischemic cardiomyopathy: four-year follow-up*. *Circulation*, 2005. **112**(12): p. 1748-55.
16. Siminiak, T., et al., *Autologous skeletal myoblast transplantation for the treatment of postinfarction myocardial injury: phase I clinical study with 12 months of follow-up*. *Am Heart J*, 2004. **148**(3): p. 531-7.
17. Smits, P.C., et al., *Catheter-based intramyocardial injection of autologous skeletal myoblasts as a primary treatment of ischemic heart failure: clinical experience with six-month follow-up*. *J Am Coll Cardiol*, 2003. **42**(12): p. 2063-9.
18. Atkins, B.Z., et al., *Intracardiac transplantation of skeletal myoblasts yields two populations of striated cells in situ*. *Ann Thorac Surg*, 1999. **67**(1): p. 124-9.
19. Murry, C.E., et al., *Skeletal myoblast transplantation for repair of myocardial necrosis*. *J Clin Invest*, 1996. **98**(11): p. 2512-23.
20. Ott, H.C., et al., *On the fate of skeletal myoblasts in a cardiac environment: down-regulation of voltage-gated ion channels*. *J Physiol*, 2004. **558**(Pt 3): p. 793-805.
21. Menasche, P., *Cellular transplantation: hurdles remaining before widespread clinical use*. *Curr Opin Cardiol*, 2004. **19**(2): p. 154-61.
22. Beauchamp, J.R., et al., *Dynamics of myoblast transplantation reveal a discrete minority of precursors with stem cell-like properties as the myogenic source*. *J Cell Biol*, 1999. **144**(6): p. 1113-22.
23. Huard, J., et al., *Human myoblast transplantation: preliminary results of 4 cases*. *Muscle Nerve*, 1992. **15**(5): p. 550-60.
24. Cao, B., et al., *Muscle stem cells differentiate into haematopoietic lineages but retain myogenic potential*. *Nat Cell Biol*, 2003. **5**(7): p. 640-6.

25. Deasy, B.M., R.J. Jankowski, and J. Huard, *Muscle-derived stem cells: characterization and potential for cell-mediated therapy*. Blood Cells Mol Dis, 2001. **27**(5): p. 924-33.
26. Huard, J., B. Cao, and Z. Qu-Petersen, *Muscle-derived stem cells: potential for muscle regeneration*. Birth Defects Res C Embryo Today, 2003. **69**(3): p. 230-7.
27. Jankowski, R.J., B.M. Deasy, and J. Huard, *Muscle-derived stem cells*. Gene Ther, 2002. **9**(10): p. 642-7.
28. Qu-Petersen, Z., et al., *Identification of a novel population of muscle stem cells in mice: potential for muscle regeneration*. J Cell Biol, 2002. **157**(5): p. 851-64.
29. Lee, J.Y., et al., *Clonal isolation of muscle-derived cells capable of enhancing muscle regeneration and bone healing*. J Cell Biol, 2000. **150**(5): p. 1085-100.
30. Oshima, H., et al., *Differential myocardial infarct repair with muscle stem cells compared to myoblasts*. Mol Ther, 2005. **12**(6): p. 1130-41.
31. Payne, T.R., et al., *Regeneration of dystrophin-expressing myocytes in the mdx heart by skeletal muscle stem cells*. Gene Ther, 2005. **12**(16): p. 1264-74.
32. Payne, T.R., et al., *A relationship between vascular endothelial growth factor, angiogenesis, and cardiac repair after muscle stem cell transplantation into ischemic hearts*. J Am Coll Cardiol, 2007. **50**(17): p. 1677-84.
33. Sakai, T., et al., *The use of ex vivo gene transfer based on muscle-derived stem cells for cardiovascular medicine*. Trends Cardiovasc Med, 2002. **12**(3): p. 115-20.
34. Anversa, P., et al., *Life and death of cardiac stem cells: a paradigm shift in cardiac biology*. Circulation, 2006. **113**(11): p. 1451-63.
35. Beltrami, A.P., et al., *Adult cardiac stem cells are multipotent and support myocardial regeneration*. Cell, 2003. **114**(6): p. 763-76.
36. Matsuura, K., et al., *Adult cardiac Sca-1-positive cells differentiate into beating cardiomyocytes*. J Biol Chem, 2004. **279**(12): p. 11384-91.
37. Urbanek, K., et al., *Myocardial regeneration by activation of multipotent cardiac stem cells in ischemic heart failure*. Proc Natl Acad Sci U S A, 2005. **102**(24): p. 8692-7.
38. Hierlihy, A.M., et al., *The post-natal heart contains a myocardial stem cell population*. FEBS Lett, 2002. **530**(1-3): p. 239-43.
39. Moretti, A., et al., *Multipotent embryonic isl1+ progenitor cells lead to cardiac, smooth muscle, and endothelial cell diversification*. Cell, 2006. **127**(6): p. 1151-65.

40. Ott, H.C., et al., *The adult human heart as a source for stem cells: repair strategies with embryonic-like progenitor cells*. Nat Clin Pract Cardiovasc Med, 2007. **4 Suppl 1**: p. S27-39.
41. Wu, X., et al., *Small molecules that induce cardiomyogenesis in embryonic stem cells*. J Am Chem Soc, 2004. **126**(6): p. 1590-1.
42. Zhou, X., E. Quann, and G.I. Gallicano, *Differentiation of nonbeating embryonic stem cells into beating cardiomyocytes is dependent on downregulation of PKC beta and zeta in concert with upregulation of PKC epsilon*. Dev Biol, 2003. **255**(2): p. 407-22.
43. Sachinidis, A., et al., *Identification of platelet-derived growth factor-BB as cardiogenesis-inducing factor in mouse embryonic stem cells under serum-free conditions*. Cell Physiol Biochem, 2003. **13**(6): p. 423-9.
44. Pittenger, M.F., et al., *Multilineage potential of adult human mesenchymal stem cells*. Science, 1999. **284**(5411): p. 143-7.
45. Kawada, H., et al., *Nonhematopoietic mesenchymal stem cells can be mobilized and differentiate into cardiomyocytes after myocardial infarction*. Blood, 2004. **104**(12): p. 3581-7.
46. Fukuda, K., *Development of regenerative cardiomyocytes from mesenchymal stem cells for cardiovascular tissue engineering*. Artif Organs, 2001. **25**(3): p. 187-93.
47. Makino, S., et al., *Cardiomyocytes can be generated from marrow stromal cells in vitro*. J Clin Invest, 1999. **103**(5): p. 697-705.
48. Tomita, S., et al., *Autologous transplantation of bone marrow cells improves damaged heart function*. Circulation, 1999. **100**(19 Suppl): p. II247-56.
49. Shim, W.S., et al., *Ex vivo differentiation of human adult bone marrow stem cells into cardiomyocyte-like cells*. Biochem Biophys Res Commun, 2004. **324**(2): p. 481-8.
50. Rangappa, S., et al., *Cardiomyocyte-mediated contact programs human mesenchymal stem cells to express cardiogenic phenotype*. J Thorac Cardiovasc Surg, 2003. **126**(1): p. 124-32.
51. Liu, Y., et al., *Growth and differentiation of rat bone marrow stromal cells: does 5-azacytidine trigger their cardiomyogenic differentiation?* Cardiovasc Res, 2003. **58**(2): p. 460-8.
52. Schuster, M.D., et al., *Myocardial neovascularization by bone marrow angioblasts results in cardiomyocyte regeneration*. Am J Physiol Heart Circ Physiol, 2004. **287**(2): p. H525-32.

53. Thompson, R.B., et al., *Intracardiac transplantation of a mixed population of bone marrow cells improves both regional systolic contractility and diastolic relaxation*. J Heart Lung Transplant, 2005. **24**(2): p. 205-14.
54. Jiang, X.X., et al., *Human mesenchymal stem cells inhibit differentiation and function of monocyte-derived dendritic cells*. Blood, 2005. **105**(10): p. 4120-6.
55. Yeh, E.T., et al., *Transdifferentiation of human peripheral blood CD34⁺-enriched cell population into cardiomyocytes, endothelial cells, and smooth muscle cells in vivo*. Circulation, 2003. **108**(17): p. 2070-3.
56. Deten, A., et al., *Hematopoietic stem cells do not repair the infarcted mouse heart*. Cardiovasc Res, 2005. **65**(1): p. 52-63.
57. Murry, C.E., et al., *Haematopoietic stem cells do not transdifferentiate into cardiac myocytes in myocardial infarcts*. Nature, 2004. **428**(6983): p. 664-8.
58. Aicher, A., et al., *Assessment of the tissue distribution of transplanted human endothelial progenitor cells by radioactive labeling*. Circulation, 2003. **107**(16): p. 2134-9.
59. Masuda, H., C. Kalka, and T. Asahara, *Endothelial progenitor cells for regeneration*. Hum Cell, 2000. **13**(4): p. 153-60.
60. Urbich, C., et al., *FOXO-dependent expression of the proapoptotic protein Bim: pivotal role for apoptosis signaling in endothelial progenitor cells*. Faseb J, 2005. **19**(8): p. 974-6.
61. Henning, R.J., et al., *Human umbilical cord blood mononuclear cells for the treatment of acute myocardial infarction*. Cell Transplant, 2004. **13**(7-8): p. 729-39.
62. Ma, N., et al., *Human cord blood cells induce angiogenesis following myocardial infarction in NOD/scid-mice*. Cardiovasc Res, 2005. **66**(1): p. 45-54.
63. Hirata, Y., et al., *Human umbilical cord blood cells improve cardiac function after myocardial infarction*. Biochem Biophys Res Commun, 2005. **327**(2): p. 609-14.
64. Moelker, A.D., et al., *Intracoronary delivery of umbilical cord blood derived unrestricted somatic stem cells is not suitable to improve LV function after myocardial infarction in swine*. J Mol Cell Cardiol, 2007. **42**(4): p. 735-45.
65. Reinlib, L. and L. Field, *Cell transplantation as future therapy for cardiovascular disease?: A workshop of the National Heart, Lung, and Blood Institute*. Circulation, 2000. **101**(18): p. E182-7.
66. Haider, H.K., et al., *Nonviral vector gene modification of stem cells for myocardial repair*. Mol Med, 2008. **14**(1-2): p. 79-86.

67. Askari, A.T., et al., *Effect of stromal-cell-derived factor 1 on stem-cell homing and tissue regeneration in ischaemic cardiomyopathy*. Lancet, 2003. **362**(9385): p. 697-703.
68. Duan, H.F., et al., *Treatment of myocardial ischemia with bone marrow-derived mesenchymal stem cells overexpressing hepatocyte growth factor*. Mol Ther, 2003. **8**(3): p. 467-74.
69. Hattan, N., et al., *Autologous vascular smooth muscle cell-based myocardial gene therapy to induce coronary collateral growth*. Am J Physiol Heart Circ Physiol, 2004. **287**(2): p. H488-93.
70. Miyagawa, S., et al., *Myocardial regeneration therapy for heart failure: hepatocyte growth factor enhances the effect of cellular cardiomyoplasty*. Circulation, 2002. **105**(21): p. 2556-61.
71. Murry, C.E., et al., *Muscle differentiation during repair of myocardial necrosis in rats via gene transfer with MyoD*. J Clin Invest, 1996. **98**(10): p. 2209-17.
72. Yau, T.M., et al., *Enhanced myocardial angiogenesis by gene transfer with transplanted cells*. Circulation, 2001. **104**(12 Suppl 1): p. I218-22.
73. Yau, T.M., et al., *Vascular endothelial growth factor transgene expression in cell-transplanted hearts*. J Thorac Cardiovasc Surg, 2004. **127**(4): p. 1180-7.
74. Ye, L., et al., *Transplantation of nanoparticle transfected skeletal myoblasts overexpressing vascular endothelial growth factor-165 for cardiac repair*. Circulation, 2007. **116**(11 Suppl): p. I113-20.
75. Zhang, M., et al., *SDF-1 expression by mesenchymal stem cells results in trophic support of cardiac myocytes after myocardial infarction*. FASEB J, 2007. **21**(12): p. 3197-207.
76. Nof, M. and L.D. Shea, *Drug-releasing scaffolds fabricated from drug-loaded microspheres*. J Biomed Mater Res, 2002. **59**(2): p. 349-56.
77. Tabata, Y., *Tissue regeneration based on growth factor release*. Tissue Eng, 2003. **9 Suppl 1**: p. S5-15.
78. Putnam, A.J. and D.J. Mooney, *Tissue engineering using synthetic extracellular matrices*. Nat Med, 1996. **2**(7): p. 824-6.
79. Godbey, W.T. and A. Atala, *In vitro systems for tissue engineering*. Ann N Y Acad Sci, 2002. **961**: p. 10-26.
80. Kim, B.S., C.E. Baez, and A. Atala, *Biomaterials for tissue engineering*. World J Urol, 2000. **18**(1): p. 2-9.

81. Ramaswami, P., Wagner, WR, *Cardiovascular Tissue Engineering*, in *An Introduction to Biomaterials*, S. Guelcher, JO Hollinger, Editor. 2006, CRC Press: Boca Raton, FL. p. 461-484.
82. Kofidis, T., et al., *In vitro engineering of heart muscle: artificial myocardial tissue*. J Thorac Cardiovasc Surg, 2002. **124**(1): p. 63-9.
83. Kofidis, T., et al., *A novel bioartificial myocardial tissue and its prospective use in cardiac surgery*. Eur J Cardiothorac Surg, 2002. **22**(2): p. 238-43.
84. Kofidis, T., et al., *Clinically established hemostatic scaffold (tissue fleece) as biomatrix in tissue- and organ-engineering research*. Tissue Eng, 2003. **9**(3): p. 517-23.
85. Radisic, M., et al., *Functional assembly of engineered myocardium by electrical stimulation of cardiac myocytes cultured on scaffolds*. Proc Natl Acad Sci U S A, 2004. **101**(52): p. 18129-34.
86. Zimmermann, W.H., et al., *Tissue engineering of a differentiated cardiac muscle construct*. Circ Res, 2002. **90**(2): p. 223-30.
87. Dar, A., et al., *Optimization of cardiac cell seeding and distribution in 3D porous alginate scaffolds*. Biotechnol Bioeng, 2002. **80**(3): p. 305-12.
88. Itabashi, Y., et al., *A new method for manufacturing cardiac cell sheets using fibrin-coated dishes and its electrophysiological studies by optical mapping*. Artif Organs, 2005. **29**(2): p. 95-103.
89. Shimizu, T., et al., *Electrically communicating three-dimensional cardiac tissue mimic fabricated by layered cultured cardiomyocyte sheets*. J Biomed Mater Res, 2002. **60**(1): p. 110-7.
90. Shimizu, T., et al., *Fabrication of pulsatile cardiac tissue grafts using a novel 3-dimensional cell sheet manipulation technique and temperature-responsive cell culture surfaces*. Circ Res, 2002. **90**(3): p. e40.
91. Yang, S., et al., *The design of scaffolds for use in tissue engineering. Part I. Traditional factors*. Tissue Eng, 2001. **7**(6): p. 679-89.
92. Ozawa, T., et al., *Optimal biomaterial for creation of autologous cardiac grafts*. Circulation, 2002. **106**(12 Suppl 1): p. I176-82.
93. Ozawa, T., et al., *Histologic changes of nonbiodegradable and biodegradable biomaterials used to repair right ventricular heart defects in rats*. J Thorac Cardiovasc Surg, 2002. **124**(6): p. 1157-64.
94. Matsubayashi, K., et al., *Improved left ventricular aneurysm repair with bioengineered vascular smooth muscle grafts*. Circulation, 2003. **108 Suppl 1**: p. II219-25.

95. Shin, M., et al., *Contractile cardiac grafts using a novel nanofibrous mesh*. Biomaterials, 2004. **25**(17): p. 3717-23.
96. Stankus, J.J., et al., *Microintegrating smooth muscle cells into a biodegradable, elastomeric fiber matrix*. Biomaterials, 2006. **27**(5): p. 735-44.
97. Stankus, J.J., J. Guan, and W.R. Wagner, *Fabrication of biodegradable elastomeric scaffolds with sub-micron morphologies*. J Biomed Mater Res A, 2004. **70**(4): p. 603-14.
98. Pego, A.P., et al., *Preparation of degradable porous structures based on 1,3-trimethylene carbonate and D,L-lactide (co)polymers for heart tissue engineering*. Tissue Eng, 2003. **9**(5): p. 981-94.
99. McDevitt, T.C., et al., *In vitro generation of differentiated cardiac myofibers on micropatterned laminin surfaces*. J Biomed Mater Res, 2002. **60**(3): p. 472-9.
100. McDevitt, T.C., et al., *Spatially organized layers of cardiomyocytes on biodegradable polyurethane films for myocardial repair*. J Biomed Mater Res A, 2003. **66**(3): p. 586-95.
101. Campbell, P.G., et al., *Engineered spatial patterns of FGF-2 immobilized on fibrin direct cell organization*. Biomaterials, 2005. **26**(33): p. 6762-70.
102. Endres, M., et al., *Osteogenic induction of human bone marrow-derived mesenchymal progenitor cells in novel synthetic polymer-hydrogel matrices*. Tissue Eng, 2003. **9**(4): p. 689-702.
103. Ennett, A.B., D. Kaigler, and D.J. Mooney, *Temporally regulated delivery of VEGF in vitro and in vivo*. J Biomed Mater Res A, 2006. **79**(1): p. 176-84.
104. Fischbach, C. and D.J. Mooney, *Polymers for pro- and anti-angiogenic therapy*. Biomaterials, 2007. **28**(12): p. 2069-76.
105. Gurevich, O., et al., *Fibrin microbeads for isolating and growing bone marrow-derived progenitor cells capable of forming bone tissue*. Tissue Eng, 2002. **8**(4): p. 661-72.
106. Hao, X., et al., *Angiogenic effects of sequential release of VEGF-A165 and PDGF-BB with alginate hydrogels after myocardial infarction*. Cardiovasc Res, 2007. **75**(1): p. 178-85.
107. Hishikawa, K., et al., *Gene expression profile of human mesenchymal stem cells during osteogenesis in three-dimensional thermoreversible gelation polymer*. Biochem Biophys Res Commun, 2004. **317**(4): p. 1103-7.
108. Korovessis, P.G. and D.D. Deligianni, *Role of surface roughness of titanium versus hydroxyapatite on human bone marrow cells response*. J Spinal Disord Tech, 2002. **15**(2): p. 175-83; discussion 183.

109. Levenberg, S., et al., *Differentiation of human embryonic stem cells on three-dimensional polymer scaffolds*. Proc Natl Acad Sci U S A, 2003. **100**(22): p. 12741-6.
110. Lu, H.H., et al., *Three-dimensional, bioactive, biodegradable, polymer-bioactive glass composite scaffolds with improved mechanical properties support collagen synthesis and mineralization of human osteoblast-like cells in vitro*. J Biomed Mater Res, 2003. **64A**(3): p. 465-74.
111. Murphy, W.L., et al., *Sustained release of vascular endothelial growth factor from mineralized poly(lactide-co-glycolide) scaffolds for tissue engineering*. Biomaterials, 2000. **21**(24): p. 2521-7.
112. Wang, M.L., et al., *Titanium particles suppress expression of osteoblastic phenotype in human mesenchymal stem cells*. J Orthop Res, 2002. **20**(6): p. 1175-84.
113. Xie, Y., S.T. Yang, and D.A. Kniss, *Three-dimensional cell-scaffold constructs promote efficient gene transfection: implications for cell-based gene therapy*. Tissue Eng, 2001. **7**(5): p. 585-98.
114. Laham, R.J., et al., *Local perivascular delivery of basic fibroblast growth factor in patients undergoing coronary bypass surgery: results of a phase I randomized, double-blind, placebo-controlled trial*. Circulation, 1999. **100**(18): p. 1865-71.
115. Iwakura, A., et al., *Intramyocardial sustained delivery of basic fibroblast growth factor improves angiogenesis and ventricular function in a rat infarct model*. Heart Vessels, 2003. **18**(2): p. 93-9.
116. Sakakibara, Y., et al., *Prevascularization with gelatin microspheres containing basic fibroblast growth factor enhances the benefits of cardiomyocyte transplantation*. J Thorac Cardiovasc Surg, 2002. **124**(1): p. 50-6.
117. Peattie, R.A., et al., *Stimulation of in vivo angiogenesis by cytokine-loaded hyaluronic acid hydrogel implants*. Biomaterials, 2004. **25**(14): p. 2789-98.
118. Marui, A., et al., *Simultaneous application of basic fibroblast growth factor and hepatocyte growth factor to enhance the blood vessels formation*. J Vasc Surg, 2005. **41**(1): p. 82-90.
119. Peattie, R.A., et al., *Dual growth factor-induced angiogenesis in vivo using hyaluronan hydrogel implants*. Biomaterials, 2006. **27**(9): p. 1868-75.
120. Riley, C.M., et al., *Stimulation of in vivo angiogenesis using dual growth factor-loaded crosslinked glycosaminoglycan hydrogels*. Biomaterials, 2006. **27**(35): p. 5935-43.
121. Birchmeier, C., et al., *Met, metastasis, motility and more*. Nat Rev Mol Cell Biol, 2003. **4**(12): p. 915-25.

122. Gherardi, E., et al., *Purification of scatter factor, a fibroblast-derived basic protein that modulates epithelial interactions and movement*. Proc Natl Acad Sci U S A, 1989. **86**(15): p. 5844-8.
123. Zarnegar, R. and G. Michalopoulos, *Purification and biological characterization of human hepatopoietin A, a polypeptide growth factor for hepatocytes*. Cancer Res, 1989. **49**(12): p. 3314-20.
124. Forte, G., et al., *Hepatocyte growth factor effects on mesenchymal stem cells: proliferation, migration, and differentiation*. Stem Cells, 2006. **24**(1): p. 23-33.
125. Jayasankar, V., et al., *Induction of angiogenesis and inhibition of apoptosis by hepatocyte growth factor effectively treats postischemic heart failure*. J Card Surg, 2005. **20**(1): p. 93-101.
126. Tambara, K., et al., *Administration of control-released hepatocyte growth factor enhances the efficacy of skeletal myoblast transplantation in rat infarcted hearts by greatly increasing both quantity and quality of the graft*. Circulation, 2005. **112**(9 Suppl): p. I129-34.
127. Anderson, C.D., et al., *The Role of Cytoprotective Cytokines in Cardiac Ischemia/Reperfusion Injury*. J Surg Res, 2007.
128. Mourkioti, F. and N. Rosenthal, *IGF-1, inflammation and stem cells: interactions during muscle regeneration*. Trends Immunol, 2005. **26**(10): p. 535-42.
129. Schulze, P.C. and U. Spate, *Insulin-like growth factor-1 and muscle wasting in chronic heart failure*. Int J Biochem Cell Biol, 2005. **37**(10): p. 2023-35.
130. Gneecchi, M., et al., *Paracrine action accounts for marked protection of ischemic heart by Akt-modified mesenchymal stem cells*. Nat Med, 2005. **11**(4): p. 367-8.
131. Gneecchi, M., et al., *Evidence supporting paracrine hypothesis for Akt-modified mesenchymal stem cell-mediated cardiac protection and functional improvement*. FASEB J, 2006. **20**(6): p. 661-9.
132. Liu, T.B., et al., *Enhanced IGF-1 expression improves smooth muscle cell engraftment after cell transplantation*. Am J Physiol Heart Circ Physiol, 2004. **287**(6): p. H2840-9.
133. Noiseux, N., et al., *Mesenchymal stem cells overexpressing Akt dramatically repair infarcted myocardium and improve cardiac function despite infrequent cellular fusion or differentiation*. Mol Ther, 2006. **14**(6): p. 840-50.
134. Schulze, P.C., et al., *Transgenic overexpression of locally acting insulin-like growth factor-1 inhibits ubiquitin-mediated muscle atrophy in chronic left-ventricular dysfunction*. Circ Res, 2005. **97**(5): p. 418-26.

135. Davis, M.E., et al., *Local myocardial insulin-like growth factor I (IGF-1) delivery with biotinylated peptide nanofibers improves cell therapy for myocardial infarction*. Proc Natl Acad Sci U S A, 2006. **103**(21): p. 8155-60.
136. Chen, F.M., et al., *Enhancement of periodontal tissue regeneration by locally controlled delivery of insulin-like growth factor-I from dextran-co-gelatin microspheres*. J Control Release, 2006. **114**(2): p. 209-22.
137. Luginbuehl, V., et al., *Insulin-like growth factor I-releasing alginate-tricalciumphosphate composites for bone regeneration*. Pharm Res, 2005. **22**(6): p. 940-50.
138. Singh, M., et al., *Controlled release of recombinant insulin-like growth factor from a novel formulation of polylactide-co-glycolide microparticles*. J Control Release, 2001. **70**(1-2): p. 21-8.
139. Wildemann, B., et al., *IGF-I and TGF-beta 1 incorporated in a poly(D,L-lactide) implant coating maintain their activity over long-term storage-cell culture studies on primary human osteoblast-like cells*. Biomaterials, 2004. **25**(17): p. 3639-44.
140. Yasuda, A., et al., *In vitro culture of chondrocytes in a novel thermoreversible gelation polymer scaffold containing growth factors*. Tissue Eng, 2006. **12**(5): p. 1237-45.
141. Davis, M.E., et al., *Custom design of the cardiac microenvironment with biomaterials*. Circ Res, 2005. **97**(1): p. 8-15.
142. Jang, J.H., et al., *Surface adsorption of DNA to tissue engineering scaffolds for efficient gene delivery*. J Biomed Mater Res A, 2006. **77**(1): p. 50-8.
143. Jang, J.H., T.L. Houchin, and L.D. Shea, *Gene delivery from polymer scaffolds for tissue engineering*. Expert Rev Med Devices, 2004. **1**(1): p. 127-38.
144. Tabata, Y., *Potential of Drug Delivery Technology in Tissue Regeneration Therapy*. J Hard Tissue Biology, 2006. **15**(3): p. 73-81.
145. Godbey, W.T., K.K. Wu, and A.G. Mikos, *Poly(ethylenimine) and its role in gene delivery*. J Control Release, 1999. **60**(2-3): p. 149-60.
146. Lavigne, M.D., et al., *Enhanced gene expression through temperature profile-induced variations in molecular architecture of thermoresponsive polymer vectors*. J Gene Med, 2007. **9**(1): p. 44-54.
147. Ogris, M. and E. Wagner, *Tumor-targeted gene transfer with DNA polyplexes*. Somat Cell Mol Genet, 2002. **27**(1-6): p. 85-95.
148. Kushibiki, T., et al., *Controlled release of plasmid DNA from hydrogels prepared from gelatin cationized by different amine compounds*. J Control Release, 2006. **112**(2): p. 249-56.

149. Kasahara, H., et al., *Biodegradable gelatin hydrogel potentiates the angiogenic effect of fibroblast growth factor 4 plasmid in rabbit hindlimb ischemia*. J Am Coll Cardiol, 2003. **41**(6): p. 1056-62.
150. Christman, K.L., et al., *Enhanced neovasculature formation in ischemic myocardium following delivery of pleiotrophin plasmid in a biopolymer*. Biomaterials, 2005. **26**(10): p. 1139-44.
151. Alexander, H.K., et al., *Selected technologies to control genes and their products for experimental and clinical purposes*. Arch Immunol Ther Exp (Warsz), 2007. **55**(3): p. 139-49.
152. Gossen, M. and H. Bujard, *Tight control of gene expression in mammalian cells by tetracycline-responsive promoters*. Proc Natl Acad Sci U S A, 1992. **89**(12): p. 5547-51.
153. Goverdhan, S., et al., *Regulatable gene expression systems for gene therapy applications: progress and future challenges*. Mol Ther, 2005. **12**(2): p. 189-211.
154. Sun, Y., X. Chen, and D. Xiao, *Tetracycline-inducible expression systems: new strategies and practices in the transgenic mouse modeling*. Acta Biochim Biophys Sin (Shanghai), 2007. **39**(4): p. 235-46.
155. Palli, S.R., et al., *Improved ecdysone receptor-based inducible gene regulation system*. Eur J Biochem, 2003. **270**(6): p. 1308-15.
156. Hatzistergos, K.E., et al., *Randomised comparison of growth hormone versus IGF-1 on early post-myocardial infarction ventricular remodelling in rats*. Growth Horm IGF Res, 2008. **18**(2): p. 157-65.
157. Jin, H., et al., *The therapeutic potential of hepatocyte growth factor for myocardial infarction and heart failure*. Curr Pharm Des, 2004. **10**(20): p. 2525-33.
158. Ueda, H., et al., *A potential cardioprotective role of hepatocyte growth factor in myocardial infarction in rats*. Cardiovasc Res, 2001. **51**(1): p. 41-50.
159. Urbanek, K., et al., *Cardiac stem cells possess growth factor-receptor systems that after activation regenerate the infarcted myocardium, improving ventricular function and long-term survival*. Circ Res, 2005. **97**(7): p. 663-73.
160. Baker, R.E. and P.K. Maini, *Travelling gradients in interacting morphogen systems*. Math Biosci, 2007. **209**(1): p. 30-50.
161. Haugh, J.M., et al., *Spatial sensing in fibroblasts mediated by 3' phosphoinositides*. J Cell Biol, 2000. **151**(6): p. 1269-80.
162. Kennedy, T.E., et al., *Axon guidance by diffusible chemoattractants: a gradient of netrin protein in the developing spinal cord*. J Neurosci, 2006. **26**(34): p. 8866-74.

163. Makanya, A.N., et al., *Microvascular growth, development, and remodeling in the embryonic avian kidney: the interplay between sprouting and intussusceptive angiogenic mechanisms*. *Microsc Res Tech*, 2005. **66**(6): p. 275-88.
164. Schneider, I.C. and J.M. Haugh, *Quantitative elucidation of a distinct spatial gradient-sensing mechanism in fibroblasts*. *J Cell Biol*, 2005. **171**(5): p. 883-92.
165. Guelcher, S., *Biodegradable Polyurethanes: Synthesis and Applications in Regenerative Medicine*. *Tissue Engineering: Part B*, 2008. **14**(1): p. 3-17.
166. Santerre, J.P., et al., *Understanding the biodegradation of polyurethanes: from classical implants to tissue engineering materials*. *Biomaterials*, 2005. **26**(35): p. 7457-70.
167. Rockwood, D.N., et al., *Characterization of biodegradable polyurethane microfibers for tissue engineering*. *J Biomater Sci Polym Ed*, 2007. **18**(6): p. 743-58.
168. Skarja, G.A. and K.A. Woodhouse, *In vitro degradation and erosion of degradable, segmented polyurethanes containing an amino acid-based chain extender*. *J Biomater Sci Polym Ed*, 2001. **12**(8): p. 851-73.
169. Guan, J., et al., *Synthesis, characterization, and cytocompatibility of elastomeric, biodegradable poly(ester-urethane)ureas based on poly(caprolactone) and putrescine*. *J Biomed Mater Res*, 2002. **61**(3): p. 493-503.
170. Guan, J., et al., *Preparation and characterization of highly porous, biodegradable polyurethane scaffolds for soft tissue applications*. *Biomaterials*, 2005. **26**(18): p. 3961-71.
171. Fujimoto, K.L., et al., *In vivo evaluation of a porous, elastic, biodegradable patch for reconstructive cardiac procedures*. *Ann Thorac Surg*, 2007. **83**(2): p. 648-54.
172. Guan, J., J.J. Stankus, and W.R. Wagner, *Biodegradable elastomeric scaffolds with basic fibroblast growth factor release*. *J Control Release*, 2007. **120**(1-2): p. 70-8.
173. Liu, X.J., et al., *Identification of a nonpeptide ligand that releases bioactive insulin-like growth factor-I from its binding protein complex*. *J Biol Chem*, 2001. **276**(35): p. 32419-22.
174. Bussolino, F., et al., *Hepatocyte growth factor is a potent angiogenic factor which stimulates endothelial cell motility and growth*. *J Cell Biol*, 1992. **119**(3): p. 629-41.
175. Schmidt, B., Feduska, JM, Witt AM, Deasy BM, *Robotic Cell Culture System for Stem Cell Assays*. *Industrial Robot*, 2008. **35**(2).
176. Siepe, M., et al., *Construction of skeletal myoblast-based polyurethane scaffolds for myocardial repair*. *Artif Organs*, 2007. **31**(6): p. 425-33.

177. Lamba, N., Woodhouse, KA, and Cooper, SL, *Polyurethanes in Biomedical Applications*. 1998, Boca Raton, FL: CRC Press.
178. Cohn, D., et al., *Biodegradable poly(ethylene oxide)/poly(epsilon-caprolactone) multiblock copolymers*. J Biomed Mater Res, 2002. **59**(2): p. 273-81.
179. Fromstein, J.D. and K.A. Woodhouse, *Elastomeric biodegradable polyurethane blends for soft tissue applications*. J Biomater Sci Polym Ed, 2002. **13**(4): p. 391-406.
180. Guan, J., et al., *Biodegradable poly(ether ester urethane)urea elastomers based on poly(ether ester) triblock copolymers and putrescine: synthesis, characterization and cytocompatibility*. Biomaterials, 2004. **25**(1): p. 85-96.
181. Woo, G.L., et al., *Biological characterization of a novel biodegradable antimicrobial polymer synthesized with fluoroquinolones*. J Biomed Mater Res, 2002. **59**(1): p. 35-45.
182. Yang, M. and J.P. Santerre, *Utilization of quinolone drugs as monomers: characterization of the synthesis reaction products for poly(norfloxacin diisocyanatododecane polycaprolactone)*. Biomacromolecules, 2001. **2**(1): p. 134-41.
183. Huang, X. and C.S. Brazel, *On the importance and mechanisms of burst release in matrix-controlled drug delivery systems*. J Control Release, 2001. **73**(2-3): p. 121-36.
184. Musaro, A., et al., *Stem cell-mediated muscle regeneration is enhanced by local isoform of insulin-like growth factor I*. Proc Natl Acad Sci U S A, 2004. **101**(5): p. 1206-10.
185. Musaro, A., et al., *Localized Igf-1 transgene expression sustains hypertrophy and regeneration in senescent skeletal muscle*. Nat Genet, 2001. **27**(2): p. 195-200.
186. Torella, D., et al., *Cardiac stem cell and myocyte aging, heart failure, and insulin-like growth factor-1 overexpression*. Circ Res, 2004. **94**(4): p. 514-24.
187. Stewart, C.E. and P. Rotwein, *Growth, differentiation, and survival: multiple physiological functions for insulin-like growth factors*. Physiol Rev, 1996. **76**(4): p. 1005-26.
188. Hayashi, S., et al., *Sequence of IGF-I, IGF-II, and HGF expression in regenerating skeletal muscle*. Histochem Cell Biol, 2004. **122**(5): p. 427-34.
189. Machida, S. and F.W. Booth, *Insulin-like growth factor I and muscle growth: implication for satellite cell proliferation*. Proc Nutr Soc, 2004. **63**(2): p. 337-40.
190. Barton, E.R., et al., *Muscle-specific expression of insulin-like growth factor I counters muscle decline in mdx mice*. J Cell Biol, 2002. **157**(1): p. 137-48.
191. Nakamura, T., et al., *Myocardial protection from ischemia/reperfusion injury by endogenous and exogenous HGF*. J Clin Invest, 2000. **106**(12): p. 1511-9.

192. Neuss, S., et al., *Functional expression of HGF and HGF receptor/c-met in adult human mesenchymal stem cells suggests a role in cell mobilization, tissue repair, and wound healing*. *Stem Cells*, 2004. **22**(3): p. 405-14.
193. Soeki, T., et al., *Role of circulating vascular endothelial growth factor and hepatocyte growth factor in patients with coronary artery disease*. *Heart Vessels*, 2000. **15**(3): p. 105-11.
194. Soeki, T., et al., *Serial changes in serum VEGF and HGF in patients with acute myocardial infarction*. *Cardiology*, 2000. **93**(3): p. 168-74.
195. Isobe, M., H. Futamatsu, and J. Suzuki, *Hepatocyte growth factor: Effects on immune-mediated heart diseases*. *Trends Cardiovasc Med*, 2006. **16**(6): p. 188-93.
196. Langer, R. and D.A. Tirrell, *Designing materials for biology and medicine*. *Nature*, 2004. **428**(6982): p. 487-92.
197. Alexis, F., et al., *New frontiers in nanotechnology for cancer treatment*. *Urol Oncol*, 2008. **26**(1): p. 74-85.
198. Kong, H.J., et al., *Design of Biodegradable Hydrogel for the Local and Sustained Delivery of Angiogenic Plasmid DNA*. *Pharm Res*, 2008.
199. Kost, J. and R. Langer, *Responsive polymeric delivery systems*. *Adv Drug Deliv Rev*, 2001. **46**(1-3): p. 125-48.
200. Langer, R., *Biomaterials in drug delivery and tissue engineering: one laboratory's experience*. *Acc Chem Res*, 2000. **33**(2): p. 94-101.
201. Sheridan, M.H., et al., *Bioabsorbable polymer scaffolds for tissue engineering capable of sustained growth factor delivery*. *J Control Release*, 2000. **64**(1-3): p. 91-102.
202. Storrie, H. and D.J. Mooney, *Sustained delivery of plasmid DNA from polymeric scaffolds for tissue engineering*. *Adv Drug Deliv Rev*, 2006. **58**(4): p. 500-14.
203. Tabata, Y., *Current status of regenerative medical therapy based on drug delivery technology*. *Reprod Biomed Online*, 2008. **16**(1): p. 70-80.
204. Phillippi, J.A., et al., *Microenvironments engineered by inkjet bioprinting spatially direct adult stem cells toward muscle- and bone-like subpopulations*. *Stem Cells*, 2008. **26**(1): p. 127-34.
205. Lessard, J., et al., *Characterization of the RSL1-dependent conditional expression system in LNCaP prostate cancer cells and development of a single vector format*. *Prostate*, 2007. **67**(8): p. 808-19.
206. Li, Y., et al., *Effects of filtration seeding on cell density, spatial distribution, and proliferation in nonwoven fibrous matrices*. *Biotechnol Prog*, 2001. **17**(5): p. 935-44.

207. Antczak, M. and J. Van Blerkom, *Oocyte influences on early development: the regulatory proteins leptin and STAT3 are polarized in mouse and human oocytes and differentially distributed within the cells of the preimplantation stage embryo*. *Mol Hum Reprod*, 1997. **3**(12): p. 1067-86.
208. Raftery, L.A. and D.J. Sutherland, *Gradients and thresholds: BMP response gradients unveiled in Drosophila embryos*. *Trends Genet*, 2003. **19**(12): p. 701-8.
209. Veitia, R.A. and I. Salazar-Ciudad, *Commonalities in fly embryogenesis and mammalian pituitary patterning*. *Trends Endocrinol Metab*, 2007. **18**(7): p. 261-5.
210. Moustakas, A. and C.H. Heldin, *Signaling networks guiding epithelial-mesenchymal transitions during embryogenesis and cancer progression*. *Cancer Sci*, 2007. **98**(10): p. 1512-20.
211. Christen, B., et al., *Regeneration-specific expression pattern of three posterior Hox genes*. *Dev Dyn*, 2003. **226**(2): p. 349-55.
212. Stefonek, T.J. and K.S. Masters, *Immobilized gradients of epidermal growth factor promote accelerated and directed keratinocyte migration*. *Wound Repair Regen*, 2007. **15**(6): p. 847-55.
213. Campbell, P.G. and L.E. Weiss, *Tissue engineering with the aid of inkjet printers*. *Expert Opin Biol Ther*, 2007. **7**(8): p. 1123-7.
214. Miller, E.D., et al., *Dose-dependent cell growth in response to concentration modulated patterns of FGF-2 printed on fibrin*. *Biomaterials*, 2006. **27**(10): p. 2213-21.
215. Hong, S., et al., *Covalent immobilization of p-selectin enhances cell rolling*. *Langmuir*, 2007. **23**(24): p. 12261-8.
216. Kim, D.N., W. Lee, and W.G. Koh, *Micropatterning of proteins on the surface of three-dimensional poly(ethylene glycol) hydrogel microstructures*. *Anal Chim Acta*, 2008. **609**(1): p. 59-65.
217. Wright, D., et al., *Reusable, reversibly sealable parylene membranes for cell and protein patterning*. *J Biomed Mater Res A*, 2007.
218. Zhang, G. and L.J. Suggs, *Matrices and scaffolds for drug delivery in vascular tissue engineering*. *Adv Drug Deliv Rev*, 2007. **59**(4-5): p. 360-73.
219. Guerrero, M., et al., *Vascular endothelial growth factor-165 gene therapy promotes cardiomyogenesis in reperfused myocardial infarction*. *J Interv Cardiol*, 2008. **21**(3): p. 242-51.
220. Broberg, A.M., et al., *Erythropoietin has an antiapoptotic effect after myocardial infarction and stimulates in vitro aortic ring sprouting*. *Biochem Biophys Res Commun*, 2008. **371**(1): p. 75-8.

221. Jaquet, K., et al., *Erythropoietin and VEGF exhibit equal angiogenic potential*. *Microvasc Res*, 2002. **64**(2): p. 326-33.
222. Laham, R.J., et al., *Intrapericardial delivery of fibroblast growth factor-2 induces neovascularization in a porcine model of chronic myocardial ischemia*. *J Pharmacol Exp Ther*, 2000. **292**(2): p. 795-802.
223. Virag, J.A., et al., *Fibroblast growth factor-2 regulates myocardial infarct repair: effects on cell proliferation, scar contraction, and ventricular function*. *Am J Pathol*, 2007. **171**(5): p. 1431-40.
224. Kuethe, F., et al., *Treatment with granulocyte colony-stimulating factor for mobilization of bone marrow cells in patients with acute myocardial infarction*. *Am Heart J*, 2005. **150**(1): p. 115.
225. Kuethe, F., et al., *Treatment with granulocyte-colony stimulating factor in patients with acute myocardial infarction. Evidence for a stimulation of neovascularization and improvement of myocardial perfusion*. *Pharmazie*, 2006. **61**(11): p. 957-61.
226. Kuhn, B., et al., *Periostin induces proliferation of differentiated cardiomyocytes and promotes cardiac repair*. *Nat Med*, 2007. **13**(8): p. 962-9.
227. Shimazaki, M., et al., *Periostin is essential for cardiac healing after acute myocardial infarction*. *J Exp Med*, 2008. **205**(2): p. 295-303.